PROJECT SUMMARY REPORT 1508-1F

PERFORMANCE EVALUATION OF THE UT AUTOMATED ROAD MAINTENANCE MACHINE

Carl T. Haas, Al Traver, Young-Suk Kim, and Richard Greer

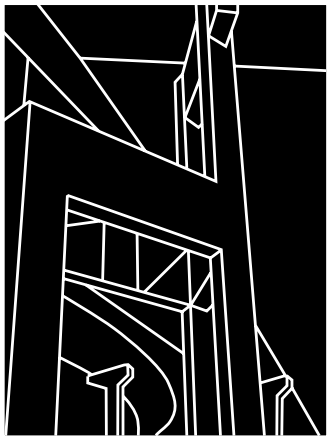

CENTER FOR TRANSPORTATION RESEARCH
BUREAU OF ENGINEERING RESEARCH
THE UNIVERSITY OF TEXAS AT AUSTIN

OCTOBER 1997

Technical Report Documentation Page

1. Report No.	2. Government Accession No.	3. Recipient's Catalog No.
FHWA/TX-99/1508-1F		

4. Title and Subtitle	5. Report Date
PERFORMANCE EVALUATION OF THE UT AUTOMATED ROAD MAINTENANCE MACHINE	October 1997

7. Author(s)	6. Performing Organization Code
Carl T. Haas, Al Traver, Young-Suk Kim, and Richard Greer	8. Performing Organization Report No. 1508-1F

9. Performing Organization Name and Address	10. Work Unit No. (TRAIS)
Center for Transportation Research The University of Texas at Austin 3208 Red River, Suite 200 Austin, TX 78705-2650	11. Contract or Grant No. 9-1508

12. Sponsoring Agency Name and Address	13. Type of Report and Period Covered
Texas Department of Transportation Research and Technology Transfer Section/Construction Division P.O. Box 5080 Austin, TX 78763-5080	Project Summary Report (9/96-8/97) 14. Sponsoring Agency Code

15. Supplementary Notes

Project conducted in cooperation with the Federal Highway Administration.

16. Abstract

This final report mainly focuses on evaluating the overall performance of The University of Texas' Automated Road Maintenance Machine (ARMM). First, the ARMM's man-machine-balanced control loop was further developed then rigorously tested and evaluated based on (1) accuracy, (2) time, and (3) quality of the resultant seal. For the efficiency evaluation, thirty pavement crack images, which included longitudinal, transverse, and block cracking, were collected from a UT research campus, and field trials were completed at five locations (Austin, San Antonio, Dallas, Corpus Christi, and Travis County) in the state of Texas. Several additional significant improvements were made to the ARMM during the course of this project.

Second, the ARMM's productivity was estimated based on (1) the results of the efficiency evaluation of the man-machine control loop, (2) observations made during the series of field trials, and (3) a productivity model. The mathematical model that predicts the productivity of the ARMM under various work conditions was developed as a means for job estimating and for rating the performance of the ARMM. The ARMM's estimated productivity was then compared with the typical productivity rate associated with conventional crack sealing methods. Evaluation results from the field trials and implementation recommendations are also made in this final project report.

It was concluded that the introduction of automated methods to the pavement crack-sealing process will improve productivity and quality and can reduce costs and safety risks. The latter is a direct result of reducing normal crew sizes of seven to eight workers to only three to four workers. The reduction in crew size and the increase in productivity of the sealing process translate directly into significant potential cost savings. By automatically recording work completed, the ARMM should help improve project controls; by its ability to work at night, the ARMM should reduce road user costs.

17. Key Words	18. Distribution Statement
Automated crack sealing, crack detection, crack sealing operations, pavement maintenance	No restrictions. This document is available to the public through the National Technical Information Service, Springfield, Virginia 22161.

19. Security Classif. (of report)	20. Security Classif. (of this page)	21. No. of pages	22. Price
Unclassified	Unclassified	138	

Form DOT F 1700.7 (8-72) Reproduction of completed page authorized

PERFORMANCE EVALUATION OF THE UT AUTOMATED ROAD MAINTENANCE MACHINE

Carl Haas
Al Traver
Young-Suk Kim
Richard Greer

Research Report 1508-1F

Research Project 9-1508
Performance Evaluation of the UT Automated Road Maintenance Machine

Conducted for the

TEXAS DEPARTMENT OF TRANSPORTATION

in cooperation with the
U.S. Department of Transportation
Federal Highway Administration

by the

CENTER FOR TRANSPORTATION RESEARCH
Bureau of Engineering Research
THE UNIVERSITY OF TEXAS AT AUSTIN

October 1997

DISCLAIMERS

The contents of this report reflect the views of the authors, who are responsible for the facts and the accuracy of the data presented herein. The contents do not necessarily reflect the official views or policies of the Federal Highway Administration and Texas Department of Transportation. This report does not constitute a standard, specification, or regulation.

There was no invention or discovery conceived or first actually reduced to practice in the course of or under this contract, including any art, method, process, machine, manufacture, design or composition of matter, or any new and useful improvement thereof, or any variety of plant, which is or may be patentable under the patent laws of the United States of America or any foreign country.

ACKNOWLEDGMENTS

The researchers acknowledge the expert assistance provided by the project director, K. Boehme (CMD), and by the project coordinator, D. Casteel (CHS).

NOT INTENDED FOR CONSTRUCTION,
BIDDING, OR PERMIT PURPOSES

Carl Haas, P.E.
Research Supervisor

TABLE OF CONTENTS

EXECUTIVE SUMMARY

This final report mainly focuses on evaluating overall performance of The University of Texas' Automated Road Maintenance Machine (ARMM). First, the ARMM's man-machine balanced control loop was further developed then rigorously tested and evaluated based on (1) accuracy, (2) time, and (3) quality of the resultant seal. For the efficiency evaluation, thirty pavement crack images, which included longitudinal, transverse, and block cracking, were collected from the UT research campus, and field trials were completed at five locations (Austin, San Antonio, Dallas, Corpus Christi, and Travis County) in the state of Texas. Several additional significant improvements were made to the ARMM during the course of this project. These improvements are summarized in Chapter 4.

Second, the ARMM's productivity was estimated based on (1) the results of the efficiency evaluation of the man-machine control loop, (2) observations made during the series of field trials, and (3) a productivity model. The mathematical model that predicts the productivity of the ARMM under various work conditions was developed as a means for job estimating and for rating the performance of the ARMM. The ARMM's estimated productivity was then compared with the typical productivity rate associated with conventional crack sealing methods. Evaluation results from the field trials and implementation recommendations are also made in this final project report.

It was concluded that the introduction of automated methods to the pavement crack sealing process will improve productivity, quality, and reduce costs and safety risks. The latter is a direct result of reducing normal crew sizes of seven-eight workers to only three-four workers. The reduction in crew size and the increase in productivity of the sealing process translate directly into significant potential cost savings. By automatically recording work completed, the ARMM should help improve project controls; by its ability to work at night, the ARMM should reduce road user costs as well. The results of the efficiency evaluation of the man-machine balanced control loop developed for the ARMM and recent field trials conducted at five locations in the state of Texas support this conclusion.

IMPLEMENTATION RECOMMENDATIONS

Implementation and commercialization of the ARMM can be completed in tandem. A final year of nationwide demonstrations should coincide with the procurement of a first commercially produced unit. Since the system demonstrates well in its current configuration, demonstrations can be interspersed throughout the year with work on improvements and field trials. Improvements that should be implemented in the next year include the following:

1. Replace the current office 486 PC with an industrial Pentium PC.
2. Use a spring-loaded, U-shaped squeegee.
3. Develop a retractable turret.
4. Modify the support arm for sealant hose.
5. Add better tinting, or mini-blinds, to reduce glare on monitor.

6. Add lighting for nighttime operations.

Field trials should be conducted in at least ten locations around the country. Potential demonstration sites include the Transportation Research Board's Annual Meeting; ASCE, NCHRP, AASHTO, and WASHTO meetings; state highway departments' research meetings; and various locations throughout the nation where a significant interest has been shown. Lead time for planning will be required to minimize inefficiencies. Objectives of the demonstrations will be to:

1. expose maintenance personnel around the country to the potential of the automated crack sealing technology,
2. generate extensive media coverage, and
3. generate hard orders for units of the system that will encourage one or more vendors (such as Crafco) to enter the market.

Secondary objectives include additional collection of productivity data, acquisition of more feedback from maintenance personnel, further proof testing of the equipment under actual working conditions, acquisition of additional video footage, and additional field experience. Each field demonstration is expected to require one week.

CHAPTER 1. INTRODUCTION TO THE MAN-MACHINE BALANCED CONTROL LOOP DEVELOPED FOR THE ARMM

1.1 INTRODUCTION

Over the course of developing four physical crack sealing prototype systems, a unique man-machine balanced control loop (Figure 1.2) for successful automation of crack sealing has been developed for computer-assisted teleoperation. The previous crack-sealing prototype systems, though fully autonomous, were slow and impractical. A complex evolution over approximately 9 years (Table 1.1) has resulted in a functional production prototype system that has achieved a good balance (Table 1.2) between manual functions and automated functions. This chapter first describes a working definition of teleoperation and identifies its common elements. It also discusses the human factors and ergonomics issues involved in the development of man-machine systems. Then, Section 1.2 illustrates the man-machine balanced control loop architecture that was originally devised for the ARMM.

1.1.1 Teleoperation

Automation of construction and maintenance operations has been advancing at an accelerated pace since the early 1980s (Haas 1995). While early works sought to completely automate some activities, experience and the resulting deeper understanding of the enabling technologies have emphasized the importance of finding an optimal balance between human and computer functions in the control of automated systems. Teleoperation has become the preferred control paradigm in these efforts.

The prefix *tele* is defined as being "at a distance or over a distance" *(Merriam Webster's Collegiate Dictionary 1993).* From this, teleoperation can be thought of as controlling equipment from a distance. Teleoperated equipment control has the following components: remote control of the device (hardwired or radio), visual feedback of the tool and work space (human, video, or graphical), and usually some form of computer assistance (path planning and motion control). Figure 1.1 shows a typical teleoperation architecture. There are several basic elements that are used to achieve teleoperation. These elements

include (1) remote video, (2) actuator feedback control loops, (3) the human-machine interfaces, (4) machine vision, (5) graphical programming, and (6) sensory cues. The ARMM has effectively used those teleoperation elements (elements 1 to 5) to accurately seal pavement cracks in real time.

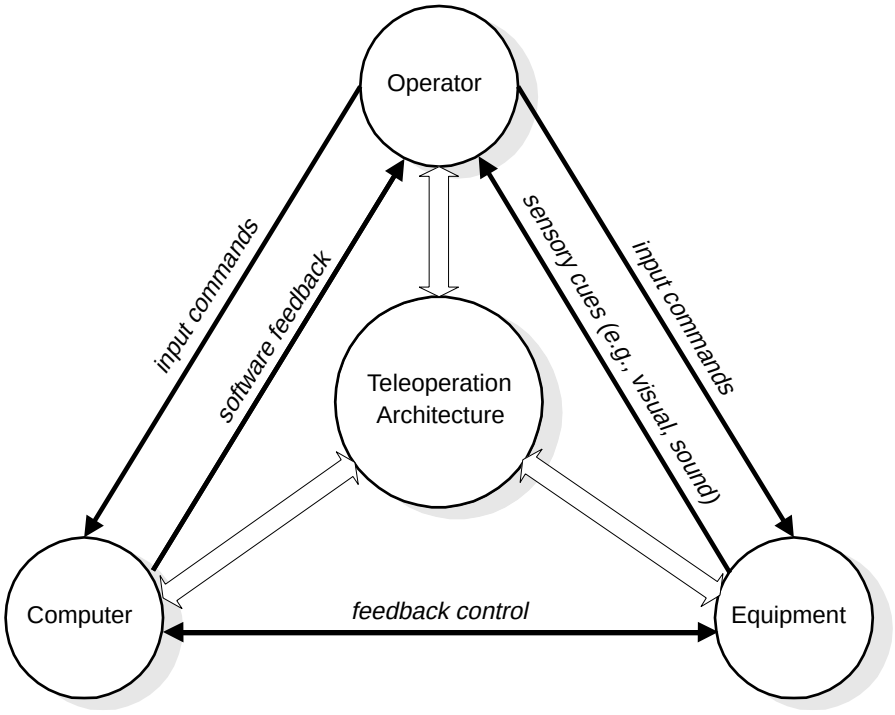

Figure 1.1. A Simplified Typical Teleoperation Architecture

1.1.2 Human Factors and Ergonomics

Complete autonomy could be achieved for automation of pavement crack sealing, but usually at a cost and speed that was unacceptable. Teleoperation alone can achieve safety benefits by removing personnel from hazardous working environments or elevated operations. Computer assistance in the form of graphical programming and machine vision can then cost effectively help to achieve improvements in productivity and quality. Successful automation in the field has used such tools to achieve a balance between complete

autonomy and manual operations (Haas 1996). Human factors and ergonomics have been an important issue in an effort to achieve such a balance.

Human factors engineering or ergonomics can be defined as the use of scientific knowledge about human behavior in specifying the design and use of a man-machine system. The aim is to improve system efficiency by minimizing human error (Adams 1989). That is, its ultimate goal is to optimize the performance, productivity, or safety of the man-machine system or work environment. This involves studying the people, tasks, and equipment involved, and designing ways for these three elements to interact in an optimal way (Helander 1981).

In any man-machine system, there are tasks that are better performed by man than by machine, and vice versa. Thus, it is very important to decide what functions of the system should be assigned to humans and what functions to machines. Usually, the decision whether a given function should be performed by machine, by the operator, or by both depends on which can perform that function more efficiently in the operational situation (Park 1989). In order to determine this, a comparison must be made between the advantages of the human and those of the machine. However, achieving an optimal balance between manual functions and automated functions in the control of an automated system is not easy, owing to the fact that (1) the complex behavior of a man-machine system is generally difficult to predict, and that (2) several experiments are required to truly determine the optimal balance (Haas 1996).

Every man-machine system, including the UT ARMM, contains certain functions that must be performed by man. Both man and machine are limited individually, but man's remarkable ability to adapt to circumstances can, when skillfully mated to the machine, create a combination having immense potential (Ganguli 1982). Even fully automated systems need human interventions in monitoring and maintaining. Indeed, the human operator is central to the ARMM operation. The system efficiency depends as much on the capabilities of the operator as on the capabilities of the machine. However, the human usually makes mistakes, and these errors can sometimes significantly degrade system performance and productivity. Consequently, ergonomics factors should be considered in every man-machine system development process to minimize human error so as to maximize system efficiency.

The preceding issues were considered and previous experience was used to decide which functions should be automated. Table 1.1 summarizes the options. Table 1.2 illustrates the balance achieved. Other ergonomics factors that affect the man-machine interface and the operator performance in the automated surface crack sealing operation are discussed in Section 1.2.1.5.

Table 1.1. A Complex Evolution for Automation of Pavement Crack Sealing

**Italicized options are currently being used in the ARMM*

SPECIFIC FUNCTIONS FOR CRACK SEALING	AUTOMATION OPTIONS	MANUAL OPTIONS
1. Image Acquisition	♦ ***Remote Video***	
2. Crack Detection and Mapping	♦ Multi-layer quadtree approach ♦ Histogram-based approach ♦ Optimal thresholding ♦ Edge detection and linking ♦ Hough transform ♦ ***Graphical programming*** ♦ Bitmap-to-graph conv.	♦ ***Manual crack detection, and mapping using a pointing device (mouse, light pen, stylus on touch sensitive monitor)***
3. Crack Representation	♦ ***Machine vision based line snapping using digital image processing and graphical programming techniques***	♦ ***Manual editing (rubberband capability)***
4. Path Planning	♦ Optimal path plan ♦ ***Greedy path plan***	♦ Implicit path plan
5. Equipment Control	♦ ***Automatic blow, seal, and squeeze in one pass***	♦ ***Move system to next crack location***

1.2 A MAN-MACHINE BALANCED CONTROL LOOP OF THE ARMM

A man-machine control loop exists when a person interacts directly with the hardware and software to drive the function of the system. Robots and humans working together as a team have strength, dexterity, speed, and quality skills exceeding those of either acting individually (Ibanez-Guzman 1994). The UT ARMM is a good example of this robot-human collaboration (Figure 1.2).

Table 1.2. An Optimal Balance Between Manual Functions and Automated Functions Achieved for Successful Automation of Crack Sealing

SPECIFIC FUNCTIONS	AUTOMATED FUNCTIONS	MANUAL FUNCTIONS
1. Image Acquisition	✓	
2. Crack Detection and Mapping	Assisted by graphical programming	✓
3. Crack Representation	✓	Assisted by manual editing (if necessary)
4. Path Planning	✓	
5. Equipment Control	✓	✓

As shown in Figure 1.2, the ARMM currently employs an open-loop architecture, since there is no direct link between the output and input in sealing cracks in the machine's work space. That is, the equipment control (manipulator and end effector control) relies wholly on (1) the path generation result, (2) good calibration, and (3) the reliable behavior of the actuator system. However, by using human vision as a vision sensor, three man-machine interface closed loops are utilized within the overall system control loop. Better understanding of this can be accomplished by examining Figure 1.2.

Through such closed man-machine interface loops, both machine and human errors caused in the man-machine control loop of the ARMM are sensed and corrected by human vision and judgment. Data are fed back into the computer to generate an optimal path. The xy-manipulator and end effector is then effectively controlled by the path generation results. In terms of quality, the unique man-machine balanced control loop used in the ARMM creates a potentially error-free environment for automated crack sealing. It is also anticipated that such a man-machine control loop can greatly improve system efficiency (productivity) by minimizing both human and machine errors, and by reducing the computational time and load required to automate crack sealing. A more detailed description of this man-machine control loop will be presented in Section 1.2.1.

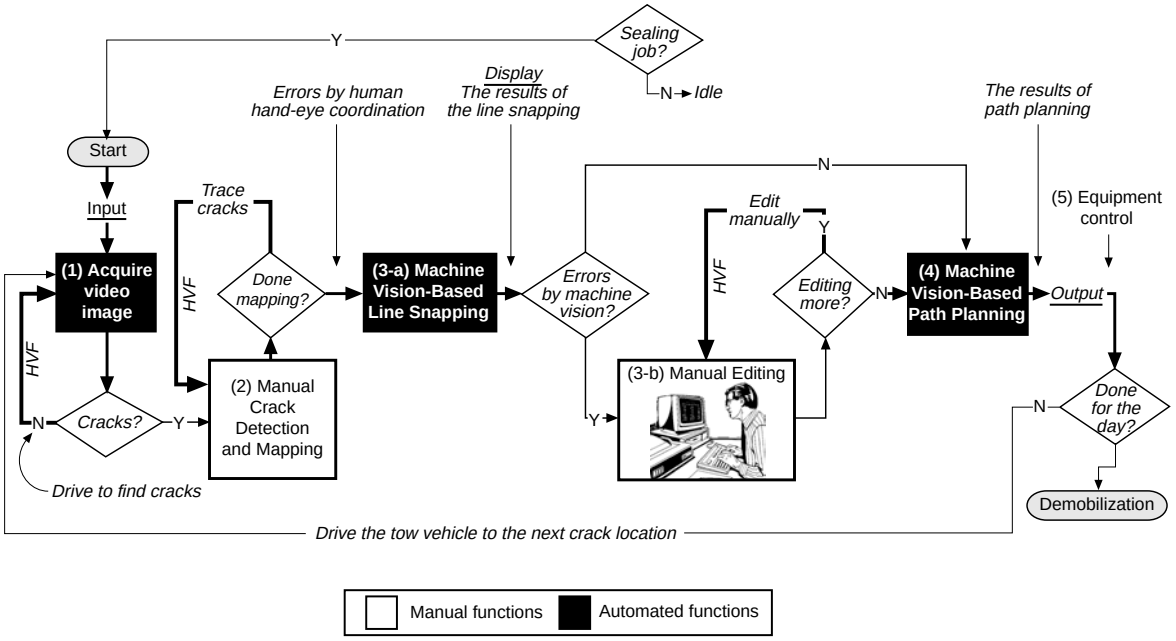

Figure 1.2. A Man-Machine Balanced Control Loop of the ARMM

1.2.1 An Optimal Man-Machine Balance Proposed in the Control Loop

This section describes in detail the man-machine balance achieved in the ARMM's control loop. Figure 1.2 graphically showed an optimal balance between human and computer for five specific functions that comprise the man-machine control loop. The value of this man-machine balance proposed in the control loop is justified through the ARMM's productivity analysis to be presented in Chapter 3.

1.2.1.1 Image Acquisition

A computer imaging system is used to view cracks to be sealed on the surface. The use of remote video cameras has been a typical method for providing visual feedback within the man-machine system. To capture and digitize video images of the cracks in the machine's work space, a commercial image processing board is installed in the PC that controls the automated crack sealing system. Two security cameras mounted on the super-structure of the

xy-manipulator provide live pavement surface images that are displayed on the PC's touch-sensitive monitor. The ARMM's man-machine interface begins at this point.

1.2.1.2 Crack Detection and Manual Mapping

To automatically seal cracks, exact crack location is the most important information required. As stated, if a new image processing algorithm is to be developed for automatically sensing and mapping cracks to be sealed in pavements, the quality of the segmentation has the highest priority for overall project purposes. Overall efficiency of the algorithm is also important for project success, if the cracks are automatically detected and mapped by a computer. However, it was concluded that detecting and mapping pavement cracks to be sealed only by computer functions may not be desirable. In their digitized form at the pixel level, cracks are highly noisy and unstructured. The low contrast between the distresses (cracks) and the background (surrounding pavement) also complicates pavement analysis. As a result, it was determined that a human should interact directly with the computer in the crack detection and mapping process of the ARMM (man-machine interaction was essential).

In general, humans are good at reacting to unforeseen circumstances and at picking signals or patterns out of a noisy background. One of the most remarkable features of human information processing is the ability to recognize patterns and relationships irrespective of the magnitude of the stimuli. Humans can recognize terrain features, photographic details, etc., against a background of visual noise (Park 1987). Thus, allowing the operator to point out the existence and location of a pavement crack can be extremely economical and beneficial (Haas 1996). With proper illumination, humans can see color, brightness (intensity level), and form (cracking type), thus easily distinguishing real cracks from such pavement background noise as sealed cracks, oil marks, or skid marks. A simple graphical program can be used to generate a computer-based model of the surface crack to be sealed and to provide visual feedback to the operator. That is, when the operator traces cracks to be sealed by a pointing device, the graphic line segments (polylines) can be displayed on the screen and their coordinates can be sampled at a certain range by the computer. The work environment of the automated crack sealing operation being fairly static, a good model can be generated by

using the graphical programming. Furthermore, by selecting only the cracked regions on a video display, the operator can reduce the search area and, hence, the time required for subsequent processing.

To point out the exact location of the cracks to be sealed on the computer screen, several pointing devices can be used, including (1) a mouse, (2) a light pen, and (3) a stylus on a touch-sensitive screen. Preliminary research has shown that using a touch-sensitive screen is the fastest and most intuitive method for most people, since it allows them to draw directly over the crack (Greer 1996).

Despite such advantages, this approach has a drawback that can significantly degrade the quality of the resultant seal. In nature, imperfections of human hand-eye coordination can cause errors even in optimal work environments. Also, the arm fatigue of the operator can increase such errors when tracing cracks on the screen. Thus, machine-vision-based line snapping or manual editing are required to compensate for human hand-eye coordination errors.

1.2.1.3 Machine-Vision-Based Line Snapping and Manual Editing

Options for compensating for the errors caused by imperfect human hand-eye coordination include (1) machine-vision-based line snapping and (2) manual editing. As stated, line snapping or manual editing is required because few human operators can match a machine's accuracy in tracing cracks. Both approaches have advantages and disadvantages.

♦ Automated Line Snapping

Machines are superb at achieving speed, accuracy, consistency, power, and optimal results within well-defined constraints. Thus, within a limited search range, the computer can correct the hand-eye coordination errors caused by human operators quickly. Errors are still possible, however, because of the noise that is inherently found in video data obtained through computer vision.

♦ **Manual Editing**

Humans are effective in processing visual information and in making decisions within well-structured environments. Humans can use judgment and be very flexible in correcting errors caused by a machine, although humans must be trained. However, humans are not fast and they generally have a reaction time lag. Thus, relying on only manual editing for correcting errors may be time consuming.

The ARMM combines both approaches to accurately map and represent all cracks to be sealed within the machine's work space. That is, once the cracks are traced, the connected line segments are automatically snapped onto the exact position of the cracks using a robust, localized crack detector (automated line snapping). Noise is compensated for by using the average pixel value for the entire crack detector box. If line segments are not properly snapped onto the exact position, they can be edited manually like an elastic band using a graphical program (manual editing). As previously mentioned, the search range of the crack detector is conveniently constrained, since the segment lines drawn by the operator are normally on or very near the crack and are almost parallel. Thus, line snapping and manual editing can greatly reduce processing time. This man-machine interface can create an error-free environment in mapping and representing cracks to be sealed in the most economical way. Preliminary results obtained from initial field trials are promising for complete and accurate adjustment of the user-drawn graphical line segments using the line snapping. Also, the initial field trials indicated that the manual editing is not required in most cases, because the amount of sealant dispensed from the end effector was sufficient to cover errors (if there were any) caused by the line snapping.

1.2.1.4 Path Planning and Manipulator and End Effector Control

The graphical line segments (crack representation) generated from the results of line snapping (or, occasionally, manual editing) is directly used for path planning of the ARMM. Humans are not as good as computers at making numerous calculations, so the computer is used in this part of the process. Currently, options for generating an optimal path of the ARMM include: (1) implicit path plan and (2) automated path plan. Compared with

conventional crack sealing operations, the ARMM demonstrates superior efficiency of movement, which is a key factor in its performance. Efficiency of movement is governed by the length of the path that the tools follow to cover the whole crack network. Other performance factors include manipulator speed and accuracy and duration of crack detection and mapping.

When cracks are mapped manually, an implicit path plan is generated by the sequence of strokes made by the operator, including their beginning and end points. Generally, the system operators drag the mouse over a crack image, with their specific movements a matter of their individualism. Thus, there can be several path generation solutions offered by each user in this approach. While automated path planning is necessary when cracks are automatically mapped, to be justified in the case of manual mapping, the time taken to compute an optimal path must be less than the time saved by executing the optimal path, on average.

Previous research (Kim 1995) compared implicit path planning with automated path planning. Twenty crack images and five operators were used for the test. Efficiency comparison between both approaches indicated the benefits of implementing automated path planning in terms of time and distance. Another disadvantage of implicit path planning is the large distribution among the path solutions generated as a result of poor training and high turnover. Thus, the advantage of computing a plan rather than relying on implicit plans generated by the human operator is clear. Finally, the automated path planning information is used for effective manipulator and end effector control. During the actual sealing process, live video updates provide visual feedback to confirm that the cracks are being sealed properly. After the crack is repaired, the video image also provides verification that the crack has been sealed.

1.2.1.5 Other Ergonomics Considerations

♦Operator Performance and Training

In the ARMM operation, an experienced and trained operator will produce better results in tracing and editing on the computer's screen cracks to be sealed. For example, the

trained system operator will edit manually only those line segments that deviate from the original crack location after the automated line snapping. The trained operator knows that the minor deviation caused by the line snapping can be compensated for by the sealant to be dispensed on the crack and by the subsequent squeegeeing operation. The experienced and trained operator can intuitively respond in determining what line segments he/she should edit manually. Thus, training can enhance system performance.

- **Cab Design of the Tow Vehicle**

Workplace design deals with surfaces that are too high or too low, uncomfortable chairs that produce aching backs, controls that cannot be easily reached, or instruments that are inappropriately placed (Leavitt 1996). Currently, the ARMM operator sits in the cab of the tow vehicle and views live video images of the pavement from the towed crack sealer. For the ARMM, the cab design of the tow vehicle is very important because it can considerably affect the overall performance of the system operator. In the final system (commercial sealing robot), the cab of the tow vehicle should be designed in an ergonomically efficient manner so as to allow the operator to be the most productive. Bodily discomfort caused by a poorly designed work environment can accelerate human fatigue as well as human error. In designing the cab of the tow vehicle, the objectives would be (1) to create user-friendly manual mapping environment (e.g., proper placement of the monitor so as to minimize human fatigue and errors), and (2) to install illumination or lighting controls inside the cab that would enhance visibility in tracing cracks (Figure 1.3). This latter subject is further described in the next section, "Illumination/Lighting."

- **Illumination/Lighting**

Inadequate lighting can cause human errors and injury. Workers who are confused by glare or shadows are more prone to committing errors (Park 1987). As the illumination level decreases, visual acuity and visibility decrease, while task time increases. Currently, the monitor for providing visual feedback to the operator is mounted on the cab of the tow vehicle. Intensive lighting can significantly degrade operator's performance (productivity) by

glaring the screen surface of the monitor. In such a case, operator visual acuity is greatly impaired, increasing the potential for error. Because glare and diffusion can impede one's ability to see easily, accurately, and quickly, they have an impact on both performance reliability and productivity. As a result, an ergonomics study should be performed to better understand how to prevent these problems, with the solutions then applied to the final system.

Figure 1.3. A Temporary Design of the Current Tow Vehicle's Cab

1.3 CHAPTER SUMMARY

An investigation undertaken over several years has resulted in a functional ARMM production prototype, one that has achieved a good balance between manual and automated functions. Many tools and algorithms were developed and experimented with to implement the prototype. This chapter mainly focused on illustrating the man-machine balanced control loop developed for the ARMM. Using the developed man-machine control loop as a framework, this chapter presented an ergonomics analysis of five specific functions that are commonly required for automation of infrastructure crack sealing. Some of the design issues and trade offs involved in balancing human and machine functions were discussed in detail in this analysis. Finally, the value and applicability of the man-machine balance achieved in the control loop will be validated through the productivity analysis of the ARMM (based on its efficiency evaluation results to be performed in the next chapter).

CHAPTER 2. TEST AND EVALUATION OF THE MAN-MACHINE CONTROL LOOP AND MACHINE VISION ALGORITHM DEVELOPED

2.1 INTRODUCTION

The ARMM's man-machine balanced control loop and the machine vision algorithm have been tested and evaluated based on (1) accuracy, (2) time, and (3) quality of the resultant seal. For the efficiency evaluation, thirty pavement crack images, which include longitudinal, transverse, and block cracking, have been collected from the UT research campus and field trials undertaken at five locations (Austin, San Antonio, Dallas, Corpus Christi, and Travis county line) in the state of Texas. All the pavement crack images collected for the efficiency evaluation are shown in Appendix A.

The image collection and categorization method, along with criteria and methodology for the efficiency evaluation, are presented in Sections 2.2.1 and 2.2.2. Figure 2.1 briefly describes a process flow for the efficiency evaluation of the man-machine loop and the algorithm. More in-depth descriptions of the efficiency evaluation processes and the experimental results are presented in Sections 2.2.2.1 to 2.2.2.3. Finally, the experimental results obtained from the efficiency evaluation are then effectively used to predict the productivity of the ARMM in Chapter 3.

2.2 OVERALL PERFORMANCE EVALUATION

2.2.1 Image Collection and Categorization

In general, pavement distress can be divided into five major categories, including (1) longitudinal cracking, (2) transverse cracking, (3) block cracking, (4) alligator cracking, and (5) joints. The ARMM was originally designed to seal all cracking types except alligator cracking. Alligator cracking consists of interconnecting cracks that form small, irregularly shaped blocks resembling an alligator's skin (Figure 2.2).

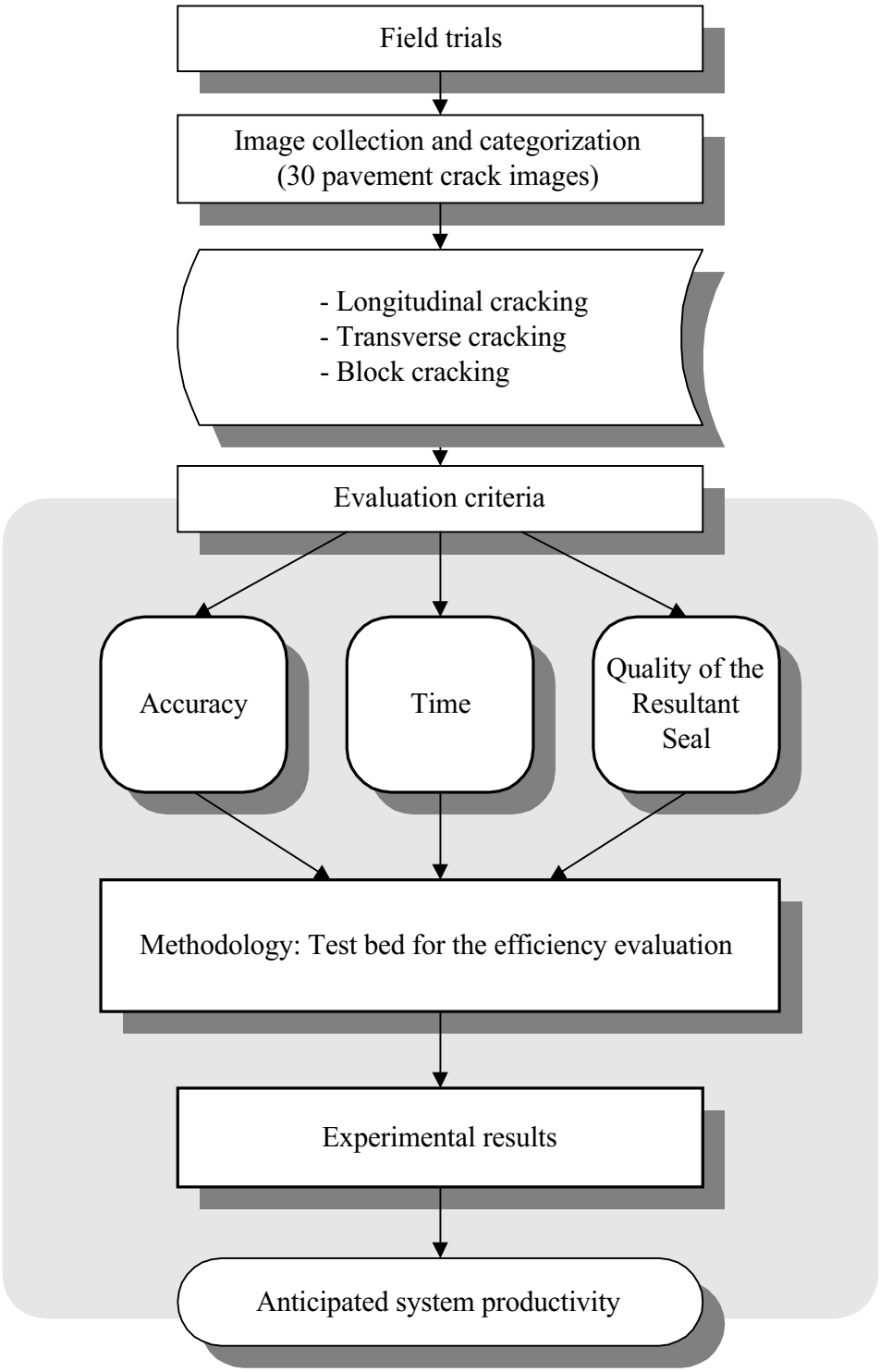

Figure 2.1. Efficiency Evaluation Process of the Man-Machine Control Loop and the Machine Vision Algorithm Developed

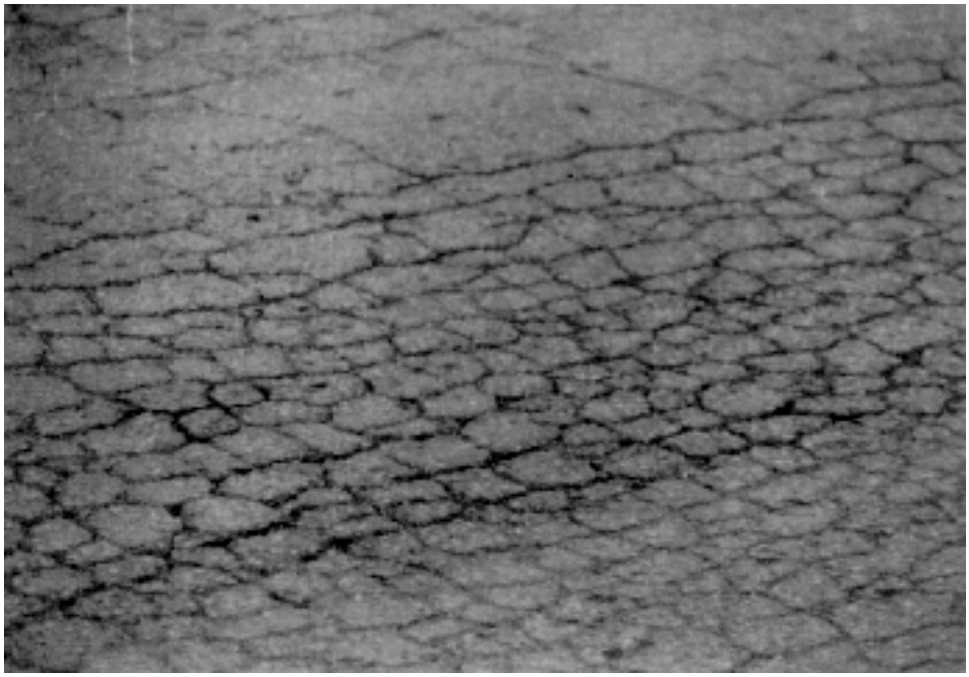

Figure 2.2. An Example of Alligator Cracking (TxDOT PMIS Rater's Manual)

Blocks formed by alligator cracks are less than 1-foot-by-1-foot (0.3-meter-by-0.3-meter) wide and usually cover a large area of the pavement section. Alligator cracking is mainly formed whenever the pavement surface is repeatedly flexed under heavy traffic loads. As a result, alligator cracking may indicate improper design or weak structural layers (*TxDOT PMIS Rater's Manual*). For these reasons, other surface crack maintenance options, such as placing patches or overlays instead of routing and sealing, are preferred in repairing alligator cracking. Thus, images of alligator cracking have not been sampled for the efficiency evaluation of the man-machine control loop and the machine vision algorithm.

Although joint sealing would be a valuable application of the ARMM man-machine control loop, images of joints have not been collected for the efficiency evaluation, since they are similar to cracks and easier to handle. Figure 2.3 shows (1) a longitudinal joint image and the result of the manual mapping over the image, and (2) its resultant seal. Thus, only three types of pavement distress — longitudinal, transverse, and block cracking — have been sampled and tested in the efficiency evaluation of the man-machine loop and algorithm

developed in this project. Sections 2.2.1.1 to 2.2.1.3 describe the characteristics of each type of cracking used in this efficiency evaluation.

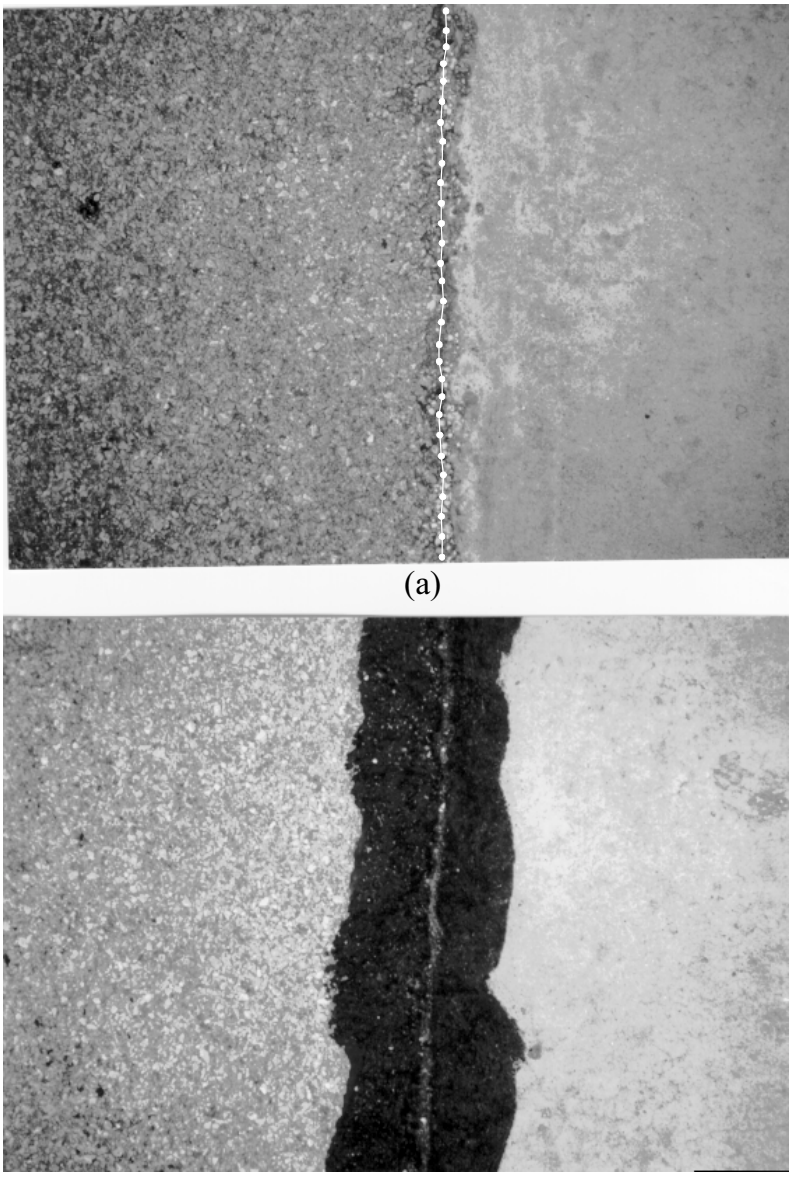

(a)

(b)

Figure 2.3. Results of the ARMM's Manual Mapping of a Longitudinal Joint (a) and its Resultant Seal (b)

2.2.1.1 Longitudinal Cracking

Longitudinal cracking can be defined as cracks or breaks that run approximately parallel to the pavement centerline (Figure 2.4). Differential movement beneath the surface is the primary cause of longitudinal cracking. Edge cracks, joint or slab cracks, and reflective cracking on composite pavement (i.e., overlaid concrete pavement) may all be regarded as instances of longitudinal cracking.

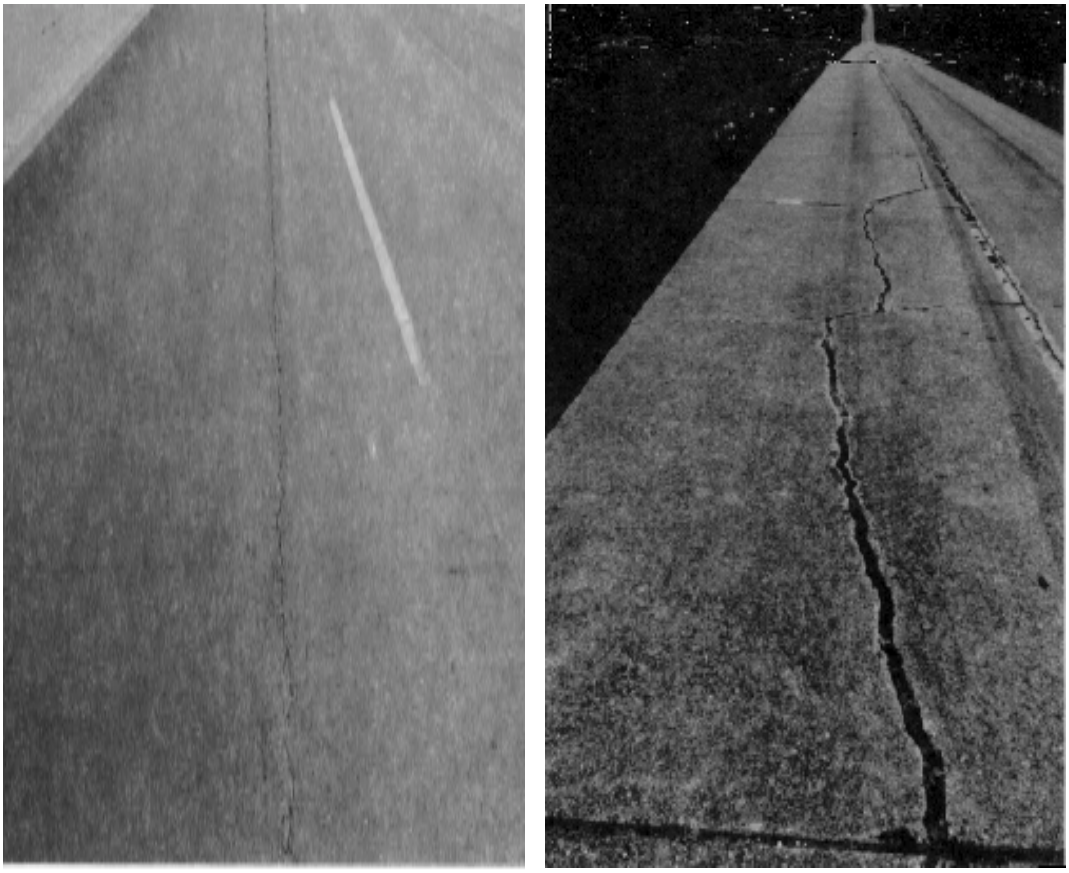

Figure 2.4. Examples of Longitudinal Cracks (TxDOT PMIS Rater's Manual)

2.2.1.2 Transverse Cracking

Transverse cracking can be defined as cracks or breaks that travel at right angles to the pavement centerline (Figure 2.5). Transverse cracks are usually caused by differential movement beneath the pavement surface. They may also be caused by surface shrinkage because of extreme temperature variations. Joint cracks may also be regarded as instances of transverse cracking.

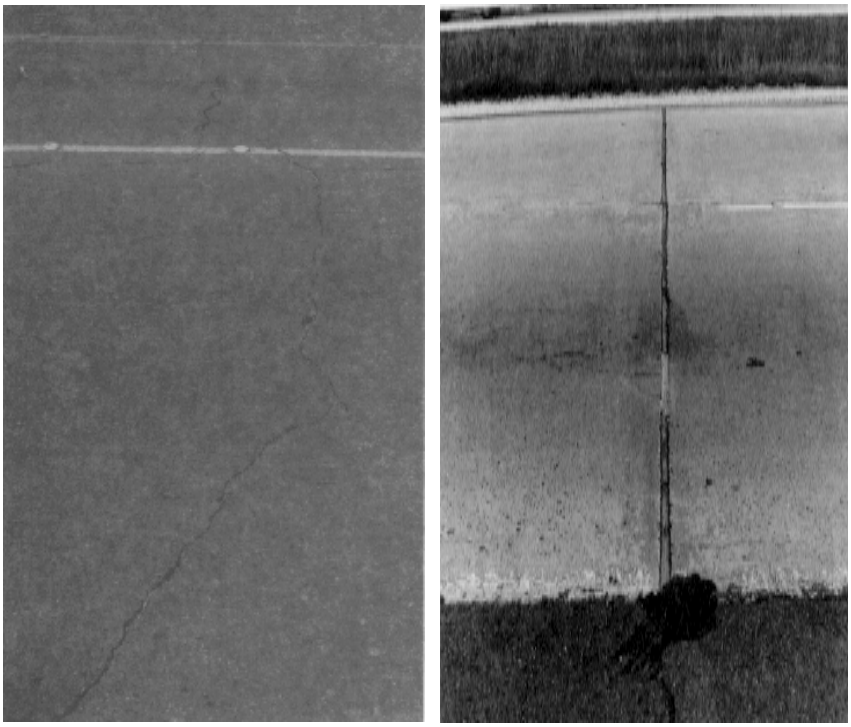

Figure 2.5. Examples of Transverse Cracking and a Joint
(TxDOT PMIS Rater's Manual)

2.2.1.3 Block Cracking

Block cracks are interconnecting cracks that divide the pavement surface into approximately rectangular pieces varying in size from 1-foot-by-1-foot (0.3-meter-by-0.3-meter) wide up to 10-feet-by-10-feet (3-meters-by-3-meters) wide (Figure 2.6). Although

similar in appearance to alligator cracking, block cracking is much larger. It is a distress caused not by loading, but by shrinkage of the asphalt concrete or of the cement or lime-stabilized base.

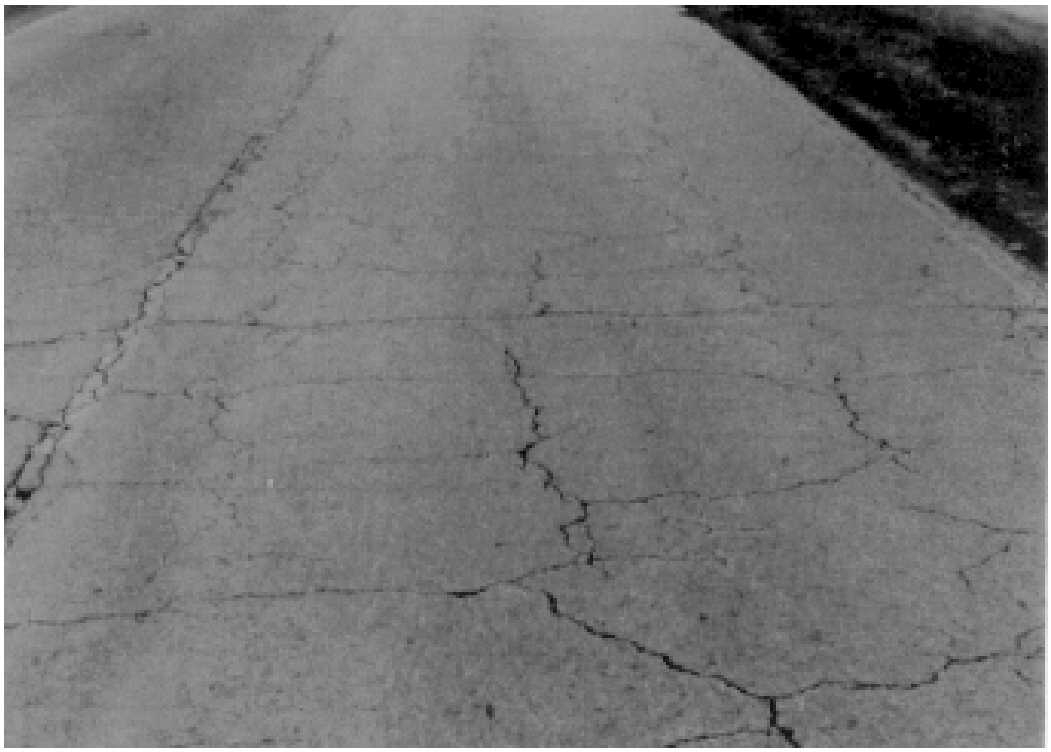

Figure 2.6. An Example of Block Cracking (TxDOT PMIS Rater's Manual)

2.2.2 Evaluation Criteria and Methodology and the Experimental Results

This section describes the methodology developed for the efficiency evaluation of the man-machine control loop and the machine vision algorithm. Criteria established for the efficiency evaluation include: (1) accuracy, (2) time, and (3) quality of the resultant seal.

In terms of the accuracy of crack identification, mapping, and representation, the current man-machine control loop, including the machine vision algorithm, promises 100 percent accuracy, if a good calibration of the work space is achieved. Recent field trials of the

full-scale crack sealer appear to support this conclusion. Highly accurate, automated crack sealing is now possible by using this unique man-machine control loop.

In conventional crack sealing operations, the quality of the seal may be inferior to the quality achieved by an automated crack sealer (compare Figures 2.19 and 2.20). For instance, worker fatigue, inattention, skill variance, and adverse weather conditions (i.e., extremes of temperature, wind, and debris) can significantly lower both the quality of the seal and the overall productivity of the crew. If there are no productivity concerns in crack sealing operations, the quality of the resultant seal achieved by the automated method should equal or exceed that achieved by the conventional method. Such quality is due to the fact that (1) the system operator tracing and adjusting the crack network shown on the computer screen has the time sufficient to guarantee very accurate crack sealing, and (2) automated crack sealing can be accomplished under various field conditions. However, enhancing the operating speed of the automated crack sealing system was the most significant and critical factor to overall project success. Thus, both the quality *and* productivity of the ARMM have been major concerns in this project.

Typically, the quality and productivity of the ARMM would depend heavily on the results of the crack detection, mapping, representation, and path planning obtained by the man-machine control loop. This section first discusses the advantages and disadvantages, revealed in laboratory tests and field trials, for each control step employed for crack detection, mapping, and representation in the man-machine loop. These control steps include (1) manual mapping, (2) line snapping, and (3) manual editing. Using these results, the next section examines and compares two control options (Figure 2.7) that have been highly recommended for use in the final system. It first evaluates and compares the manual mapping and line snapping functions included in the two control options in terms of accuracy and time. These comparison issues have become important in so far as recent field trials have shown that a sufficient amount of sealant is dispensed from the end effector to compensate for trivial errors made during manual mapping or line snapping. For these comparisons, a survey was conducted and a simple rule was established. System productivity and the quality of the resultant seal are the primary concerns in comparing the two options. From these

comparisons, the more feasible control Option In terms of providing the best quality and productivity for automated crack sealing will be selected for use in the final system. A more detailed description of the survey procedure and the rule are provided in the next section. The computational efficiency of the path planning algorithm, along with the quality of the resultant seal, is also evaluated and shown in Section 2.2.2.3.

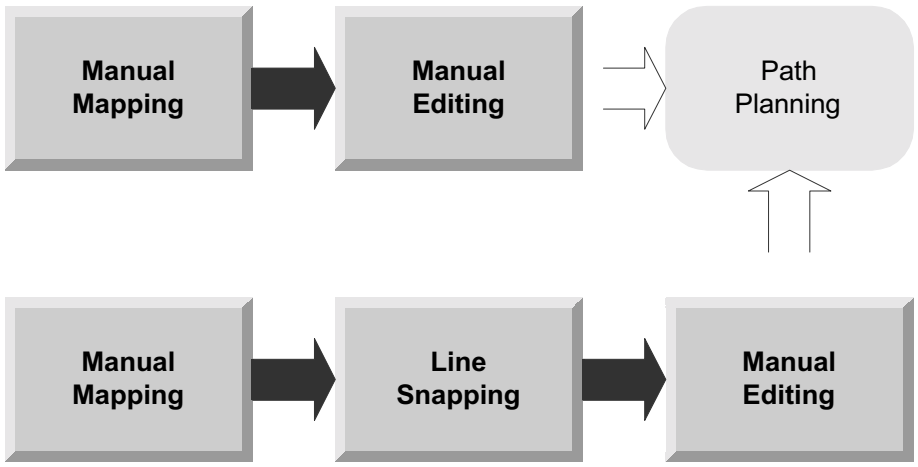

Figure 2.7. Two Control Options Recommended for the Final System

Advantages and Disadvantages of Manual Mapping, Line Snapping, and Manual Editing Revealed in Laboratory Tests and Field Trials

- **Manual Mapping**

Advantages

1. If the results of manual mapping can be directly used as input data for the path planning for manipulator and end effector control, manual mapping (Option I) would be the fastest method for automated crack sealing.

2. In the case of longitudinal or transverse joints that are typically straight, a trained operator can usually trace the joints fairly well. Thus, line snapping and manual editing may not be essential for joint sealing.
3. There is a sufficient amount of sealant dispensed from the end effector to correct for trivial errors occurring during manual mapping.

Disadvantages

1. In the case of block cracking (i.e., loop type), tracing errors generated by the system operator as a result of imperfect hand-eye coordination significantly increase according to the degree of crack network curve and complexity. Even if sufficient time is allowed for crack tracing, it is difficult to accurately trace such a crack network. Errors in manual mapping are often very significant in the case of block cracking.
2. Depending only on manual mapping would increase human fatigue, given that the system operator would have to concentrate on accurately tracing the cracks in order to avoid errors.
3. If line snapping and/or manual editing are not used in the ARMM, there will be no way that the system operator can correct errors occurring during manual mapping. Thus, the entire crack network would have to be retraced, which is very time consuming. The errors introduced by manual mapping could be large enough to degrade the quality of the resultant seal, even with a sufficient amount of sealant being dispensed onto the crack position to account for minor errors.

♦ **Line Snapping**

Advantages

1. The biggest advantage of line snapping is that the system operator can trace the crack network faster and easier than would be possible with manual mapping alone, because the line snapping will move the user-drawn lines onto the exact crack locations to be sealed. That is, faster and easier crack tracing (Figure 2.8) in

manual mapping is highly possible, if line snapping is to be used in the final system (Option II).

2. Through laboratory tests and field trials, line snapping has been shown to be very accurate in adjusting manual mapping errors in most cases. Also, it is anticipated that line snapping will work with any type of cracking.
3. The line snapping algorithm is highly flexible in extracting an object of interest from the background image. In the algorithm, the best box is the box having the lowest average pixel value (i.e., the darkest box). Because of this feature, the line snapping algorithm works properly even in shadows.
4. The amount of sealant dispensed from the end effector will be sufficient to correct for trivial errors created by the line snapping algorithm.

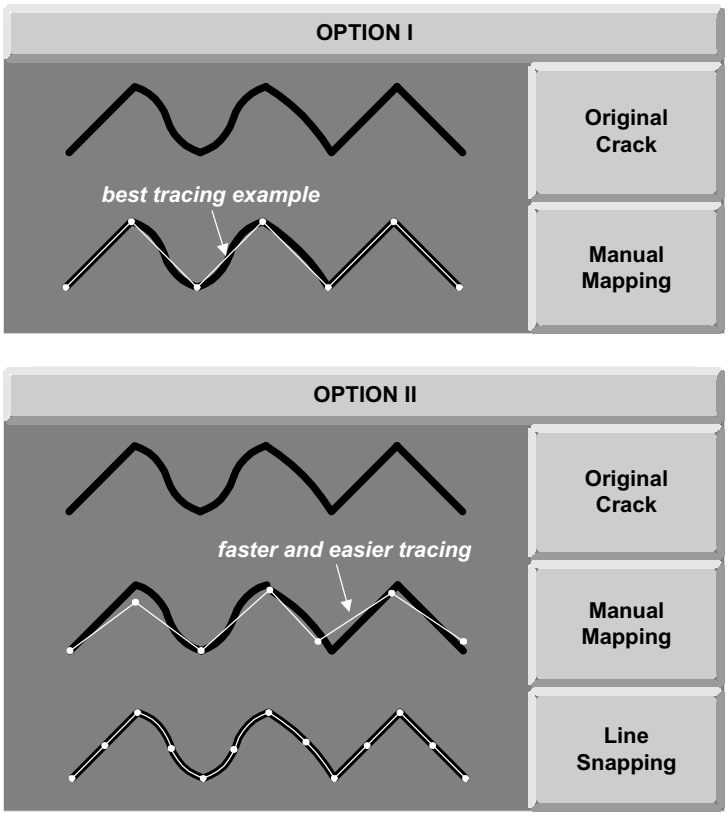

Figure 2.8. An Example of Faster and Easier Crack Tracing Considering Line Snapping

Disadvantages

1. If there is a wide range of pixel intensities in the background that overlap the range of intensities in the crack region, the line snapping algorithm may be misled.
2. Inherent noise that is often found in pavement images may also cause an error.

♦ **Manual Editing**

Using manual editing, which employs rubberband line segments, the system operator can completely correct any errors created by manual mapping and line snapping. That is, it guarantees 100 percent accuracy. However, the biggest problem of manual editing is that it usually requires an excessive adjusting time. Also, manual editing is a very repetitive process that increases human fatigue. As a result, it is recommended that manual editing be used only to correct the extremely deviated line segments occurring after either manual mapping or line snapping. Following this recommendation can maximize the quality and productivity of the ARMM.

This section has described the advantages and disadvantages of each of the control steps (manual mapping, line snapping, and manual editing) currently being used for crack detection, mapping, and representation in the man-machine control loop developed for the ARMM. In terms of quality and productivity, options I and II shown in Figure 2.7 are the best candidates for the control of the ARMM. As shown in Figure 2.7, manual mapping and line snapping are central functions in the efficiency comparisons described in this report. The manual editing function was also included in either control option for the efficiency comparison, since both options would eventually require manual editing to eliminate any large errors caused by imperfect hand-eye coordination or by line snapping. That is, the manual editing function was considered in the comparison process because it would be used as an optional function in the final system. Thus, the time required for manual editing in both options are also measured and presented in this report. Sections 2.2.2.1 through 2.2.2.3 will describe in detail a survey procedure devised to evaluate and compare the overall efficiencies

of the two control options. Finally, Section 2.2.2.4 summarizes the research findings revealed in the efficiency evaluation conducted in this project.

2.2.2.1 Time and Accuracy Comparison between Manual Mapping and Line Snapping

In the case of Option II, the computer automatically conducts line snapping after manual mapping. Poorly traced line segments are thus aligned exactly onto the crack to be sealed. If there are errors introduced by severe noise, an occasional manual editing function can be used to eliminate these errors. For Option I, crack representation depends only on manual mapping. There is no way to easily measure the degree of hand-eye coordination errors occurring. Furthermore, the degree of such errors will vary with (1) the tracing skills of each different system operator, and (2) the complexity of the crack network to be traced. Even when the same operator traces the same crack image multiple times, the result of the manual mapping will differ with each tracing. As described in Section 2.2.2, the errors caused by manual mapping are often very significant. Currently, one pixel on the computer screen represents about 3.7 millimeters. Thus, significant hand-eye coordination errors can compromise the quality of the resultant seal when using Option I (Figure 2.9).

Sections of poorly sealed pavement usually crack again after a certain period of time. Accordingly, reducing future maintenance demands can improve surface performance. Manual mapping will thus require manual editing if the line snapping function is not used in the final system. However, directly using manual editing after manual mapping without executing the line snapping function may be a very time- consuming process, owing to the fact that there are often several line segments that require editing (if the system operator does not accurately trace a given crack network). A more frequent manual editing will be usually required in the case of Option I. This excessive adjusting time greatly degrades system productivity. As a result, it is anticipated that using only manual mapping for crack representation (i.e., Option I) would not be feasible in terms of the best quality and productivity of the ARMM.

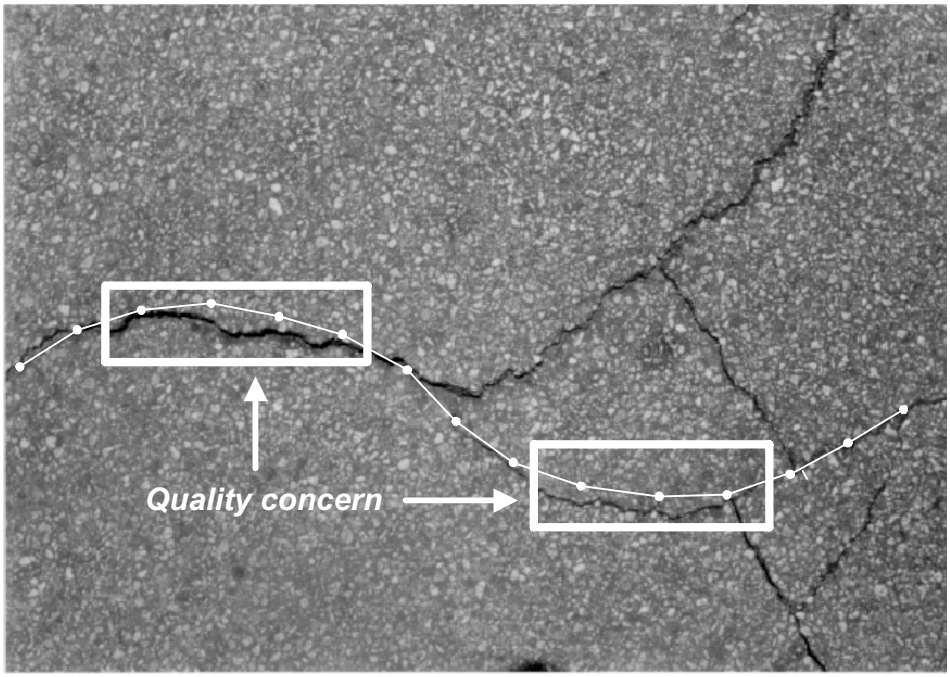

Figure 2.9. An Example of Poorly Traced Manual Mapping

To verify the prevalence of Option II, this section first evaluates and compares the efficiencies of the two options in terms of time and accuracy.

As previously mentioned, a survey was conducted to evaluate and compare the time and accuracy of the manual mapping and line snapping functions used in the options I and II. For this survey, thirty pavement crack images collected from the J. J. Pickle Research Campus and from field trials were prepared and displayed to each participant to allow him/her to trace and snap the crack network using the touch sensitive monitor (Figure 2.10). Since trained operators will be used to control the system, the survey participants consisted of three members of the automated crack sealer project team who understood the project objectives and the survey procedures. The evaluation methodology for the time and accuracy comparison and the survey procedure are described in detail in this section. This section also presents the experimental results obtained in the survey.

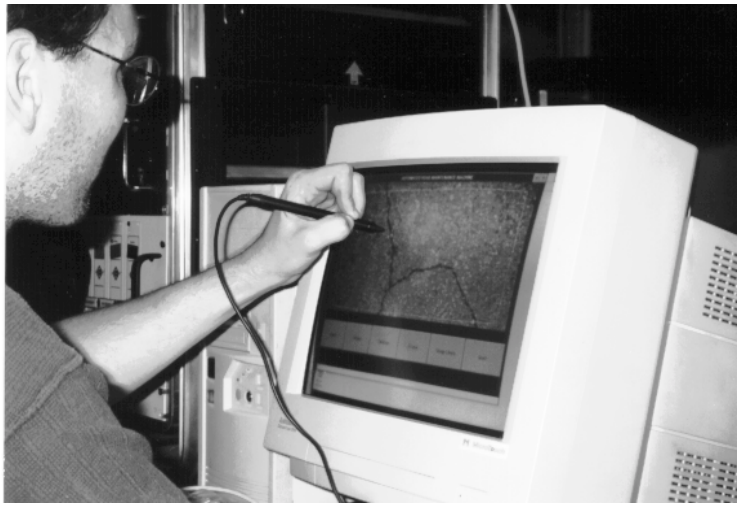

Figure 2.10. Executing Survey Procedure

♦ **A Methodology for Time and Accuracy Comparison**

Time

As mentioned previously, there are time variances between Option I, which depends on crack representation based solely on the tracing skill of the system operator, and Option II, which depends on manual mapping combined with line snapping. First, to justify the necessity of the line snapping function in the man-machine control loop to be used in the final system, the time taken to compute the line snapping function must be on average less than the time (time difference between manual mappings in options I and II) saved by performing the manual mapping where there will be subsequent line snapping. Second, to justify the overall prevalence of Option II, the total processing time of Option II must also be less than that of Option I. In practice, the time taken for manual editing is divided into the following two categories: (1) system operator's judgment time, and (2) actual line editing time. However, in estimating the manual editing time in both options, this report measures only total time taken for both processes (judgment and editing). This decision is based on the fact that (1) it is hard to accurately quantify and average system operator's judgment time, and (2) the judgment time would vary with each system operator and with the results of the

manual mapping or line snapping. The overall time comparisons for options I and II are illustrated in Figure 2.11. In the survey, each participant traced a given pavement crack image three times in an effort to obtain an average time for manual mapping and manual editing used in both options, and for the line snapping in Option II.

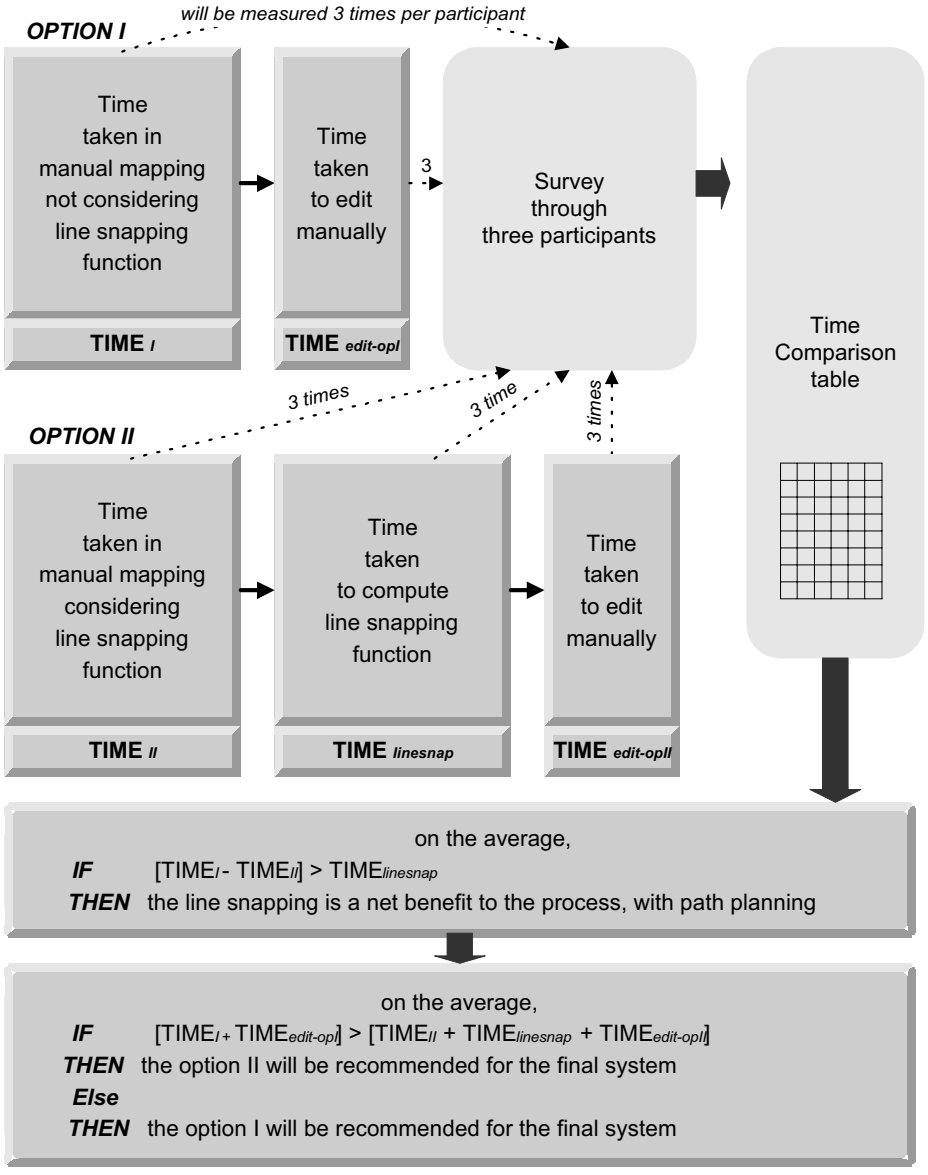

Figure 2.11. Overall Time Comparison Process for Options I and II

Accuracy

A simple rule has been established to effectively evaluate and compare the accuracy of the two options. The quality of the resultant seal was the primary concern in establishing the rule. As long as the crack network to be sealed is thin, shallow, and relatively well traced, the ARMM will dispense the amount of sealant sufficient to cover trivial manual mapping or line snapping errors. Accordingly, the line snapping function (or manual editing) may not be essential, because the errors are compensated for by the amount of the sealant. However, if the crack network to be sealed is wide, deep, or poorly traced, the amount of sealant may not be sufficient to correct for manual mapping errors. In such cases, the quality of the resultant seal will degrade. This situation is illustrated in Figure 2.12.

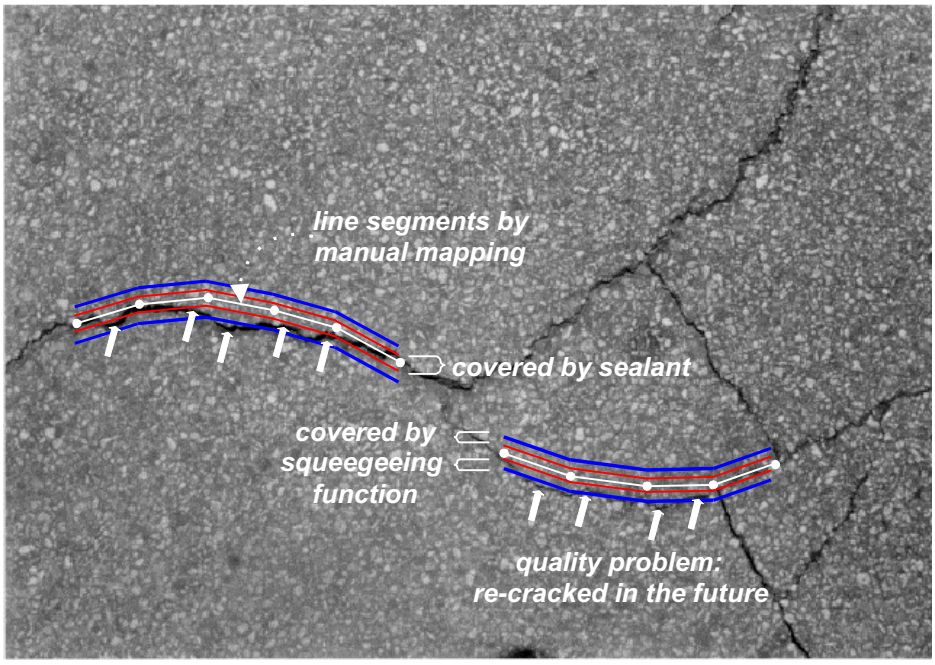

Figure 2.12. Quality Concern in the Poorly Traced Manual Mapping

As mentioned in Section 2.2.2, high quality crack sealing can minimize future maintenance demands by ensuring improved surface performance. High quality crack sealing requires accurate crack tracing and representation. Accordingly, we established a rule for

comparing the accuracies of both options. This rule is shown in Figure 2.13. For the accuracy evaluation rule, node points that connect each line segment in a crack network have been used as a primitive. It is anticipated that sealing cracks based on this rule would guarantee the best sealing quality in all cases, since it could be applied to any type of cracking irrespective of the width and depth of the crack network to be sealed.

- ***IF*** *a node point in manual mapping or line snapping exists inside or on the boundary of the crack*
- ***THEN*** *accept the node point as an accurate point for sealing*

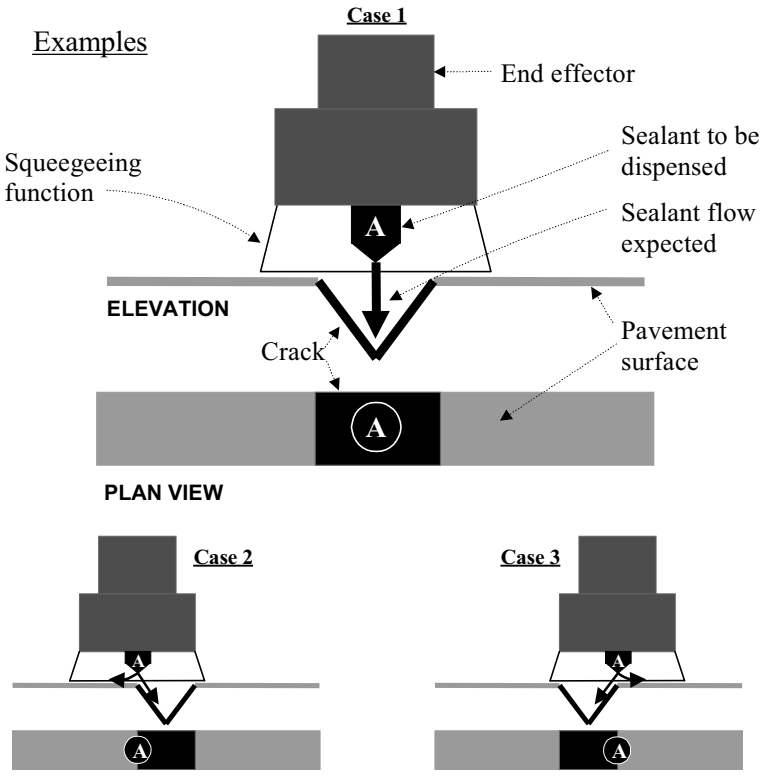

(a) Node Points to be Accepted for Sealing

- ***ELSE*** *a node point in manual mapping or line snapping exists outside of the boundary of the crack edge*
- ***THEN*** *deny the node point and do line snapping or manual editing*

Examples

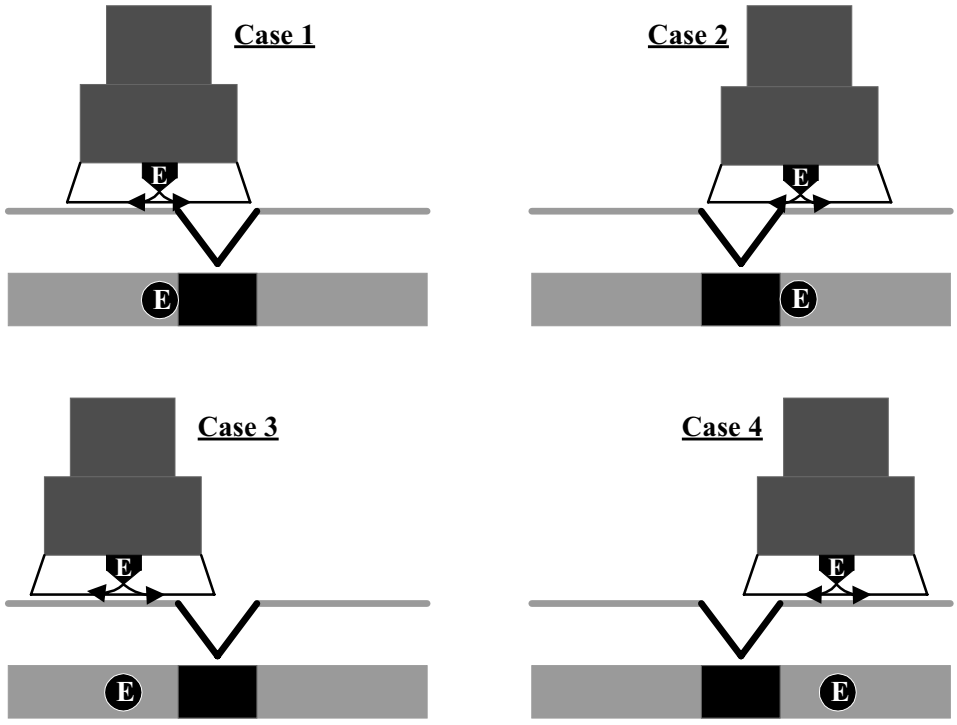

(b) Node Points to be Counted as Errors

Figure 2.13. Illustration of the Rule Established for the Accuracy Comparison of the Two Options

In an effort to evaluate the accuracy of manual mapping and line snapping in the two control options to be examined, this section first calculates the accuracy of (1) manual mapping in Option I, (2) manual mapping in Option II, and (3) line snapping in Option II. The accuracy of the developed line snapping algorithm is derived from this comparison process. Based on these results, the accuracies of options I and II are directly compared; an increment of the accuracy of the manual mapping in Option II resulting from the subsequent line snapping function can also be identified. Figure 2.14 briefly illustrates this situation.

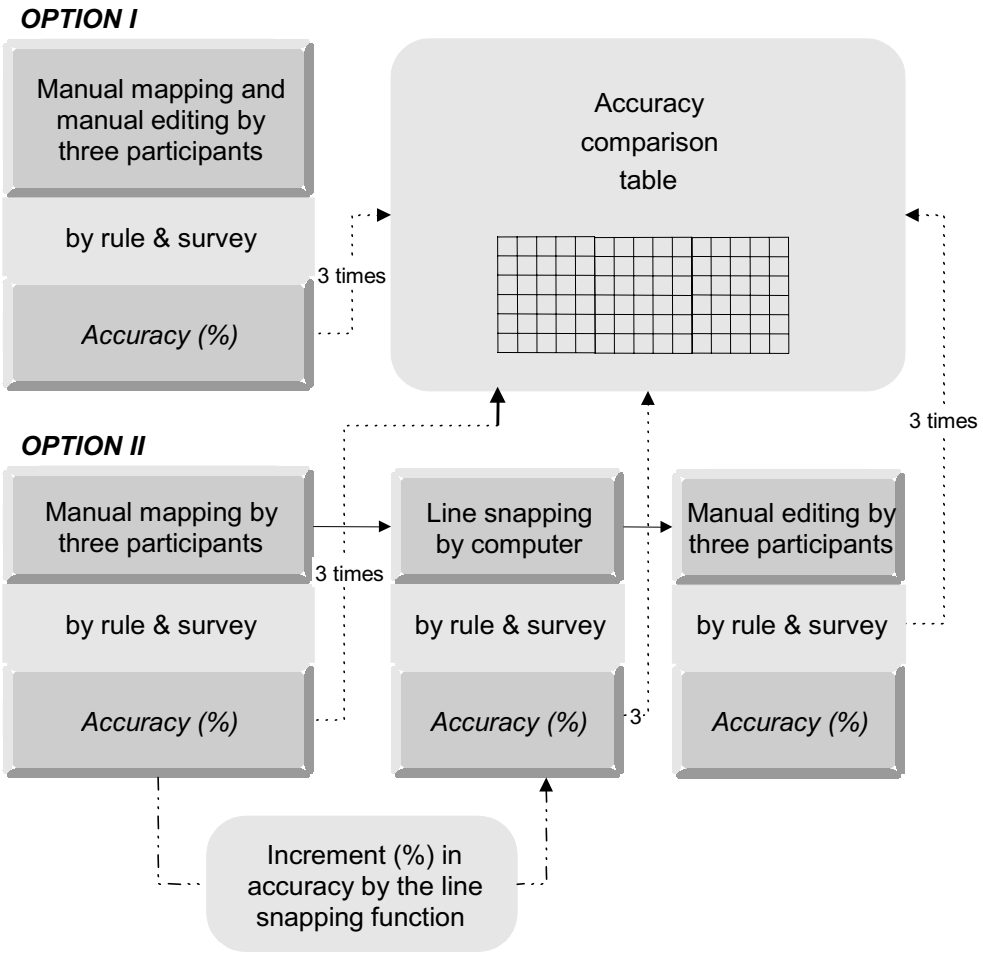

Figure 2.14. Accuracy Comparison of Options I and II

Using the results of the time and accuracy comparisons for the two options, we will then identify the more feasible control option for the ARMM.

2.2.2.2 Survey Procedure for Time and Accuracy Comparison and Results

Using (1) three project members who are familiar with the current push-button graphical user interface (Appendix C), (2) thirty pavement crack images, and (3) the established accuracy rule, a survey was conducted to evaluate and compare the time and accuracy of the manual mapping, line snapping, and manual editing functions used in the two options. To precisely monitor times required for manual mapping, line snapping, and manual editing (as well as for subsequent path planning in a given image), simple functions capable of tracking times have been added to the current vision software. (Using the computer to record these times is much more accurate than using hand timers.) The survey procedure is described in the next section, while the overall process flow of the survey is shown in Figure 2.15. Finally, summaries of the experimental results are shown in Tables 2.1 and 2.2, and in Figures 2.16 through 2.18. The complete set of experimental results can be found in Appendix B.

- **Survey Procedure**

Option I:

Step 1: *Trace a crack image to measure the time and accuracy of manual mapping in Option I. Tracing as accurately as possible is required, since the line snapping function is not to be used in Option I.*

Step 2: *The computer function:*

- *Record and store the time (seconds) taken to manually map the crack network.*

The visual inspection of each participant using the established rule:

- *Edit manually, if there are any node points violating the rule.*
- *Record and store the time (seconds) taken to manually edit the crack network.*
- *Count the total number of node points generated by manual mapping in the crack image.*

- *Count the total number of the node points that were manually edited (errors) in the crack image.*
- *Observe the accuracy (%) of the manual mapping in the crack image.*

Step 3: *Repeat the above processes until the three participants have traced the thirty pavement crack images, three times each.*

Step 4: *Get average times (seconds) of the manual mapping and manual editing for the thirty images traced three times by the three participants.*

Step 5: *Get average accuracy (%) of the manual mapping for the thirty images traced three times by the three participants.*

Option II:

Step 1: *Trace a crack image to measure the time and accuracy of the manual mapping in Option II. Tracing should be easier and faster than that of Option I, since the line snapping function is to be used in Option II.*

Step 2: *The computer function:*

- *Record and store the time (seconds) taken to manually map the crack network.*

The visual inspection of each participant using the established rule:

- *Count the total number of node points generated by the manual mapping in the crack image.*
- *Count the total number of errors caused by manual mapping in the crack image.*
- *Observe the accuracy (%) of the manual mapping in the crack image.*

Step 3: *Click on the "line snap" push-button to measure the computational time and accuracy of the line snapping function for each crack image.*

Step 4: *The computer function:*

- *Record and store the time (seconds) taken to complete the line snapping in the crack image.*

The visual inspection of each participant using the established rule:

- *Edit manually if there are any node points violating the rule.*
- *Record and store the time (seconds) taken to manually edit the crack network.*
- *Count the total number of node points generated by the line snapping in the crack image.*

- *Count the total number of the node points that were manually edited (errors) in the crack image.*
- *Get the accuracy (%) of the line snapping in the crack image.*

Step 5: *Repeat the above processes until the three participants have traced the thirty pavement crack images, three times each.*

Step 6: ***Get average times (seconds) of the manual mapping, line snapping, and manual editing for the thirty images traced three times by the three participants.***

Step 7: *Get average accuracies (%) of the manual mapping and line snapping for the thirty images traced three times by the three participants.*

Step 8: *Finally, compare the time and accuracy of the two options as described in Figure 2.15.*

- **Time and Accuracy Comparison Results of Options I and II**

Table 2.1. Time and Accuracy Evaluation Results by Three Participants in Option I

Option / Participant & Trial		Option I		
		Manual mapping		Manual editing
		Avg. accuracy per image in each trial (%)	Avg. time per image in each trial (second)	Avg. time per image in each trial (second)
Participant 1	1st	88	20	29
	2nd	88	20	28
	3rd	88	18	27
Average		88	19	28

(a) Result by Participant 1

Option / Participant & Trial		Option I		
		Manual mapping		Manual editing
		Avg. accuracy per image in each trial (%)	Avg. time per image in each trial (second)	Avg. time per image in each trial (second)
Participant 2	1st	82	25	36
	2nd	85	30	35
	3rd	81	27	38
Average		83	27	36

(b) Result by Participant 2

Option / Participant & Trial		Option I		
		Manual mapping		Manual editing
		Avg. accuracy per image in each trial (%)	Avg. time per image in each trial (second)	Avg. time per image in each trial (second)
Participant 3	1st	86	25	20
	2nd	86	23	19
	3rd	86	23	18
Average		86	24	19

(c) Result by Participant 3

Option / Participant		Option I		
		Manual mapping		Manual editing
		Avg. accuracy per image in each trial (%)	Avg. time per image in each trial (second)	Avg. time per image in each trial (second)
Participant	1	88	19	28
Participant	2	83	27	36
Participant	3	86	24	19
Average		86	23	28

(d) Summary of the Experimental Results in Option I

Table 2.2. Time and Accuracy Evaluation Results by three Participants in Option II

*acc.: accuracy

Option / Participant & Trial		Option II				
		Manual mapping		Line snapping		Manual edit
		Avg. acc. per image in each trial (%)	Avg. time per image in each trial (second)	Avg. acc. per image in each trial (%)	Avg. time per image in each trial (second)	Avg. time per image in each trial (second)
Participant 1	1st	72	7	99	1	7
	2nd	78	7	98	1	7
	3rd	77	7	99	1	6
Average		76	7	99	1	7

(a) Result by Participant 1

Option / Participant & Trial		Option II				
		Manual mapping		Line snapping		Manual edit
		Avg. acc. per image in each trial (%)	Avg. time per image in each trial (second)	Avg. acc. per image in each trial (%)	Avg. time per image in each trial (second)	Avg. time per image in each trial (second)
Participant 2	1st	58	8	98	1	7.00
	2nd	60	8	99	1	5
	3rd	58	8	99	1	5
Average		59	8	99	1	6

(b) Result by Participant 2

Option / Participant & Trial		Option II				
		Manual mapping		Line snapping		Manual edit
		Avg. acc. per image in each trial (%)	Avg. time per image in each trial (second)	Avg. acc. per image in each trial (%)	Avg. time per image in each trial (second)	Avg. time per image in each trial (second)
Participant 3	1st	65	8	99	1	6
	2nd	68	7	99	1	5
	3rd	69	7	99	1	5
Average		67	7	99	1	5

(c) Result by Participant 3

Option / Participant	Option II				
	Manual mapping		Line snapping		Manual editing
	Avg. acc. per image in each trial (%)	Avg. time per image in each trial (second)	Avg. acc. per image in each trial (%)	Avg. time per image in each trial (second)	Avg. time per image in each trial (second)
Participant 1	76	7	99	1	7
Participant 2	59	8	99	1	6
Participant 3	67	7	99	1	5
Average	67	7	99	1	6

(d) Summary of the Experimental Results in Option II

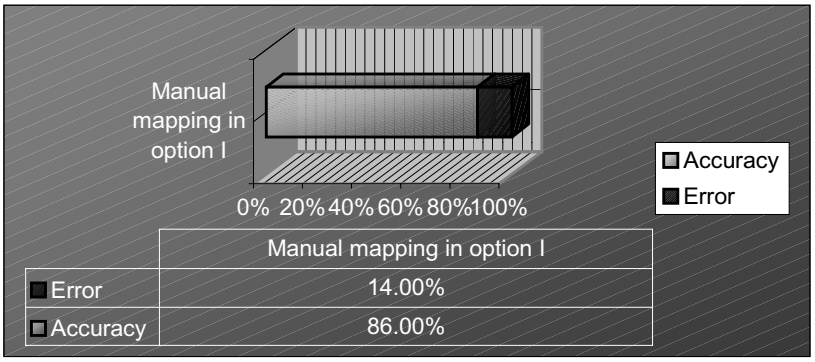

(a) Average Accuracy of Manual Mapping in Option I

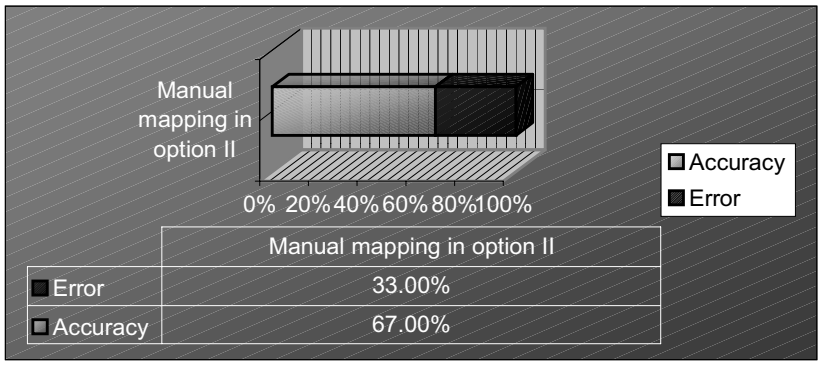

(b) Average Accuracy of Manual Mapping in Option II

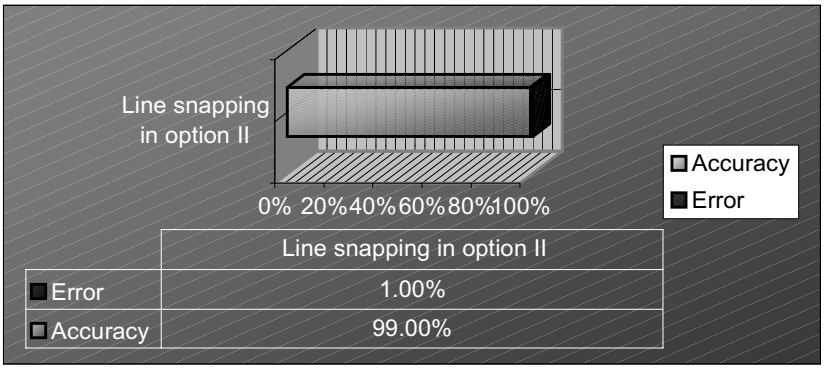

(c) Average Accuracy of Line Snapping in Option II

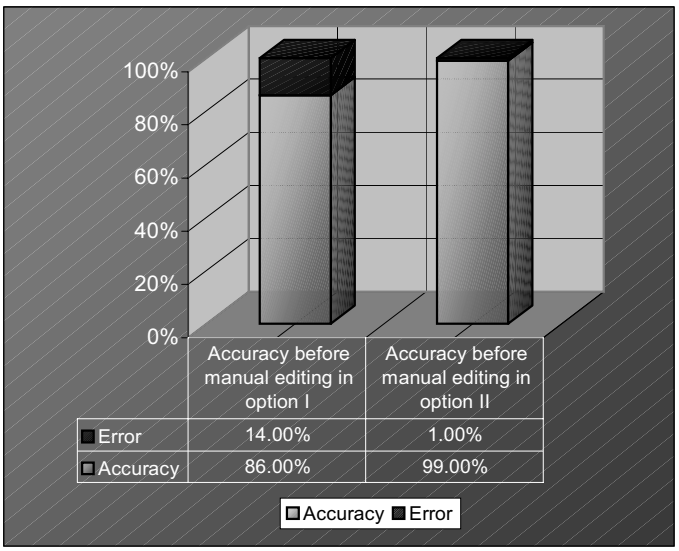

(d) Crack Representation Results before Manual Editing in Options I and II

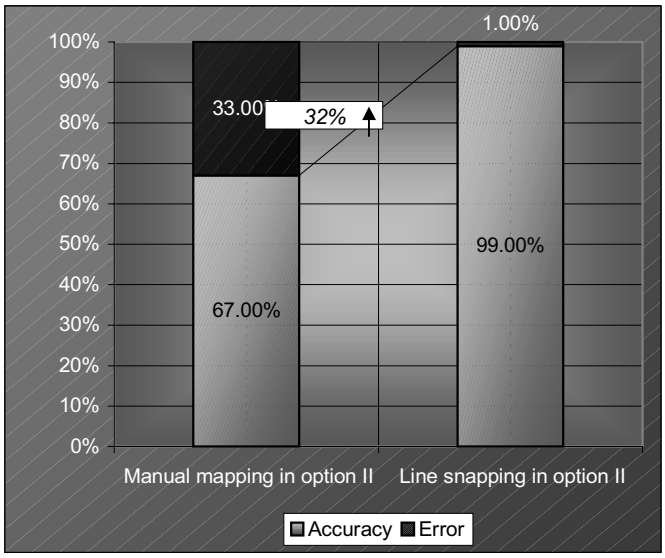

(e) Accuracy Increment Resulting from Line Snapping in Option II

Figure 2.16. Average Accuracy Comparison per Image of Options I and II

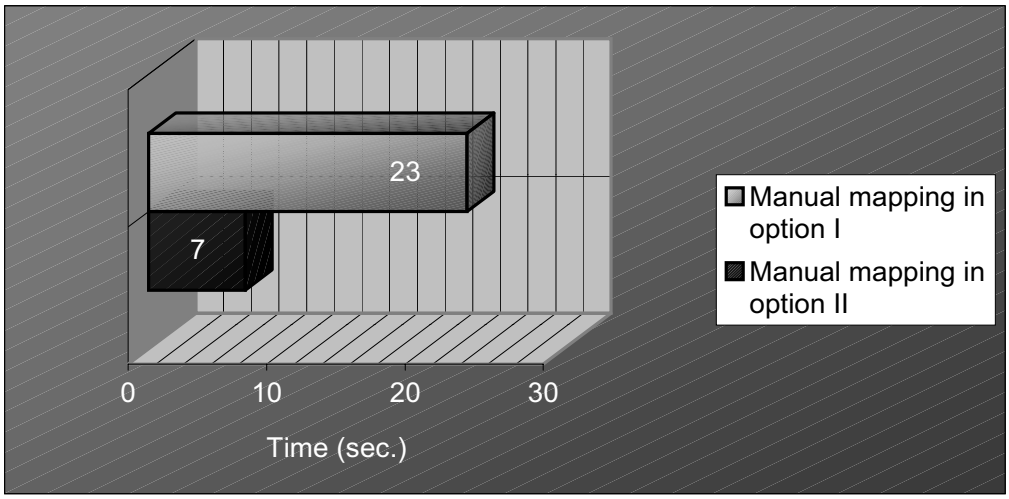

(a) Manual Mapping Time Comparison of Options I and II

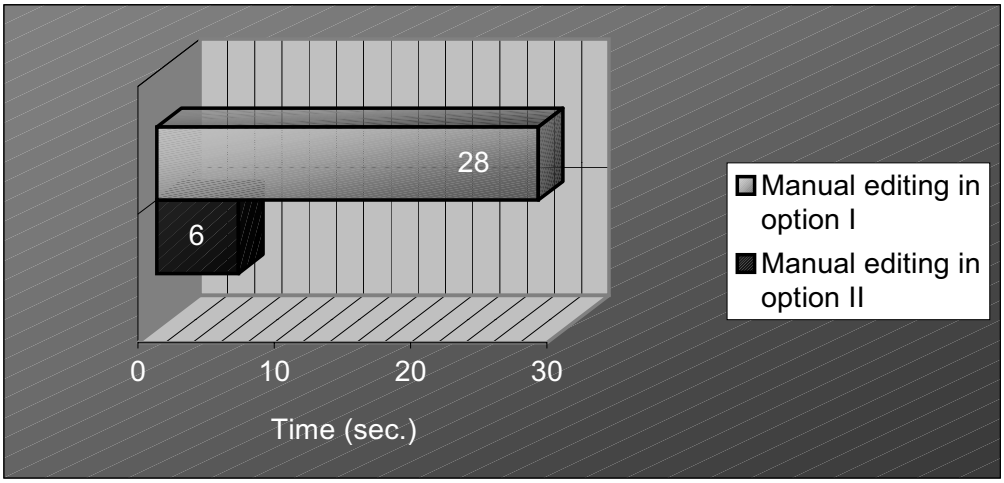

(b) Manual Editing Time Comparison of Options I and II

Figure 2.17. Average Time Comparison per Image of Common Control Elements in Options I and II

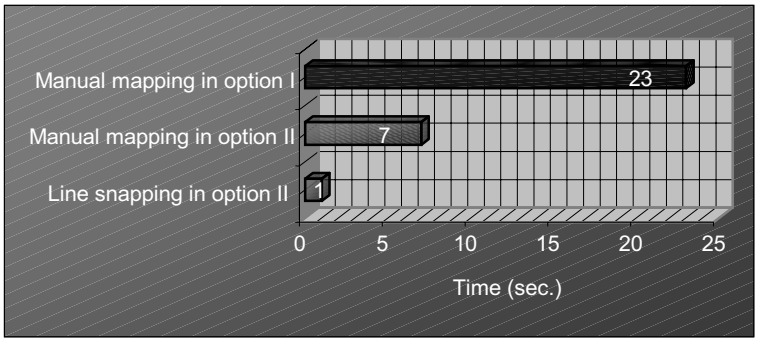

(a) Justification of the Line Snapping Function

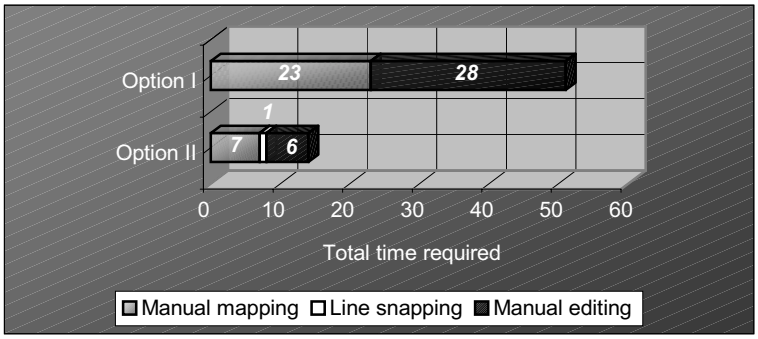

(b) Time Comparison of Each Control Step Used in Options I and II

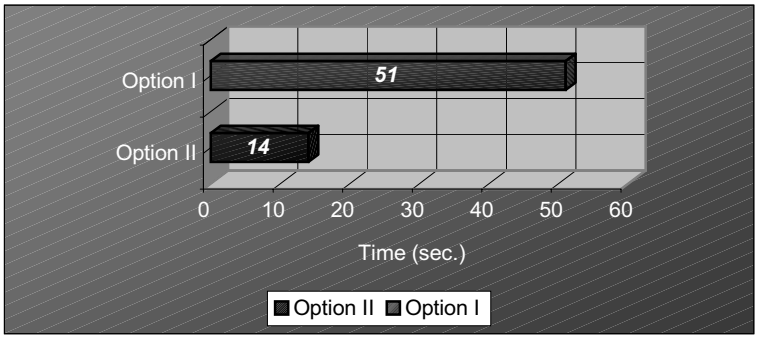

(c) Total Process Time Comparison per Image of Options I and II

Figure 2.18. Overall Time Comparison Process
to Verify the Prevalence of Option II

2.2.2.3 Path Generation Results and the Quality of the Resultant Seal

This section presents the results of the path planning on the thirty pavement crack images collected for the efficiency evaluation. Previous research by the author indicated that the time saved by the path generation was much greater than the time required to compute the path and, thus, well worth the effort. Consequently, a comparison of the implicit path plan and automated path plan was not performed in this study.

In this section, the efficiency of the path planning algorithm is simply evaluated based on (1) its computational time and on (2) the percentage of the idle distance relative to the total traversed distance of the turret required for sealing. In path planning, the idle distance is referred to as the length traveled by the turret between each crack component and/or from home position to the first crack component. That is, no sealing is being performed on this path. This idle distance will be considered in the productivity calculation of the ARMM discussed in the next chapter.

First, the test results showed that the times taken to compute a path plan in each of the thirty pavement crack images were almost zero seconds. Based on the algorithm, the computer could almost instantaneously traverse a few node points shown on the computer screen in order to generate the paths. Therefore, the time required for the path generation was negligible and assumed to be zero. We observed that the decrease in computational time brought about through modification of the previous path planning software was significant. Second, the comparison result of the total traversed distance, actual crack distance, and idle distance for the thirty pavement images, shown in Table 2.3. revealed that the idle distance accounts for approximately 13 percent of the total traversed distance. Finally, Figure 2.19 displays several pavement crack images from the field trials and their resultant ARMM seals. The quality of the automated crack sealing method is then visually compared with that of the conventional crack sealing methods shown in Figure 2.20.

Table 2.3. Comparison of the Total Traversed Distance, Actual Crack Distance, and Idle Distance for the Thirty Pavement Crack Images

Crack image	**Crack length (pixel)**	**Idle length (pixel)**	**Total length (pixel)**
Image 1	1,762.30	342.12	2,104.42
Image 2	1,192.29	115.83	1,308.12
Image 3	890.45	132.08	1,022.53
Image 4	1,013.65	235.89	1,249.54
Image 5	1,383.62	48.51	1,432.13
Image 6	436.19	85.45	521.64
Image 7	864.73	91.40	956.13
Image 8	1,604.52	323.18	1,927.70
Image 9	1,193.88	151.79	1,345.67
Image 10	1,177.17	156.73	1,333.90
Image 11	1,452.24	139.79	1,592.03
Image 12	1,183.81	289.72	1,473.53
Image 13	1,525.86	130.43	1,656.29
Image 14	1,015.93	204.92	1,220.85
Image 15	1,480.51	202.19	1,682.70
Image 16	1,290.36	298.09	1,588.45
Image 17	1,258.10	32.27	1,290.37
Image 18	893.62	104.50	998.12
Image 19	489.86	83.17	573.03
Image 20	910.90	123.91	1,034.81
Image 21	467.22	179.08	646.30
Image 22	892.81	80.41	973.22
Image 23	954.86	158.92	1,113.78
Image 24	915.91	278.57	1,194.48
Image 25	1,060.87	177.39	1,238.26

Crack image	**Crack length (pixel)**	**Idle length (pixel)**	**Total length (pixel)**
Image 26	1,514.53	78.16	1,592.69
Image 27	849.73	170.27	1,020.00
Image 28	1,045.98	92.96	1,138.94
Image 29	493.57	180.38	673.95
Image 30	1,246.90	172.91	1,419.81
Total	32,462.37	4,861.02	37.323.39
Average	1,082 pixels per image	162 pixels per image	1,244 pixels per image
Conversion factor	1 pixel = 0.37 by 0.37 (centimeters)		
Distance in centimeters	**Total crack distance**	**Total idle distance**	**Total traversed distance**
	32,462.37 x 0.37 = 12,012.08 cm	4861.02 x 0.37 = 1,798.58 cm	13,810.66cm
Percentage	**87 %**	**13 %**	**100 %**

- **Examples of the ARMM's Resultant Seals**

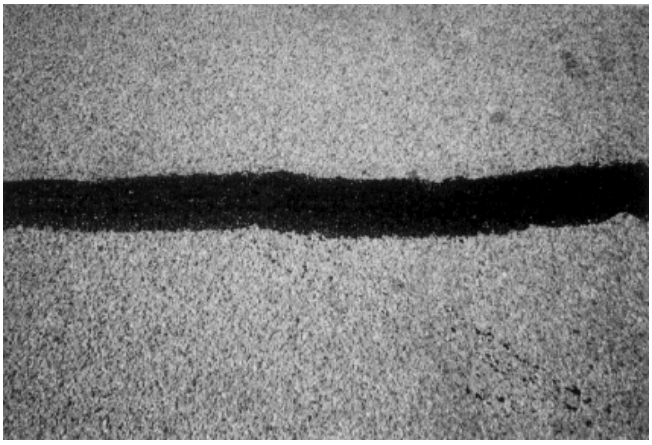

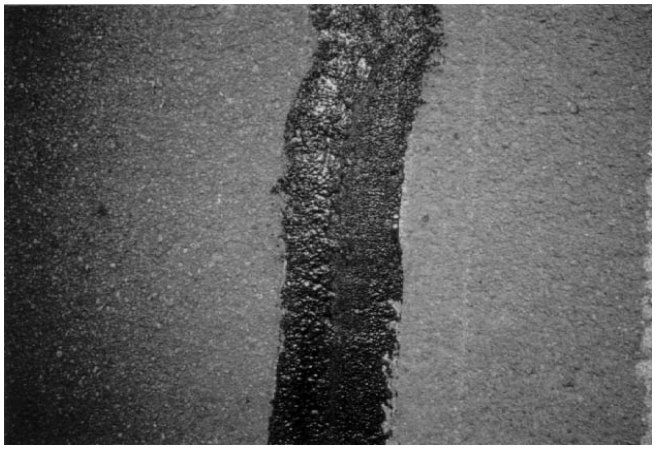

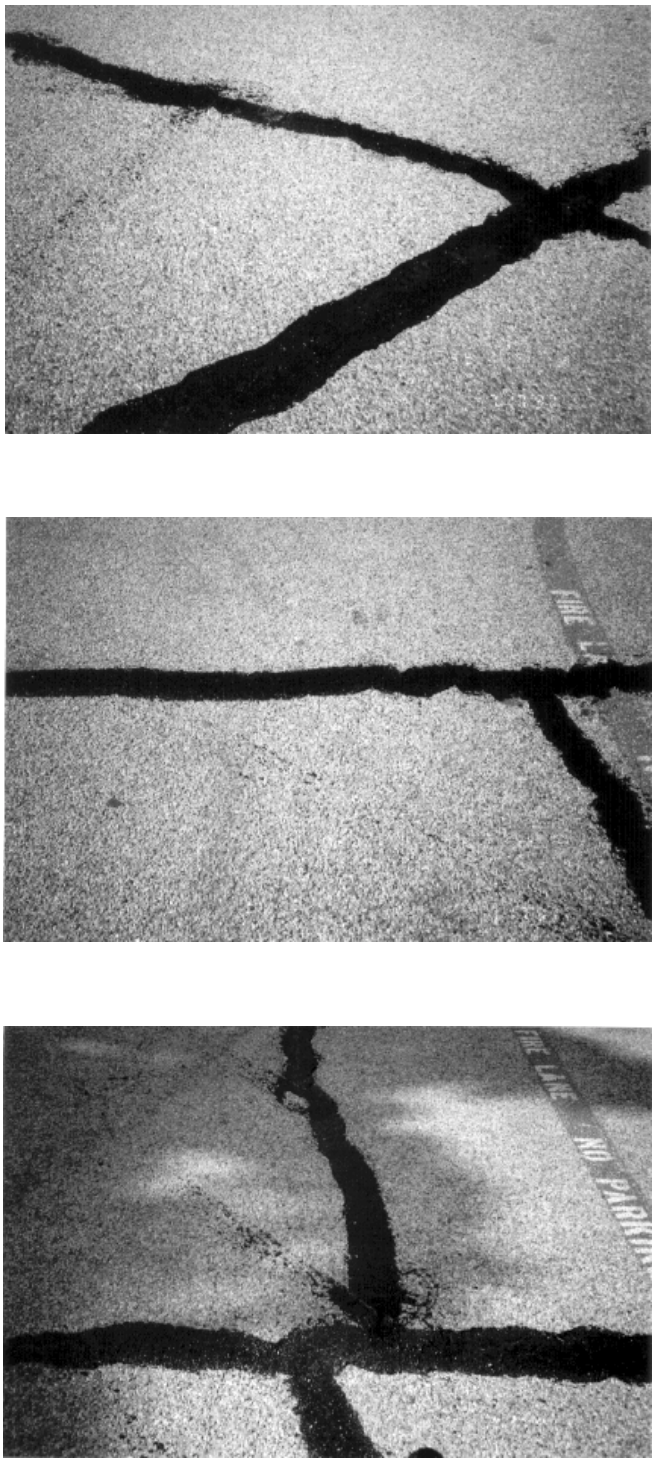

Figure 2.19. Examples of the ARMM's Resultant Seals

- **Examples of the Resultant Seals created by Conventional Methods**

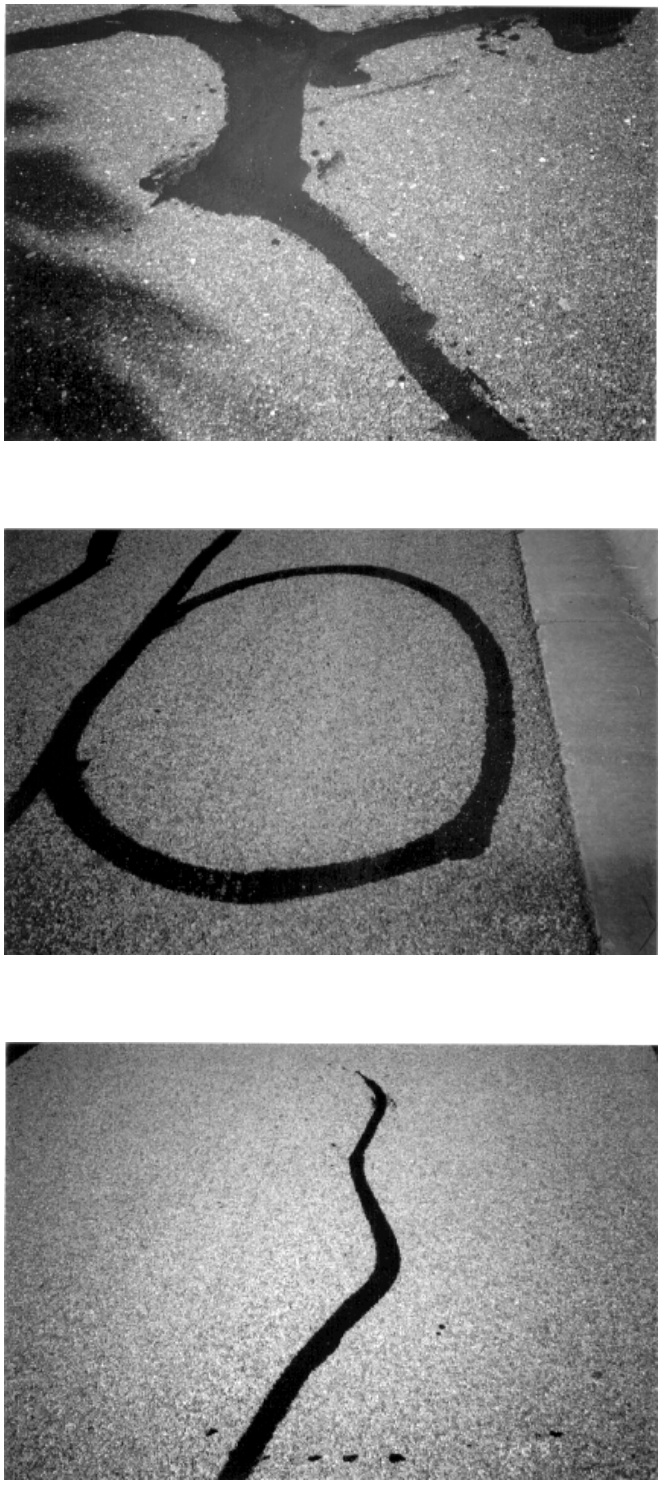

Figure 2.20. Examples of the Resultant Seals Created by Conventional Methods

2.3 CHAPTER SUMMARY

First, the results of the efficiency evaluation for the man-machine balanced control loop verified the superiority of Option II in terms of both accuracy and time. Efficiencies of the developed line snapping and path planning algorithms were derived from the comparison process. In terms of accuracy, the crack representation (99%) in Option II before manual editing was more accurate (and involved less time) than that (86%) in Option I (Figure 2.16-[d]). Also, there was an accuracy increment of 32 percent owing to the use of line snapping function in Option II (Figure 2.16-[e]). In terms of time, the survey results indicated that the time (1 sec) taken to compute the line snapping function was on average much less than the time (24-8 = 16 sec) saved by performing the manual mapping where there will be subsequent line snapping (Figures 2.17-[a] and 2.18-[a]). In the case of Option I, the use of the manual editing function was essential when taking into account the quality of the resultant seal. The time taken for the manual editing was 28 seconds per image in Option I, while it took 6 seconds per image in Option II (Figure 2.17-[b]). In the case of Option II, the time for the manual editing could be saved, because the recent field trials indicated that the trivial errors (1%) caused by line snapping were negligible and could be compensated for by the amount of sealant. The total processing time (14 sec) taken in Option II was much less than that (51 sec) taken in Option I (Figure 2.18-[c]). These results underscore both the necessity of the line snapping function in the man-machine control loop of the final system and the overall superiority of Option II. As a result, Option II will be recommended for the final crack sealing system.

Second, the results of the efficiency evaluation for the developed path planning software indicated that the time required for the path generation was almost zero seconds. There was a significant improvement (0.78 sec/image) in the computational time owing to the modification of the previous path planning software. Also, the test result revealed that the idle distance was about 13 percent of the total traversed distances traveled by the turret (Table 2.3).

Finally, the quality of the automated crack sealing method was visually compared with that of conventional crack sealing methods. Since a sufficient amount of sealant could be dispensed from the end effector onto the exact crack position represented by the automated method, the ARMM is capable of consistently sealing cracks on pavements (Figure 2.19). Moreover, the substantial performance variation observed among the individuals within the sealing crews led to variation in the quality of the resultant seal created by conventional methods (Figure 2.20). It is anticipated that the quality of the resultant seal created by the automated method would, on average, equal or exceed that created by conventional methods.

CHAPTER 3. ANTICIPATED ARMM PRODUCTIVITY

3.1 ANTICIPATED SYSTEM PRODUCTIVITY

In this section, the productivity of the ARMM is predicted based on (1) the results of the efficiency evaluation of the man-machine control loop and the machine vision algorithm, (2) a series of field trials, (3) a section of road assumed using the collected thirty pavement crack images and the current ARMM's work space, and (4) a productivity model that was developed. The mathematical model that predicts the productivity of the ARMM was developed as a means of rating the performance of the ARMM (Kim et al. 1997, Husbands 1997).

3.1.1 Methodology

To quantitatively rate the overall performance of the ARMM, the tasks associated with its operation were divided into five major components. These components were then itemized and individual subtasks were identified. These subtasks were then isolated and evaluated separately. The evaluation results of each subtask were next added to determine the overall productivity of the system. Figure 3.1 shows the major tasks and subtasks associated with the operation of the ARMM.

As shown in Figure 3.1, the first and fifth component of the automated crack sealing process represent the time required to set up the ARMM at the beginning of the work day (T_{comp1}) and the time required to break down the ARMM at the end of the work day (T_{comp5}), respectively. These times do not vary according to the type of cracking on a given section of road and, thus, constants in the model. These constant values have been estimated through a series of field trials (Table 3.1). Consequently, the general productivity model developed incorporates three of the five major components. These components include the time required to (1) trace the crack image and perform the line snapping, manual editing and path planning (T_{comp2}); (2) blow, seal, and squeegee the work space (T_{comp3}); and (3) move to the next work space (T_{comp4}).

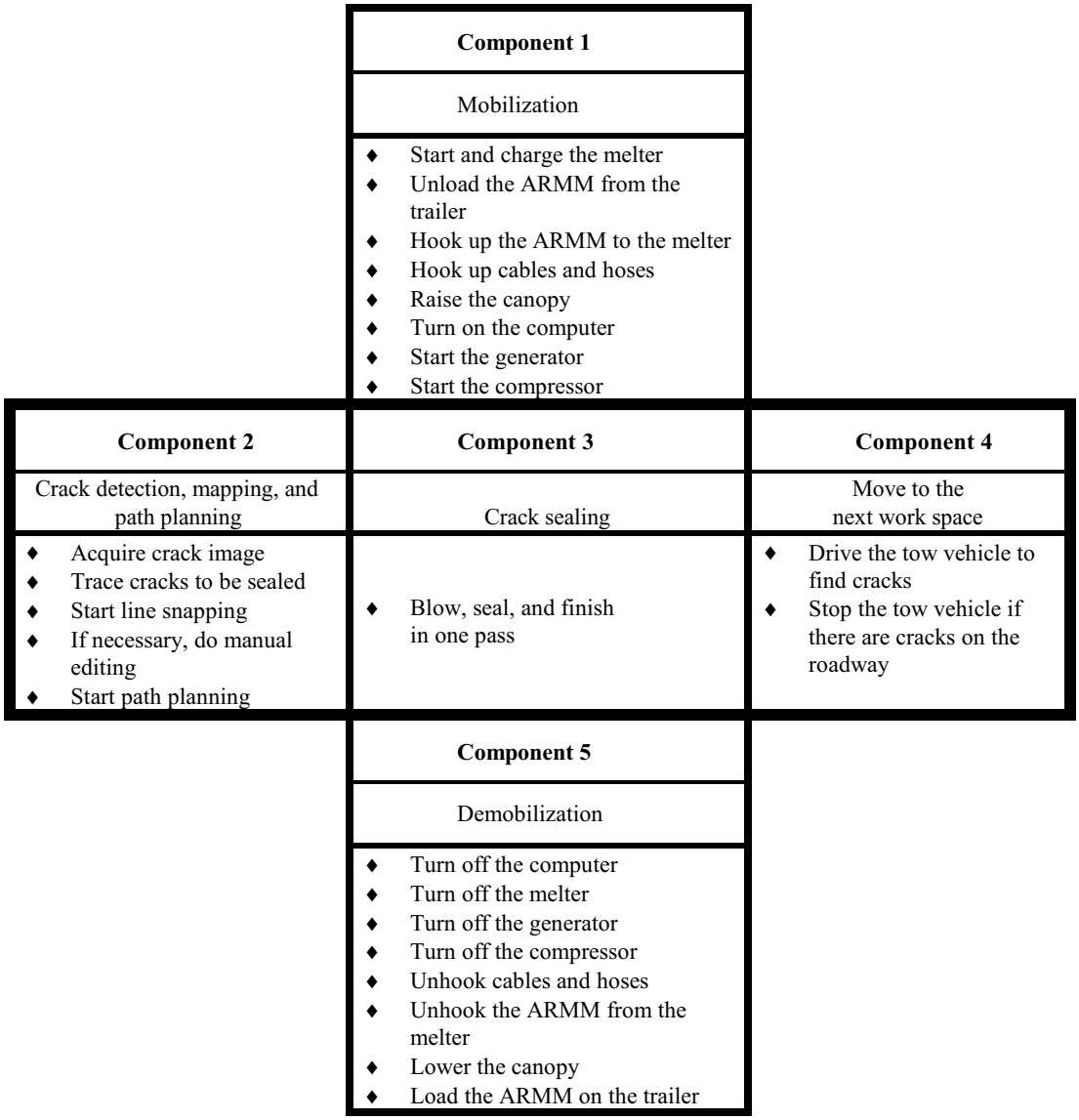

Figure 3.1. Five Components Classified for Productivity Study of the ARMM

First, as shown in Figure 3.1, the second component (T_{comp2}) reflects the time to trace (t_t), line snap (t_{ls}), and path plan (t_{pp}) given linear meters of cracking. Recent field trials showed that line snapping accuracy and effectiveness reduces the need to manually edit crack images. Therefore, the manual editing factor was not considered in the following model:

- [trace time/work space] * [no. of work spaces] = total trace time (t_t)
- [(line snap + path plan time)/work space] * [no. of work spaces] = total line snap and path plan time ($t_{ls} + t_{pp}$)
- T_{comp2} = [total trace time + total line snap and path plan time]
    - $= t_t + t_{ls} + t_{pp}$

Thus, the experimental results presented in Table 2.2 (the results of Option II) are directly applied to the T_{comp2} in the model.

Second, the third component (T_{comp3}) accounts for the time required to blow, seal, and squeegee all cracks in a work space. Since the turret assembly on the ARMM moves at constant velocity, the time required to blow, seal, and squeegee cracks is easily determined by dividing the linear meters of cracking on a given pavement section by the velocity of the ARMM's end effector. In most cases, there are multiple cracks in a single work space. In these cases, the turret assembly takes time to move from crack to crack. As mentioned previously, the time taken for the turret to traverse the idle distance must be accounted for in the productivity calculation. This time is referred to as *idle time*. There are two series of idle distances traversed by the turret (Figure 3.2). These are (1) the idle distance between each crack component and/or from home position to the start node point of the first crack component to be sealed (idle distance I), and (2) the idle distance from the end node point of the last crack component sealed to the home position (idle distance II). Once sealing for all the cracks in a work space is complete, the ARMM starts to move to the next work space. Thus, the time taken for traversing idle distance II was not considered in the productivity calculation of the ARMM. As a result, only the time taken for idle distance I will be added to

the time required to seal actual cracks in determining the total time spent traversing the entire work space.

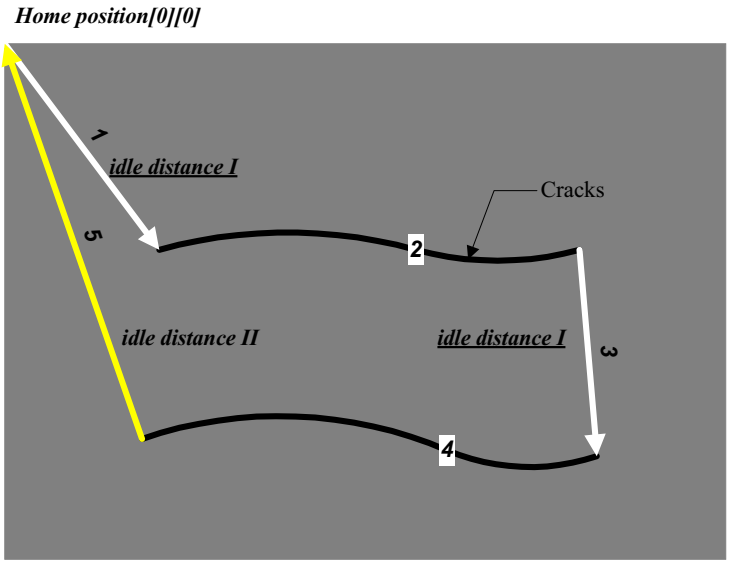

Figure 3.2. Idle Distance I vs. Idle Distance II

Therefore

- T_{comp3} = [total actual crack distance + total idle distance]/[average velocity of manipulator (30 cm/second)] = total blow, seal, squeegee time

Finally, the fourth component (T_{comp4}) relates to the time required for travel. This component includes the activities involved in advancing the ARMM to subsequent following work space or series of work spaces. The value of this component will vary according to the position of cracking to be sealed on a section of road (distance between the work spaces). For the estimation of the T_{comp4}, the ARMM has been timed to determine the acceleration, maximum speed, and deceleration at which it can be towed. With the length of the pavement section known, the required travel distance can be divided by the maximum travel speed of

the ARMM to determine the time required to move that section. The time lost through acceleration and deceleration is also included in the equation. Thus, T_{comp4} can be calculated

- T_{comp4} = [required travel distance/velocity] + [average time loss due to
- acceleration and deceleration] = total time to move

Since T_{comp4} is determined based on the ARMM's maximum travel speed and the time loss owing to acceleration and deceleration, the value of T_{comp4} estimated by the above equation would reflect the travel time in both successive work space and series of work spaces.

The complete productivity model for the ARMM incorporates all five components detailed in Figure 3.1. Thus, the total equation is:

- [T_{comp1} (time to mobilize) + T_{comp2} ($t_t + t_{ls} + t_{pp}$) + T_{comp3} + T_{comp4} + T_{comp5} (time to demobilize)]/ total length of sealed pavement = ARMM productivity (time to seal a given section of road in units of hours)

Based on this model, the ARMM's daily productivity rate is predicted in units of lane-kilometers per day.

3.1.2 A Section of Road Assumed for the ARMM's Productivity Prediction

In general, the degree of pavement distress and the types of cracking are the dominant factors affecting crack sealing productivity. For example, the more distressed a pavement section, the longer it takes to seal that pavement section (Husbands 1997). In this report, the ARMM's productivity will be estimated based on a section of road (Figure 3.3) assumed using the thirty pavement crack images (Appendix A) and the current ARMM's work space (12 ft by 5.5 ft). Because the thirty pavement crack images consist of three major crack types (longitudinal, transverse, and block) and show various degrees of pavement distress and

complexity, it is expected that the final result would represent the ARMM's generalized productivity.

As stated, an imaginary section of road with the thirty pavement crack images has been assumed in order to predict the ARMM's productivity. As shown in Figure 3.3, "one section of road" defined in this productivity study is equal to 100 linear meters (328 linear feet). Since the ARMM currently has a length of 5.5 feet and a width of 12 feet, the total cracking area for the thirty pavement crack images in the assumed section of road would be equal to approximately 50 percent (5.5 ft x 12 ft x 30 work spaces (images) = 1980 ft^2) of its total surface area (328 ft x 12 ft = 3936 ft^2). This is illustrated in Figure 3.3.

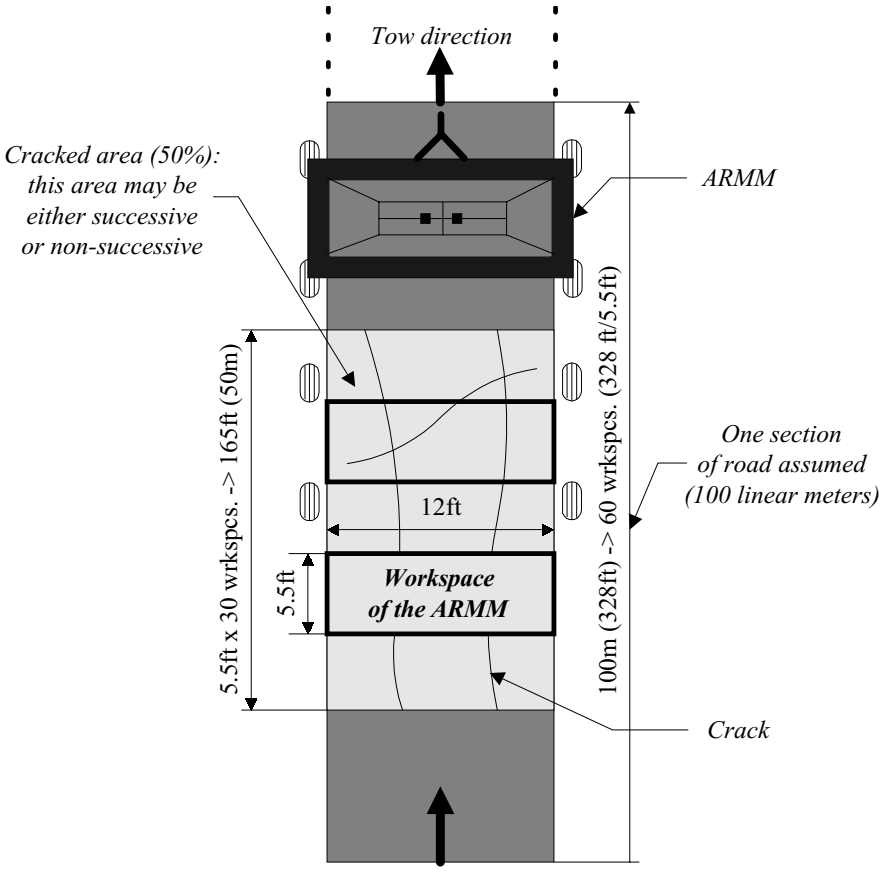

Figure 3.3. A Section of Road Assumed for Productivity Analysis of the ARMM

3.1.3 Estimation of the ARMM's Productivity

Based on the productivity model developed, on the experimental results revealed in the laboratory tests and field trials, and on the section of road assumed, this section first determines the total time required to seal the section of road (with pavement distresses of 50 percent in 100 linear meters) assumed in Figure 3.3. It then projects the ARMM's productivity (time to seal in units of hours) according to the degree of pavement distresses by varying the number of work spaces in the 10 sections (1 kilometer) of assumed road (Table 3.2). From the results, the ARMM's daily productivity rates measured according to the degree of pavement distresses are predicted in units of lane-kilometers per day.

(1) Mobilization and Demobilization (T_{comp1} and T_{comp5})

As mentioned previously, the time for mobilization and demobilization of the ARMM at the beginning and end of the work day has been estimated through a series of field trials. As shown in Table 3.1, experienced crews should be able to mobilize the ARMM in 20 minutes (T_{comp1}) and demobilize the ARMM in 15 minutes (T_{comp5}). These times will be added to the final result to determine the overall productivity of the ARMM.

Table 3.1. Estimation of the Times for Mobilization (T_{comp1}) and Demobilization Time (T_{comp5}) of the ARMM

Type of crew / Time	Regular crews	Experienced crews
Total mobilization time (T_{comp1})	35 minutes	20 minutes
Total demobilization time (T_{comp5})	25 minutes	15 minutes

(2) Crack Tracing, Line Snapping, and Path Planning (T_{comp2})

$\Rightarrow$ t_t = (7.53 sec/wrkspc) x (30 wrkspc) = 225.9 seconds

$\Rightarrow$ t_{ls} = (1.10 sec/wrkspc) x (30 wrkspc) = 33.0 seconds

$\Rightarrow$ t_{pp} = assumed to be 0 seconds

$\Rightarrow$ T_{comp2} = (225.9 + 33.0) sec = 258.9 sec = 0.072 hours/100 linear meters

(3) Crack Blowing, Sealing, and Squeegeeing (T_{comp3})

$\Rightarrow$ Total actual crack distance = 120.12 meters (Table 2.3)

$\Rightarrow$ Total idle distance = 17.98 meters (Table 2.3)

$\Rightarrow$ Total traversed distance = 138.10 meters (Table 2.3)

$\Rightarrow$ Avg. velocity of manipulator = 0.3 meters/second

$\Rightarrow$ T_{comp3} = [(120.12 + 17.98) meters] / [0.3 meters/sec] = 460.3 seconds
= 0.13 hours/100 linear meters

(4) Time Required for Travel (T_{comp4})

$\Rightarrow$ Maximum safe speed of the ARMM (velocity) = 15 mph

$\Rightarrow$ 15 miles = 79,200 feet = 24,140.16 meters

$\Rightarrow$ [100 meters/(24,140.16 meters/hour)] = 0.00414 hours

$\Rightarrow$ 0.00414 hours = (0.00414 x 3600) seconds = 15 seconds

$\Rightarrow$ 15 seconds per 100 meters

$\Rightarrow$ Average time loss caused by acceleration and deceleration = 7 seconds

$\Rightarrow$ (No. of work spaces -1) x 7 seconds = 29 x 7 = 203 seconds

$\Rightarrow$ T_{comp4} = [15 seconds +203 seconds] = 218 seconds = 0.06 hours/100 linear meters

Thus, the ARMM's productivity for the 100 linear meters assumed in Figure 3.3 would be

$\Rightarrow$ $T_{comp1} + T_{comp2} + T_{comp3} + T_{comp4} + T_{comp5}$ = (0.33 + 0.07 + 0.13 +0.06 +0.25) = 0.84 hours/100 linear meters

Based on the above result, the ARMM's productivity in the case of pavement distresses of 50 percent for 10 sections of road (1 kilometer) can be calculated as follows:

$\Rightarrow$ $T_{comp1} + T_{comp2} + T_{comp3} + T_{comp4} + T_{comp5}$ = [0.33 + (0.07 x 10) + (0.13 x 10) + (0.06 x 10) + 0.25)] = 3.18 hours

The ARMM's productivity (time to seal) according to the degree of pavement distresses are projected in the same manner (Table 3.2). In this analysis, the time to seal has been estimated based on the ten sections (1 kilometer) of road assumed. Since the T_{comp1} (time to mobilize) and T_{comp5} (time to demobilize) badly affected the productivity of the current prototype system (ARMM), as shown in the above calculation (0.84 hours/100 LM), assuming a certain amount of pavement section was essential in order to analyze the ARMM's productivity in a meaningful way. Thus, the ARMM's daily productivity rates according to the degree of pavement distresses are predicted in units of lane-kilometers per day (Table 3.2).

Table 3.2. ARMM's Overall Productivity Anticipation According to the Degree (10%~100%) of Pavement Distresses

Pavement distress (%)	No. of work-space	Linear meters of sealant placed	T_{comp1} (hrs/km)	T_{comp2} (hrs/km)	T_{comp3} (hrs/km)	T_{comp4} (hrs/km)	T_{comp5} (hrs/km)	Time to seal (hrs/km)	ARMM's daily productivity (lane-kilometers per day)
10%	60	240.24	0.33	0.14	0.26	0.14	0.25	1.12	7.14
20%	120	480.48	0.33	0.29	0.52	0.26	0.25	1.65	4.85
30%	180	720.72	0.33	0.43	0.78	0.37	0.25	2.16	3.70
40%	240	960.96	0.33	0.57	1.04	0.49	0.25	2.68	3.00
50%	300	1201.20	0.33	0.72	1.30	0.60	0.25	3.18	2.52
60%	360	1441.44	0.33	0.86	1.56	0.72	0.25	3.72	2.15
70%	420	1681.68	0.33	1.01	1.82	0.84	0.25	4.25	1.88
80%	480	1921.92	0.33	1.15	2.08	0.96	0.25	4.77	1.68
90%	540	2162.16	0.33	1.29	2.34	1.07	0.25	5.28	1.52
100%	600	2402.40	0.33	1.43	2.60	1.19	0.25	5.80	1.38
Average daily productivity of the ARMM (lane-kilometers per day)									**3.00** (1.9 ln-mi.)

Table 3.2 showed the rates at which the ARMM currently performs for the sections of road assumed in this report. However, these rates will be significantly enhanced by the following improvements to be employed in the commercial crack sealing system (Table 3.3). With such improvements, the ARMM's productivity rates shown in Table 3.2 will also be further increased, thus making the automated crack sealing more favorable. Achievable productivity rates should be several times those calculated in Table 3.2. This will be further discussed below.

Table 3.3. Major Elements for the ARMM's Productivity Improvement and Components to Be Enhanced

Improvements	**Components to be enhanced**
(1) Use of faster processor (Pentium™ computer)	Component 2
(2) Fabrication of the lighter X-Y manipulator	Components 3 and 4
(3) Use of faster motors	Component 3
(4) Ergonomical design of the tow vehicle's cab	Components 2 and 4
(5) Redesigning the crack sealing robot as a single unit	Components 1 and 5

♦ An example of the ARMM's productivity improvement

Using the current prototype system, the crews are spending too much time on mobilizing (20 minutes) and demobilizing (15 minutes) the ARMM. Eventually, the ARMM will be built as a single unit (improvement 5). In that case, times for mobilization (T_{comp1}) and demobilization (T_{comp5}) should be removed from the productivity model. This adjustment will significantly improve the overall productivity of the ARMM as follows:

In the case of the 100 linear meters with pavement distresses of 50 percent

⇒ 0.84 hours - (0.33+0.25) hours = 0.26 hours (15.6 minutes)/100 LM

⇒ 2.60 hours / lane-kilometer

⇒ ARMM's daily productivity: 3.08 lane-kilometers per day

In the same manner, the ARMM's overall productivity rate incorporating these improvements is recalculated in Table 3.4. When considering the other improvement elements shown in Table 3.3, achievable productivity rates of the commercial crack sealing unit should be several times those calculated in Tables 3.2 and 3.4.

Table 3.4. An Example of the ARMM's Productivity Improvement

Pavement distress (%)	Number of work space	Linear meters of sealant placed	Time to seal (hours/ kilometer)	ARMM's daily productivity (lane-kilometers per day)
10%	60	240.24	0.54	14.8
20%	120	480.48	1.07	7.48
30%	180	720.72	1.58	5.06
40%	240	960.96	2.11	3.79
50%	300	1201.20	2.60	3.08
60%	360	1441.44	3.14	2.56
70%	420	1681.68	3.66	2.19
80%	480	1921.92	4.18	1.91
90%	540	2162.16	4.70	1.70
100%	600	2402.40	5.23	1.53
Average daily productivity of the ARMM (lane-kilometers per day)				4.41 (2.73 ln-mi.)

Other productivity and cost analyses used for comparing the ARMM with conventional sealing crews (using the productivity model developed and the Pavement Management Information System [PMIS] Loop-up Table provided by the Texas Department of Transportation [TxDOT]) is described elsewhere (Husbands 1997).

CHAPTER 4. EVALUATION RESULTS FROM FIELD TRIALS

Field trials were completed at UT and at five locations (Austin, San Antonio, Corpus Christi, Dallas, Travis County) in the state of Texas. Evaluation of the technology over the last 8 months was based on field trial experiences, observations by maintenance personnel, key vendor input, and detailed productivity analysis. Key technical advances that have already been implemented include:

- merged, real-time, dual-camera viewing
- simplified graphical control buttons
- motion-control modifications
- larger motors
- computer-controlled electronic switch for the sealant wand
- variable speeds for cracks of variable widths

Improvements based on the evaluations vary in terms of their anticipated benefit/cost ratios. Improvements that are expected to have high benefit-cost ratios are highlighted in the following list of suggestions:

1. **replace current office 486 PC with industrial Pentium PC**
2. **use a spring-loaded, U-shaped squeegee**
3. **develop a retractable turret**
4. **modify support arm for sealant hose**
5. redesign hose and add hitch for lengthwise towing
6. create a training video
7. build smaller manipulator with less dead space for narrower roads
8. replace bearings, gantry, and motors to triple end-effector (tool) speed
9. hard-mount melter and other equipment on one truck to eliminate one towed unit
10. **add better tinting, or mini-blinds, to reduce glare on monitor**
11. **add lighting for nighttime operations**
12. add computer control of pump/flow rate

CHAPTER 5. CONCLUSIONS AND RECOMMENDATIONS

Automating the pavement crack sealing process will improve productivity, quality, and safety. The reduction in crew size and the increase in productivity of the sealing process will translate directly into significant potential cost savings. The results of the efficiency evaluation of the man-machine balanced control loop and machine vision algorithm described in Chapters 1 and 2 support this conclusion. It is also anticipated that the man-machine balanced control loop, including line snapping and path planning algorithms presented in this final report, should be applicable to a wide variety of infrastructure crack and joint sealing applications.

During the field trials, feedback obtained from maintenance personnel was mixed, though mostly positive. The ARMM's daily productivity rates, according to the degree (10%~100%) of pavement distresses in the assumed section of road, were determined in Chapter 3. Several elements for the ARMM's productivity improvements were also identified. Currently, the machine is competitive with conventional methods (2 lane-miles per day on average), but should easily outperform those methods in the near future.

Finally, the implementation plan presented at the beginning of this report should be followed.

BIBLIOGRAPHY

Adams, J. (1989). *Human Factors Engineering*, Macmillan Publishing Company, New York, NY.

Braggins, D. and Hollingum, J. (1986). *The Machine Vision Source Book*, IFS (publications) Ltd., UK.

Ganguli, Siddhartha (1982). *Performance Evaluation of Man-Machine Systems*, Affiliated East-West Press Put. Ltd., New Delhi, India.

Greer, R., Haas, C., Gibson, G., Traver, A., and Tucker, R. (1996). "Advances in Control Systems for Construction Manipulator," *Proceedings of the 13th International Symposium on Automation and Robotics in Construction (ISARC)*, Tokyo, Japan, 615–624.

Greer, R., Kim, Y., and Haas, C. (1997). "Telerobotic Control for Automated Construction and Maintenance," *Presented at the 76th annual TRB meeting*, Washington, D.C.

Greer, R., Kim, Y. S., and Haas, C. (1997). "Tele-operation for Construction Equipment," *Proceedings of ASCE Construction Congress V*, Minneapolis, MN.

Haas, C., Skibniewski, M., and Bundy, E. (1995). "Robotics in Civil Engineering," Microcomputers in Civil Engineering," No. 10, 371–381.

Haas, C. (1996). "Evolution of an Automated Crack Sealer: A Study in Construction Technology Development," *Automation in Construction 4*, Elsevier, 293–305.

Haas, C., Kim, Y.S., and Greer, R (1997). "A Model for Imaging Assisted Automation of Infrastructure Maintenance," *Proceedings of the 2nd International Conference on Imaging Technologies: Techniques and Applications in Civil Engineering*, Davos, Switzerland.

Helander, M. (1981). *Human Factors/Ergonomics for Building and Construction*, John Wiley & Sons, Inc., New York, NY.

Husbands, J. (1997). "Productivity of an Automated Pavement Crack Sealer," *master's thesis*, The University of Texas at Austin.

Ibanez-Guzman, J. (1994). "Comparison Between Industrial Robotic Manipulators, Agricultural and Construction Plant and Equipment," *Proc. of the 11th*

International Symposium on Automation and Robotics in Construction (ISARC), Elsevier.

Kim, Y. S. (1995). "Path Planning for an Automatic Pavement Crack Sealer," *master's thesis*, The University of Texas at Austin.

Kim, Y. S., Husbands, J., Haas, C., Greer, R., and Reagan, A. (1997). "Productivity Model for Performance Evaluation of the UT Automated Road Maintenance Machine," *Proceedings of the 14th International Symposium on Automation and Robotics in Construction (ISARC)*, Pittsburgh, PA, 443–450.

Kim, Y. S., Haas, C., and Greer, R. (1997). "Path Planning for a Machine Vision Assisted, Tele-operated Pavement Crack Sealer," *Journal of Transportation Engineering*, ASCE.

Kim, Y. S. (1997). "Man-Machine Balanced Control for Automation of Infrastructure Crack Sealing," *doctoral dissertation*, The University of Texas at Austin.

Levine, M. (1985). *Vision in Man and Machine*, McGraw-Hill, Inc., New York, NY.

Merriam Webster's Collegiate Dictionary (1993). Tenth Edition, Merriam Webster Inc., Springfield, MA, p. 1211.

National Research Council (1995). *Automation Opportunities in Highway Construction and Maintenance*, National Research Council's TR News, No. 176.

Park, K. (1987). *Human Reliability*, Elsevier Science Publishing Company Inc., New York, NY.

Taylor, P. (1990). *Understanding Robotics*, CRC Press Inc., Boca Raton, FL.

Texas Department of Transportation (TxDOT) (1997). *Pavement Management Information System Rater's Manual for Fiscal Year 1997*, Texas Department of Transportation, Austin, TX.

APPENDIX. A

Thirty Pavement Crack Images Used in Experiments

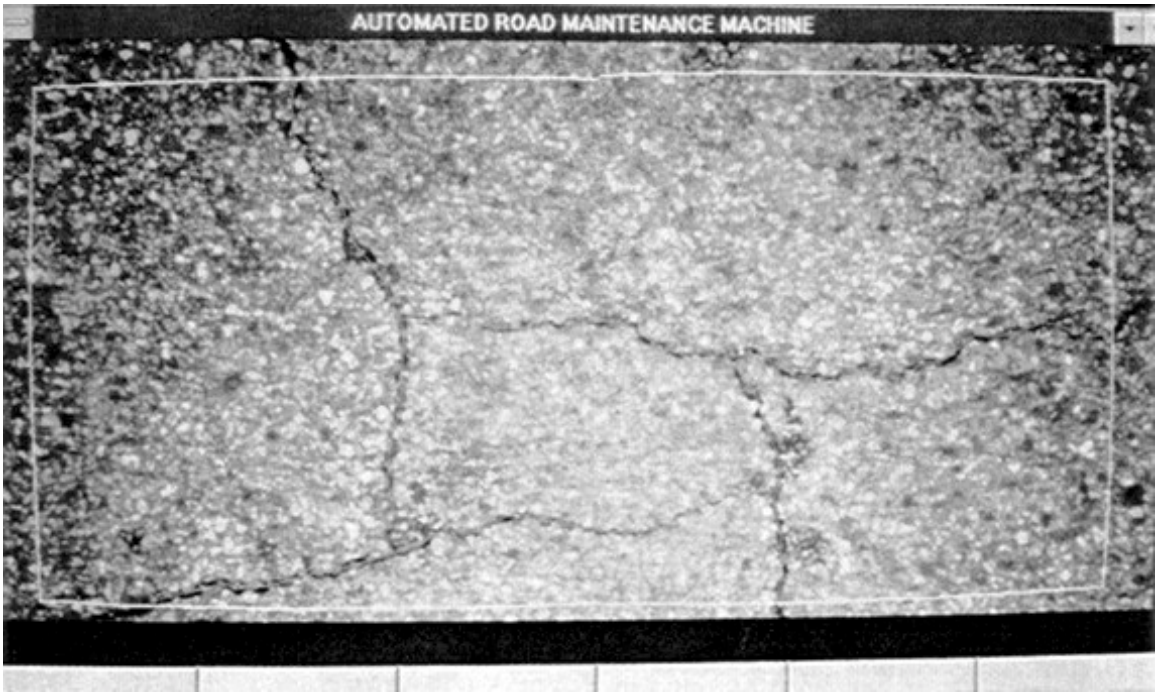

Tested Image No.1

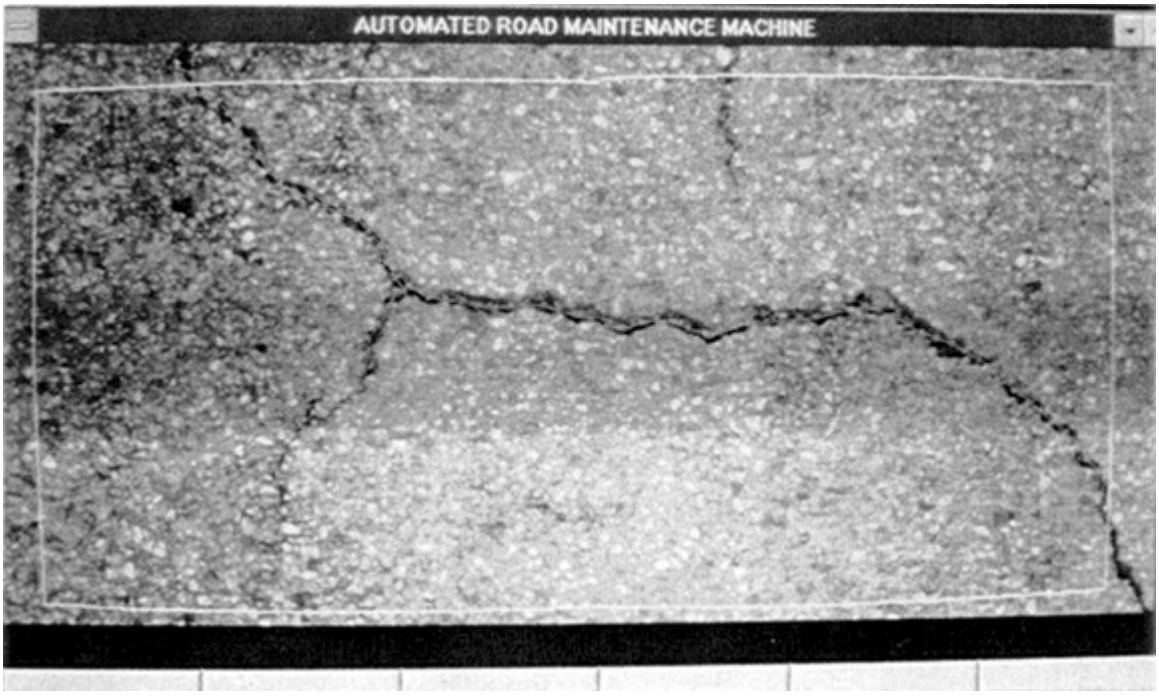

Tested Image No.2

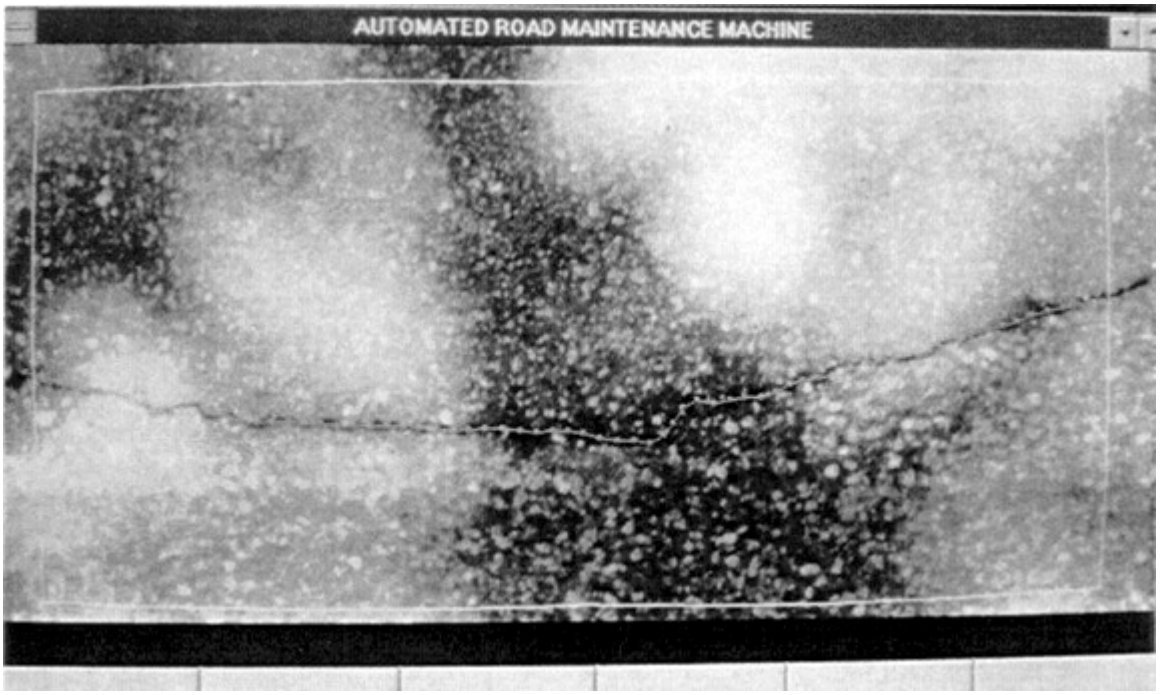

Tested Image No.3

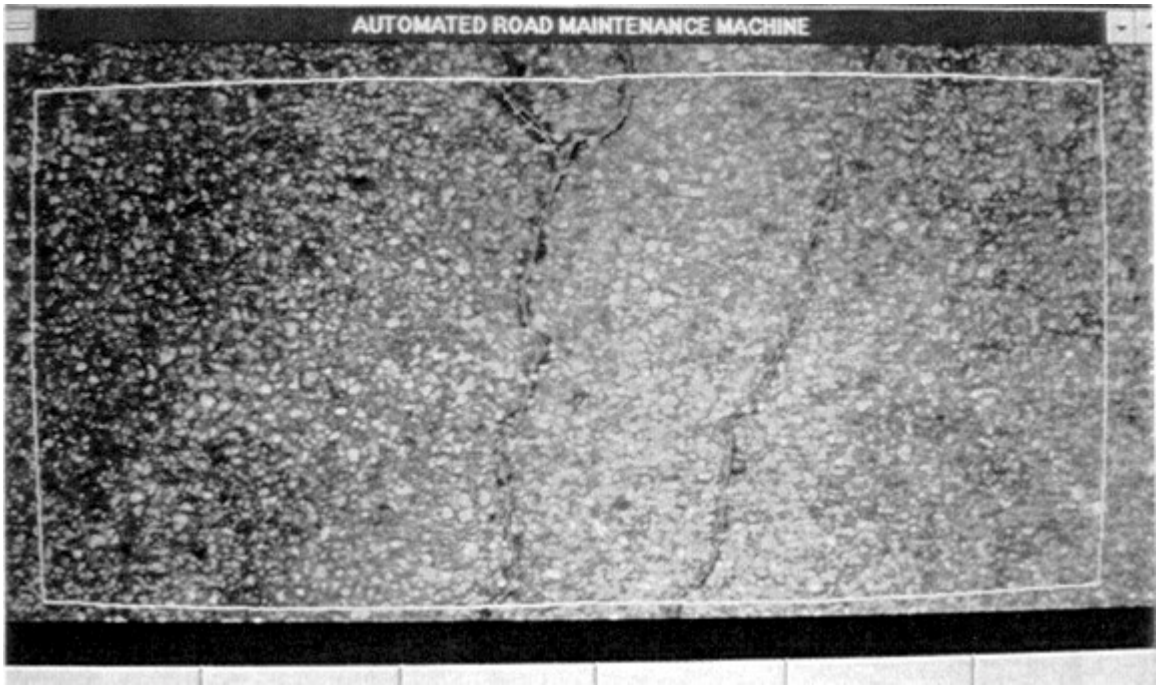

Tested Image No.4

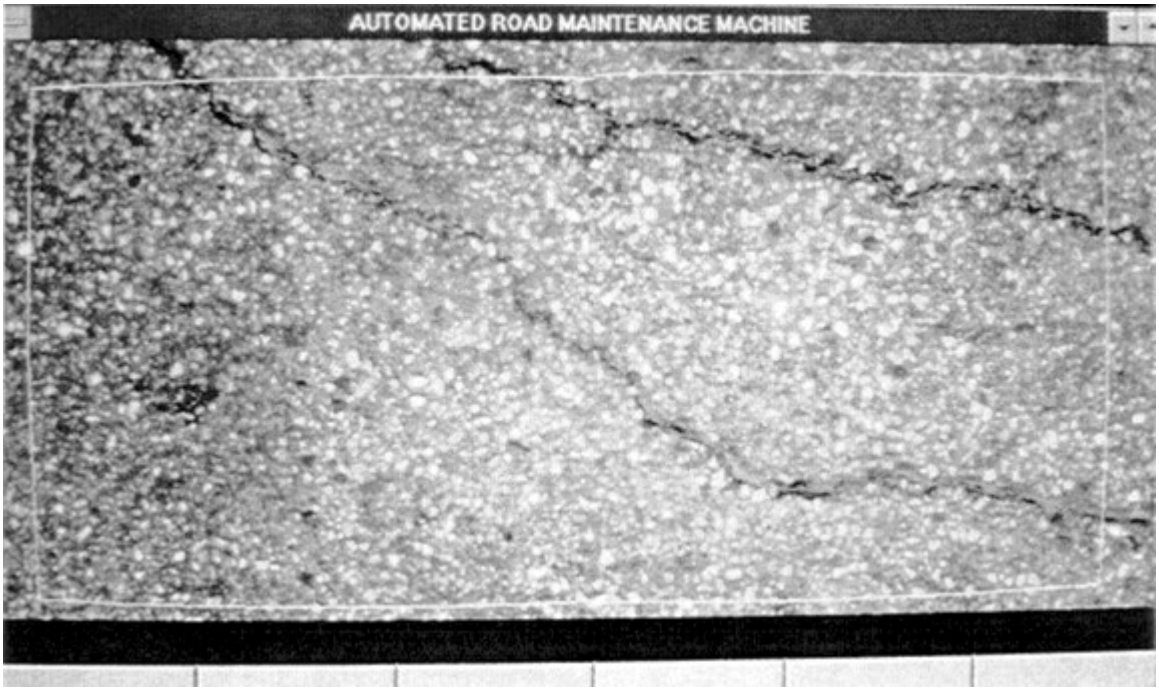

Tested Image No.5

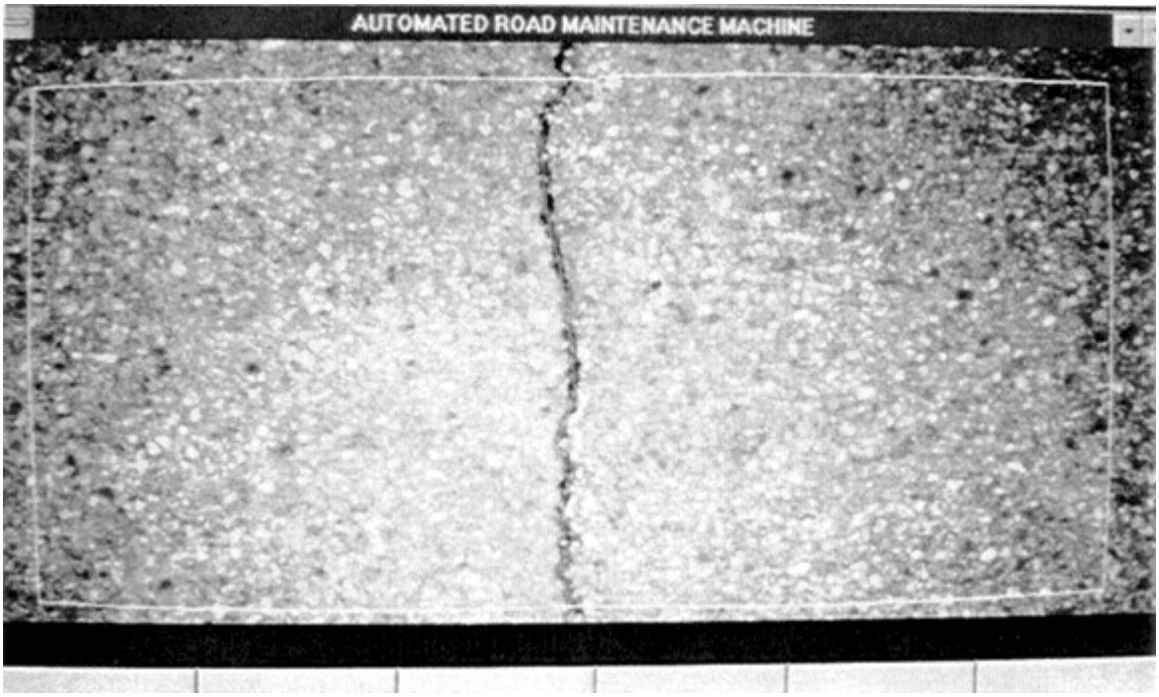

Tested Image No.6

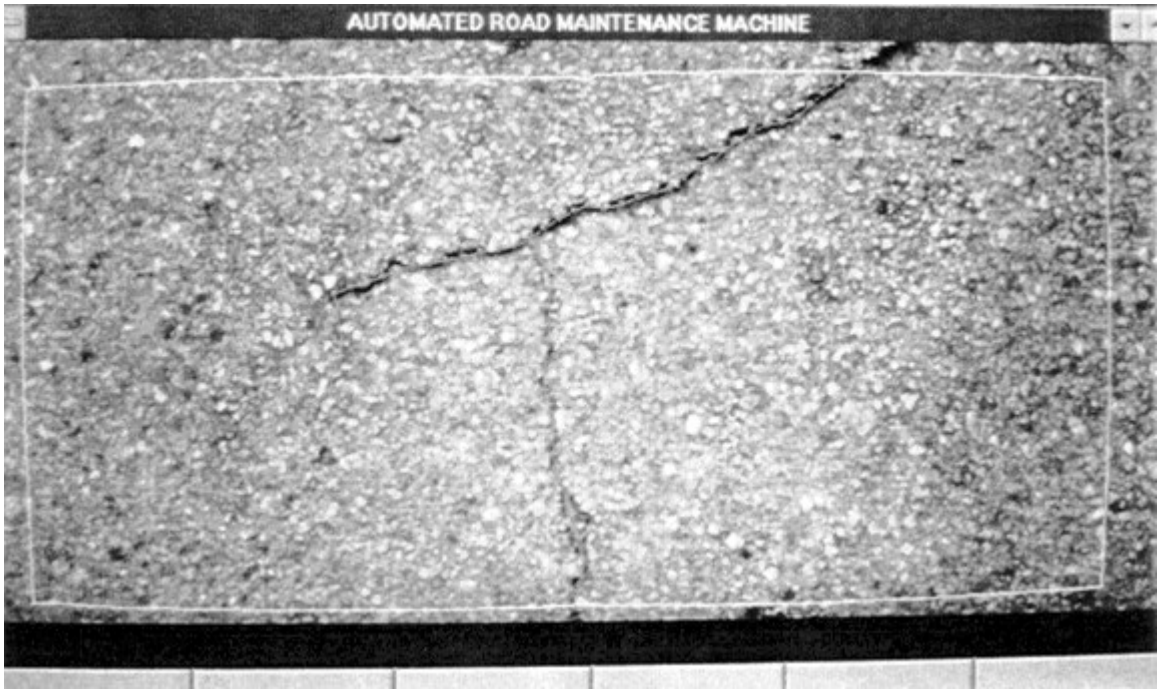

Tested Image No.7

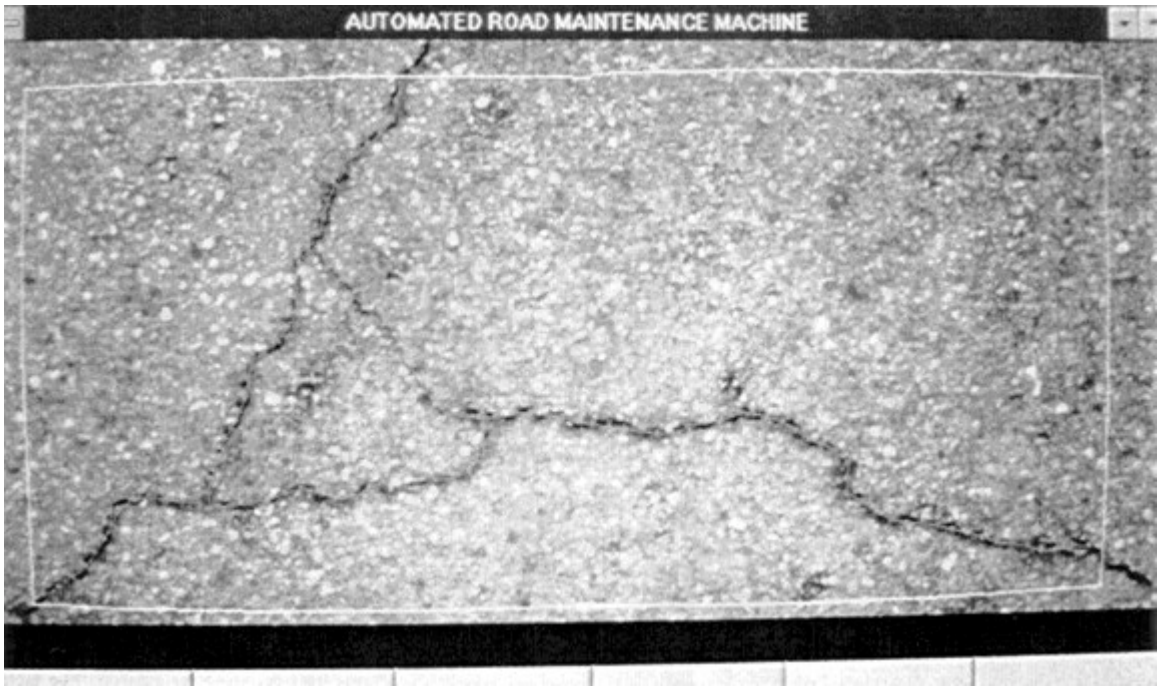

Tested Image No.8

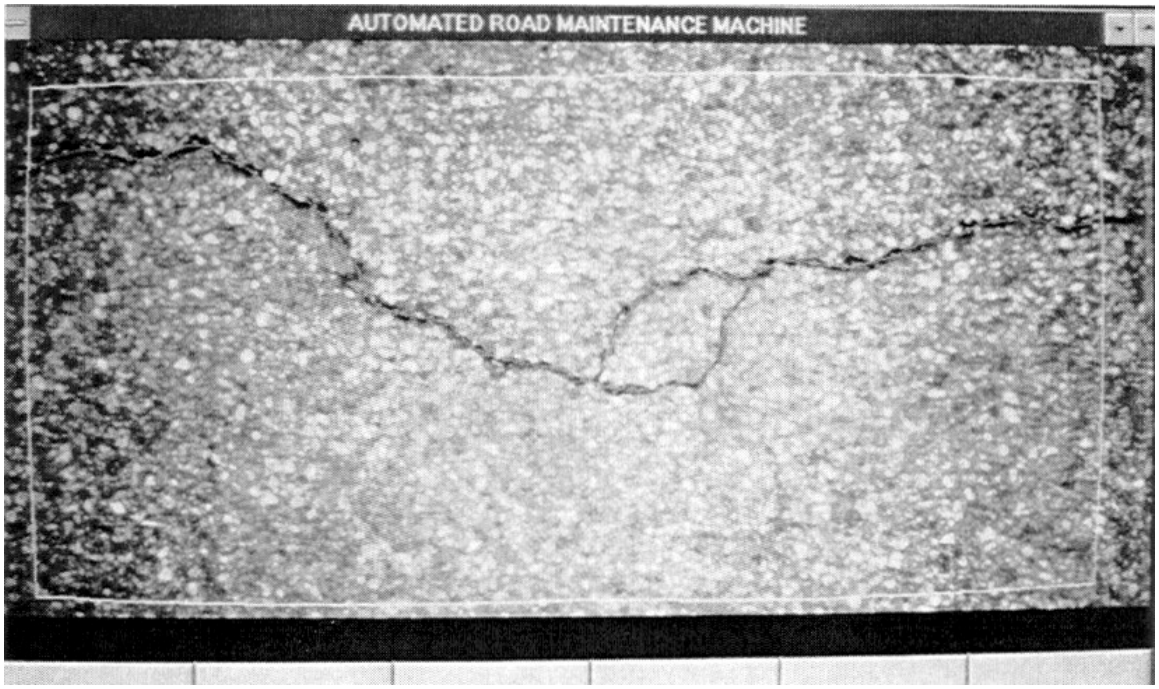

Tested Image No.9

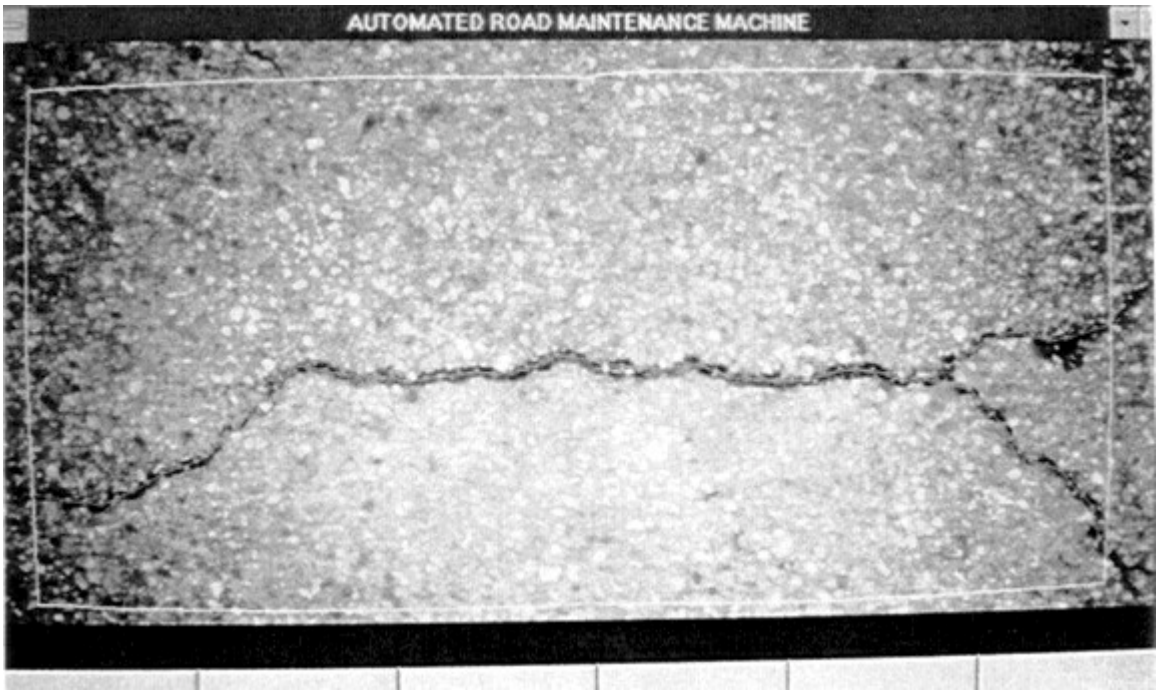

Tested Image No.10

Tested Image No.11

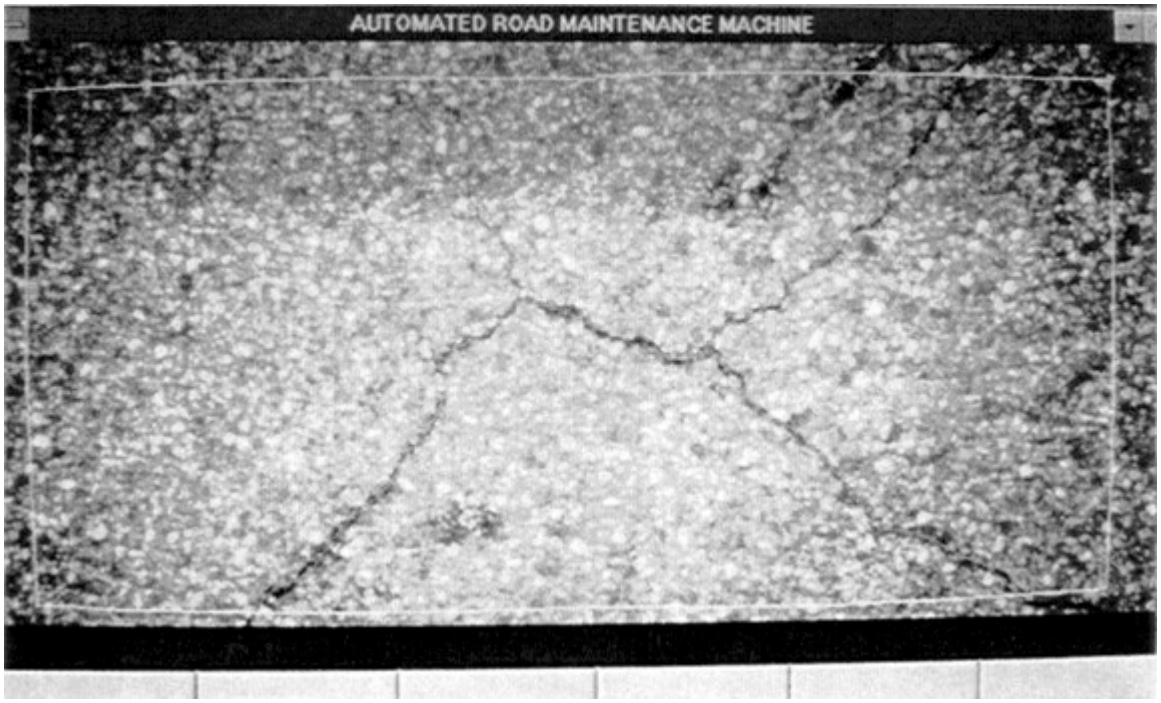

Tested Image No.12

Tested Image No.13

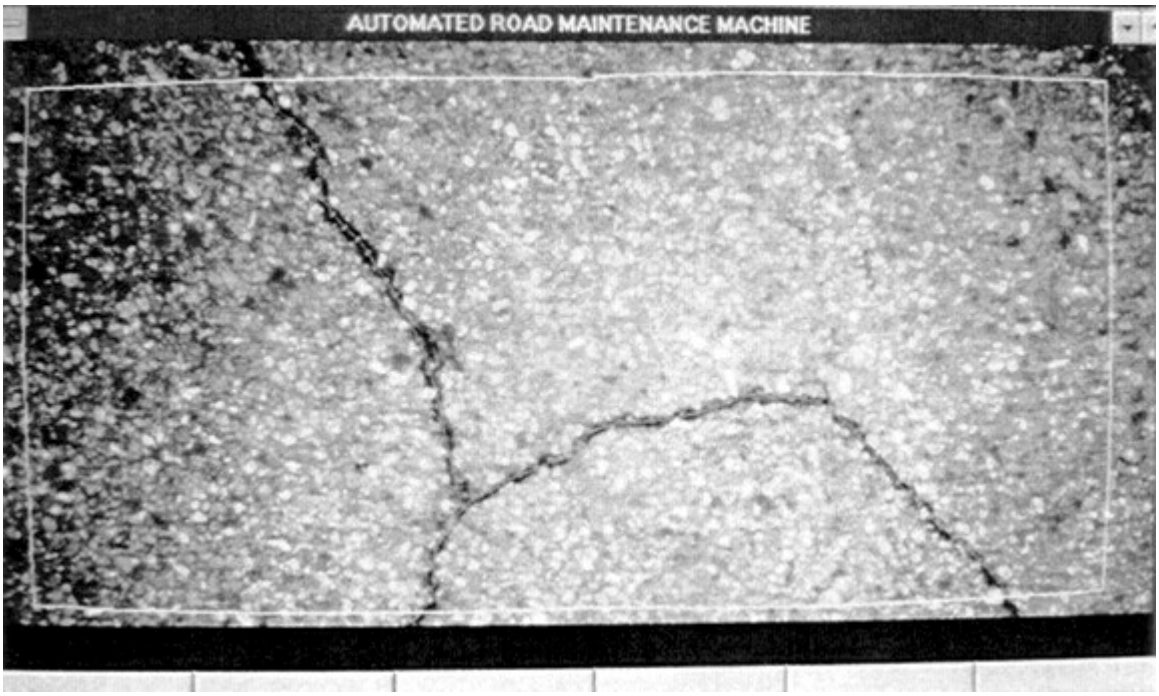

Tested Image No.14

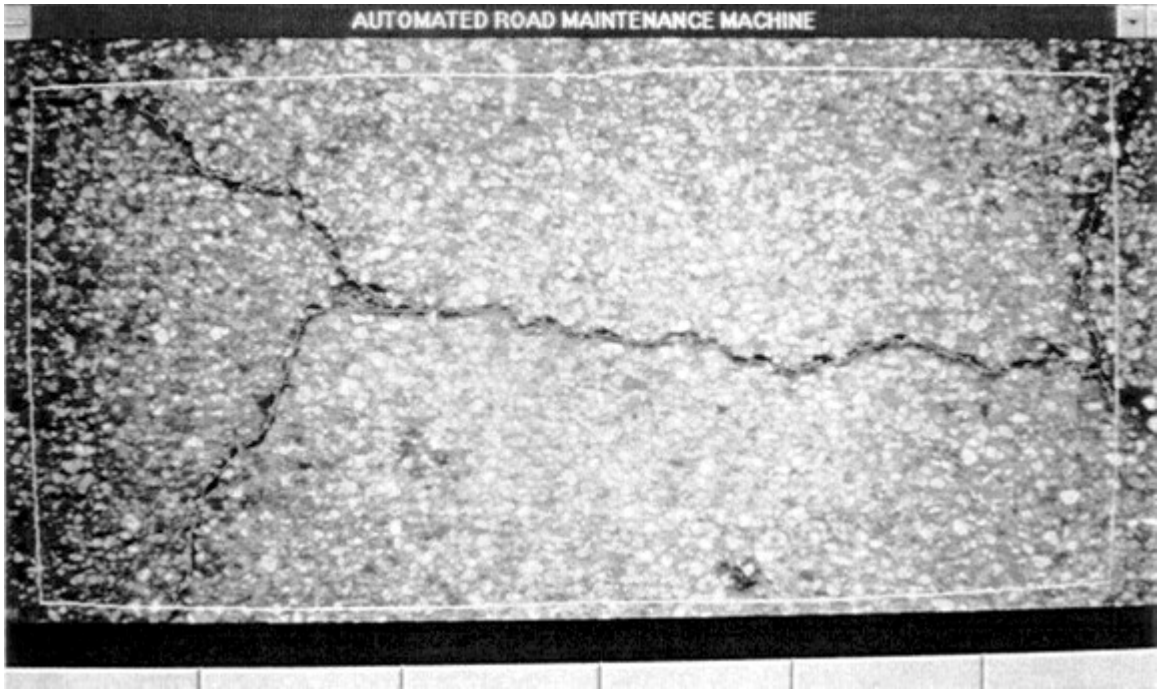

Tested Image No.15

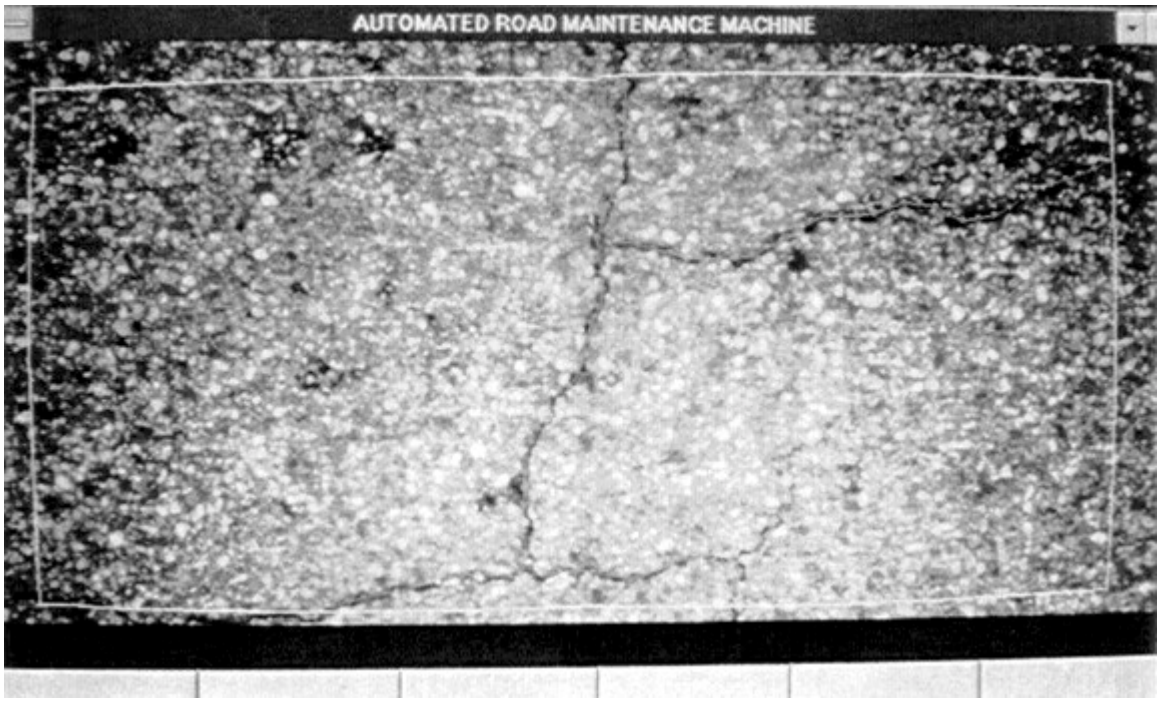

Tested Image No.16

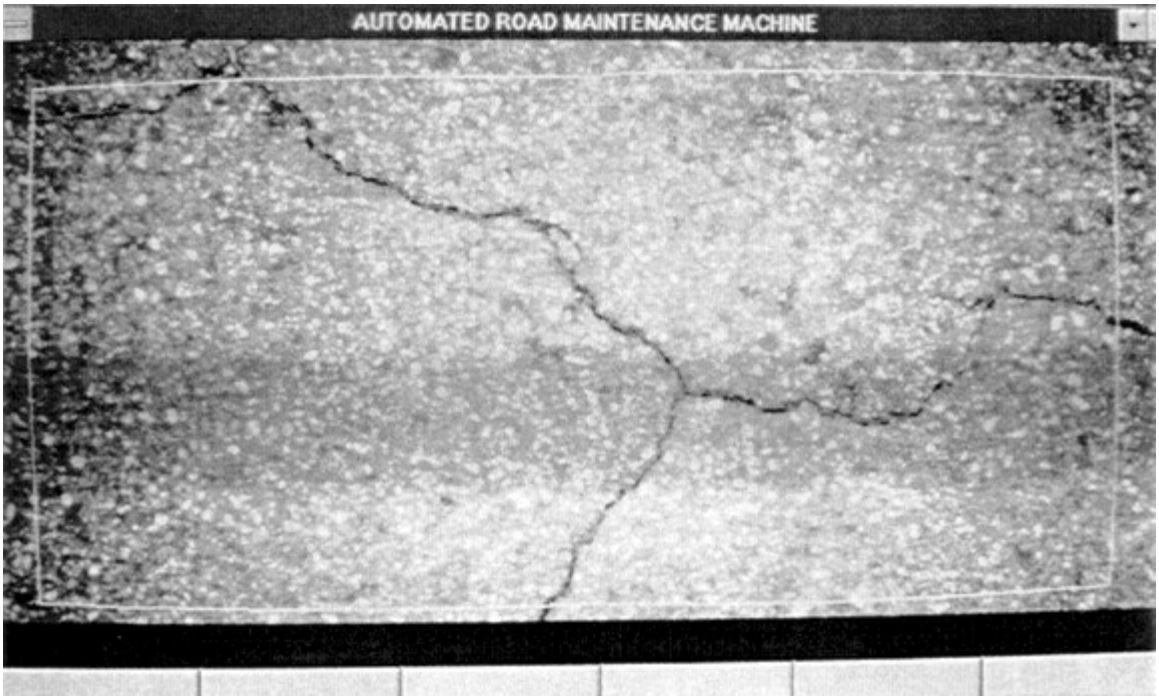

Tested Image No.17

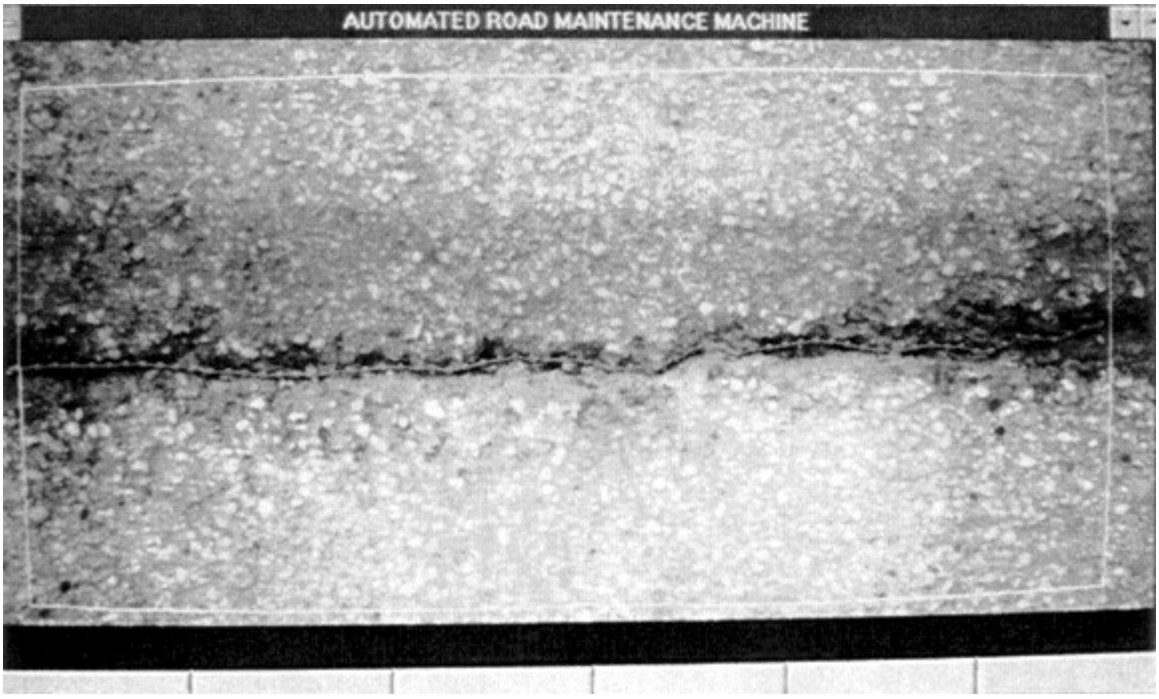

Tested Image No.18

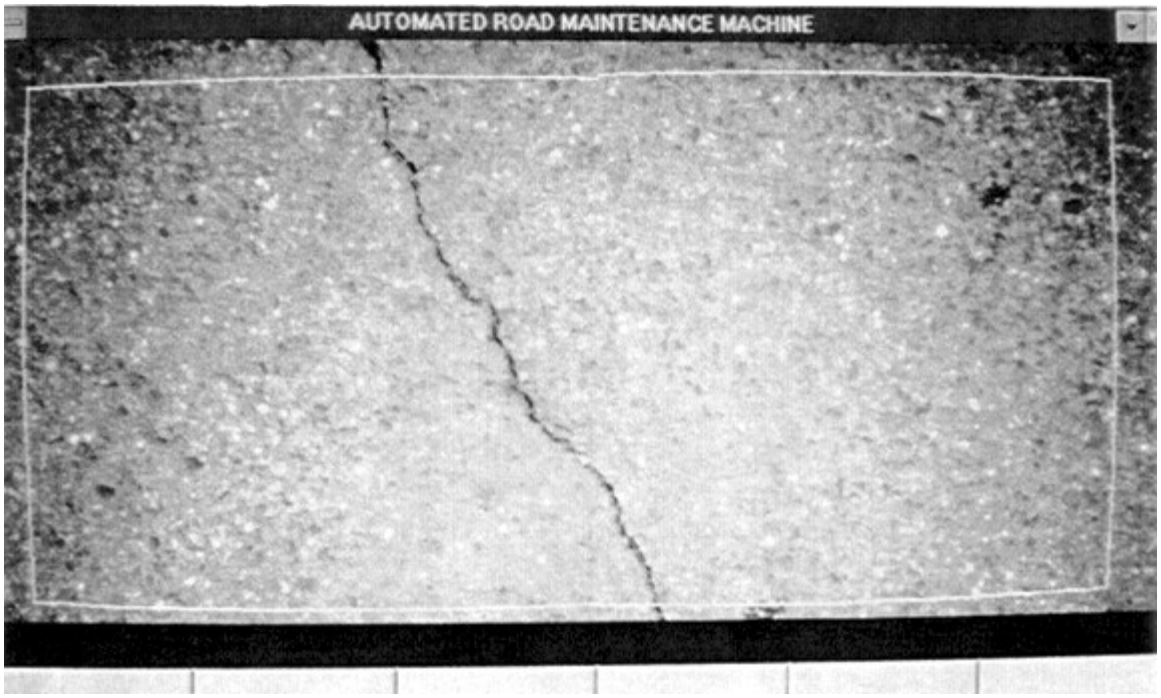

Tested Image No.19

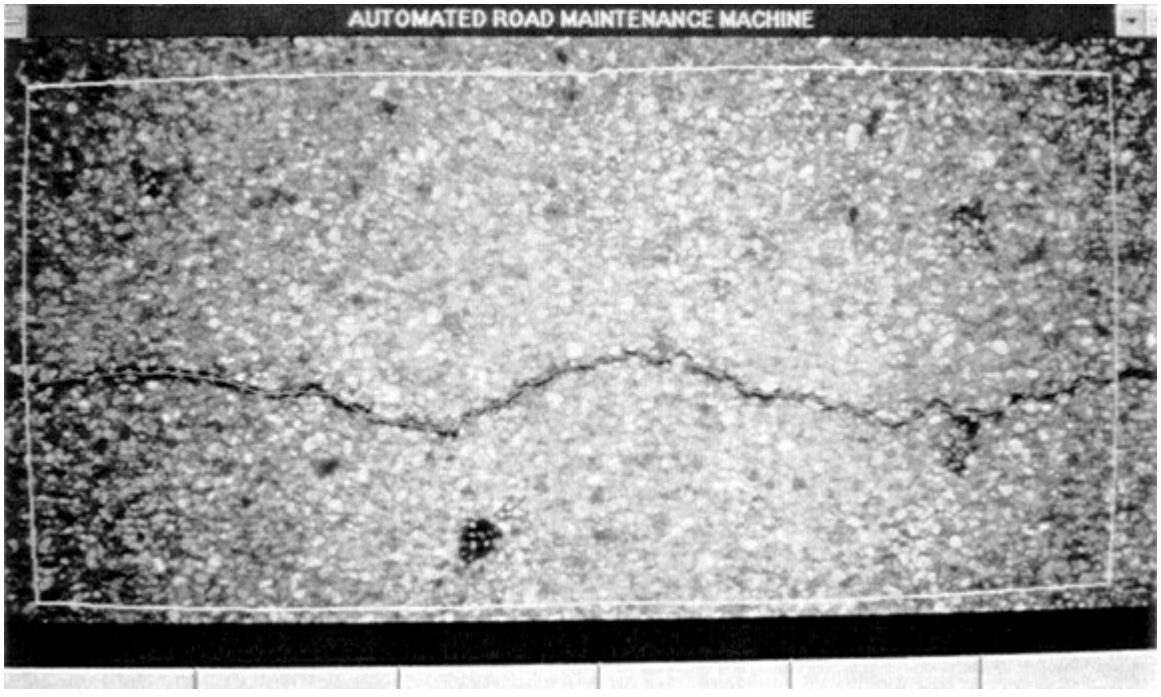

Tested Image No.20

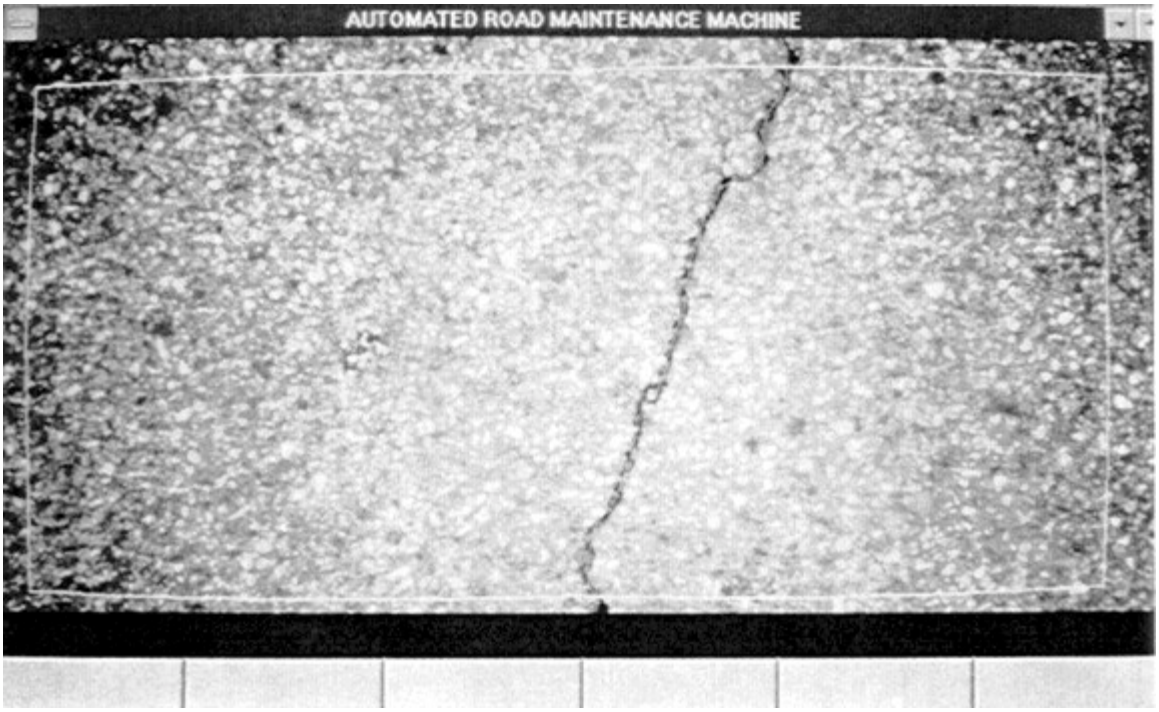

Tested Image No.21

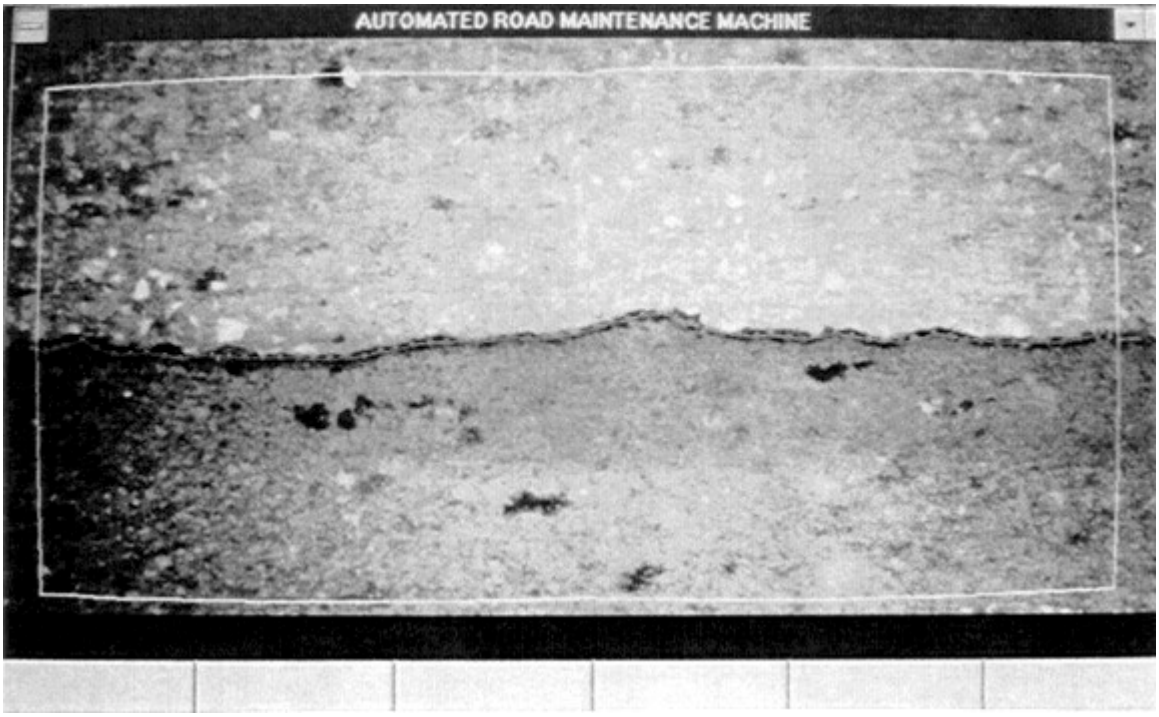

Tested Image No.22

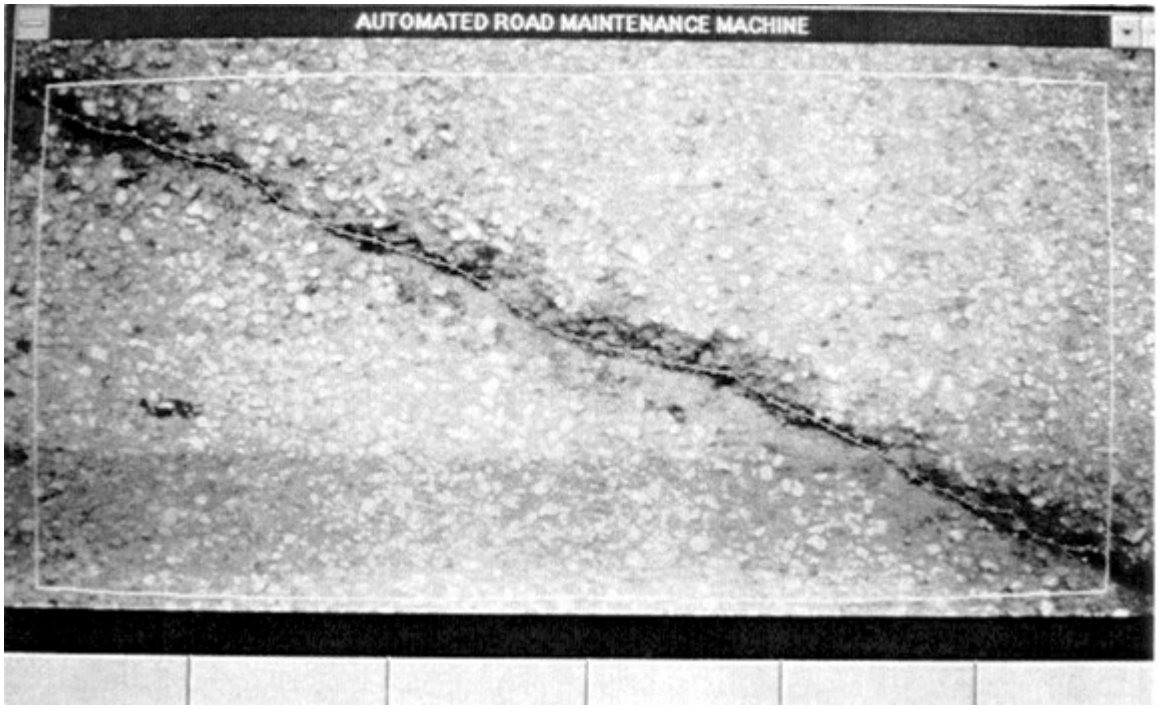

Tested Image No.23

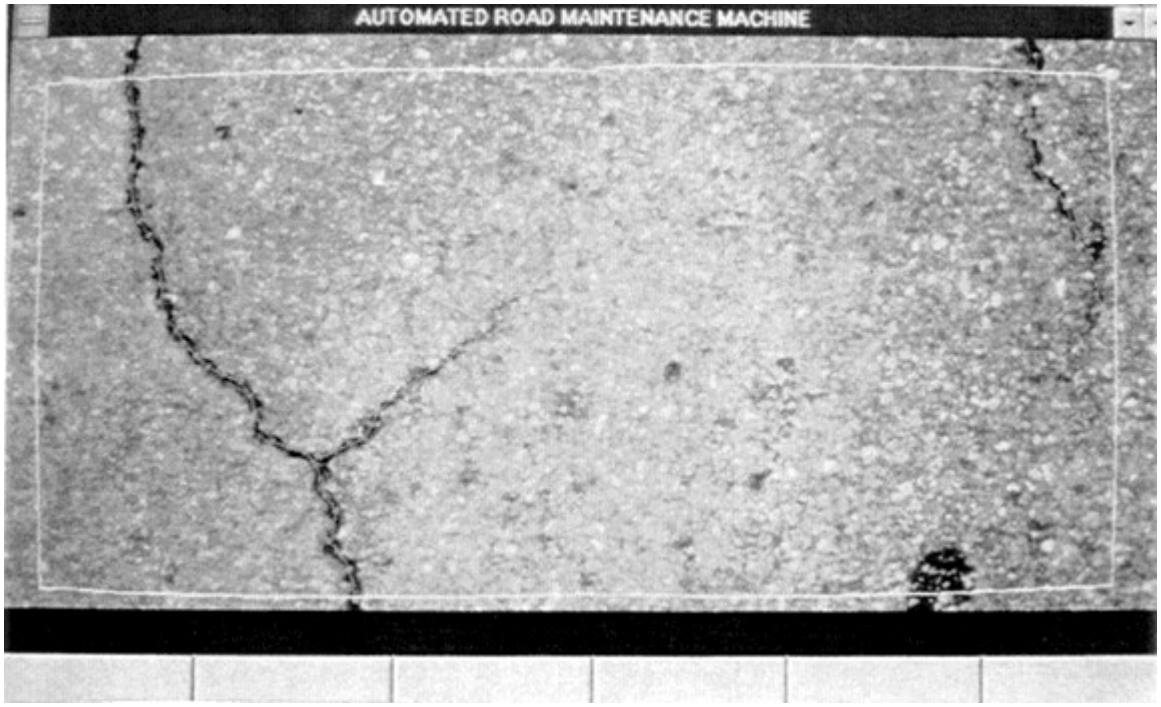

Tested Image No.24

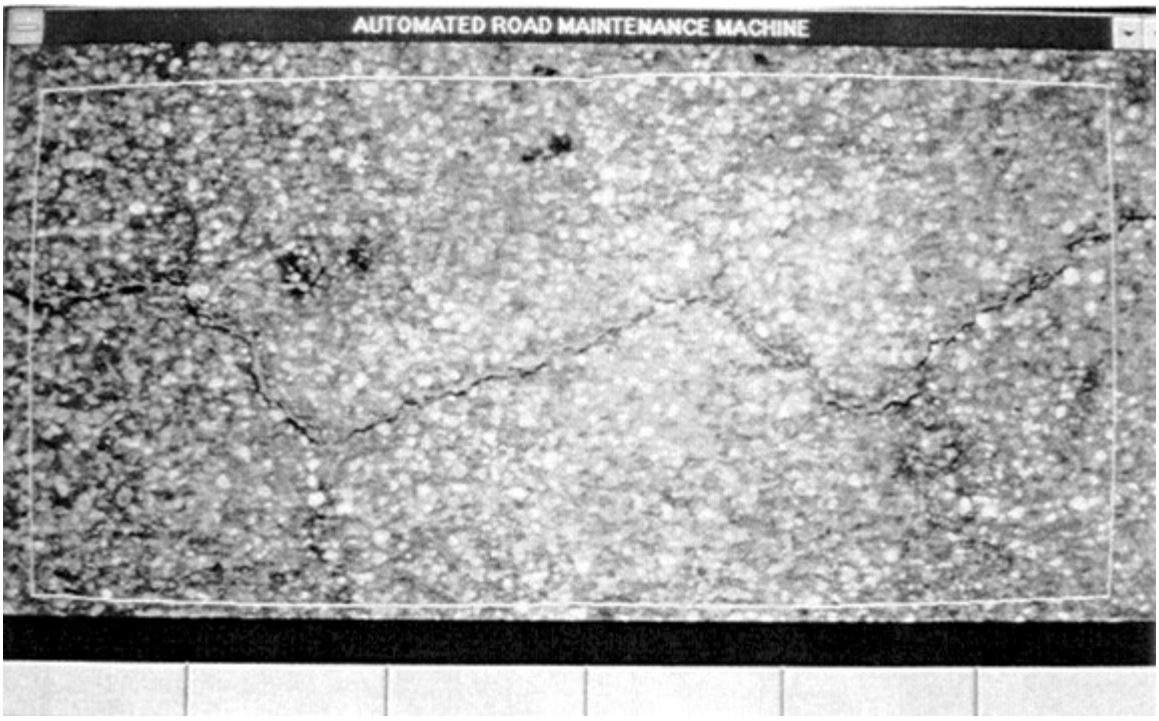

Tested Image No.25

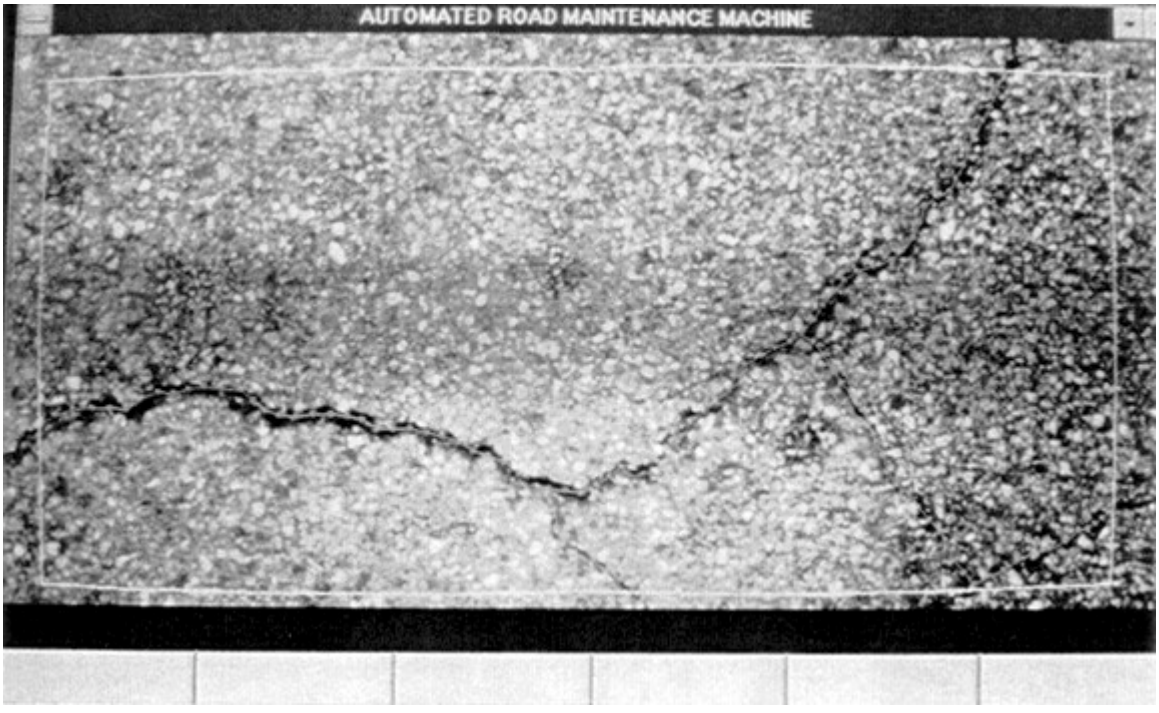

Tested Image No.26

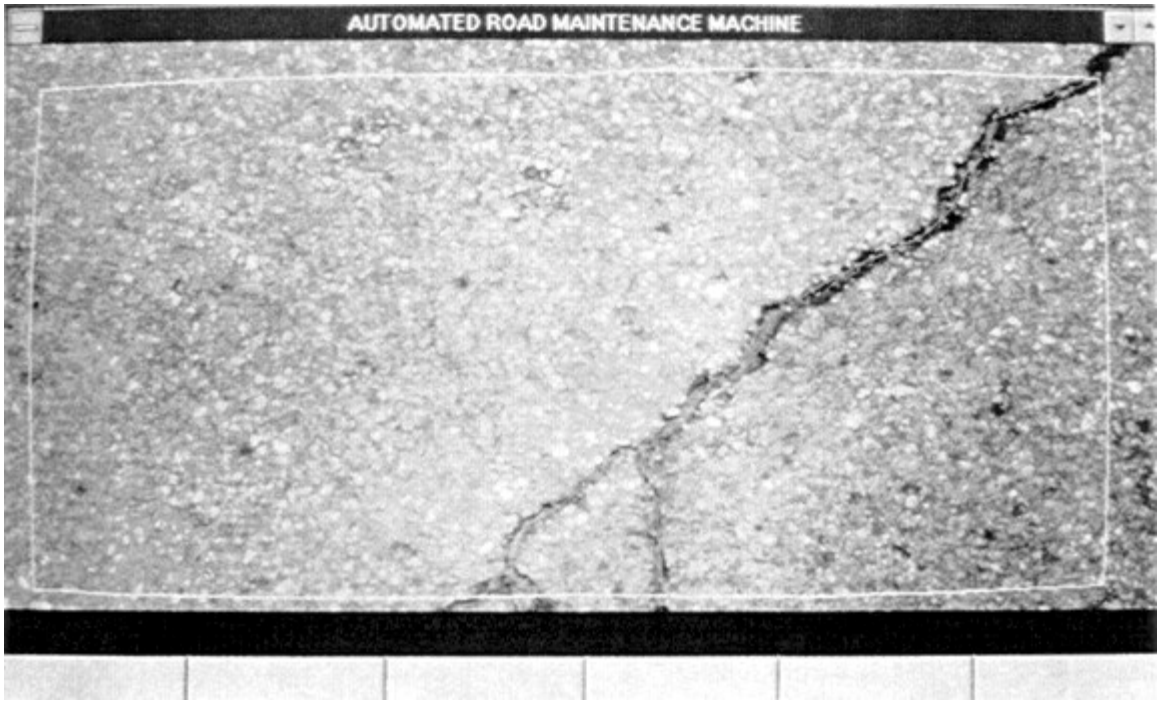

Tested Image No.27

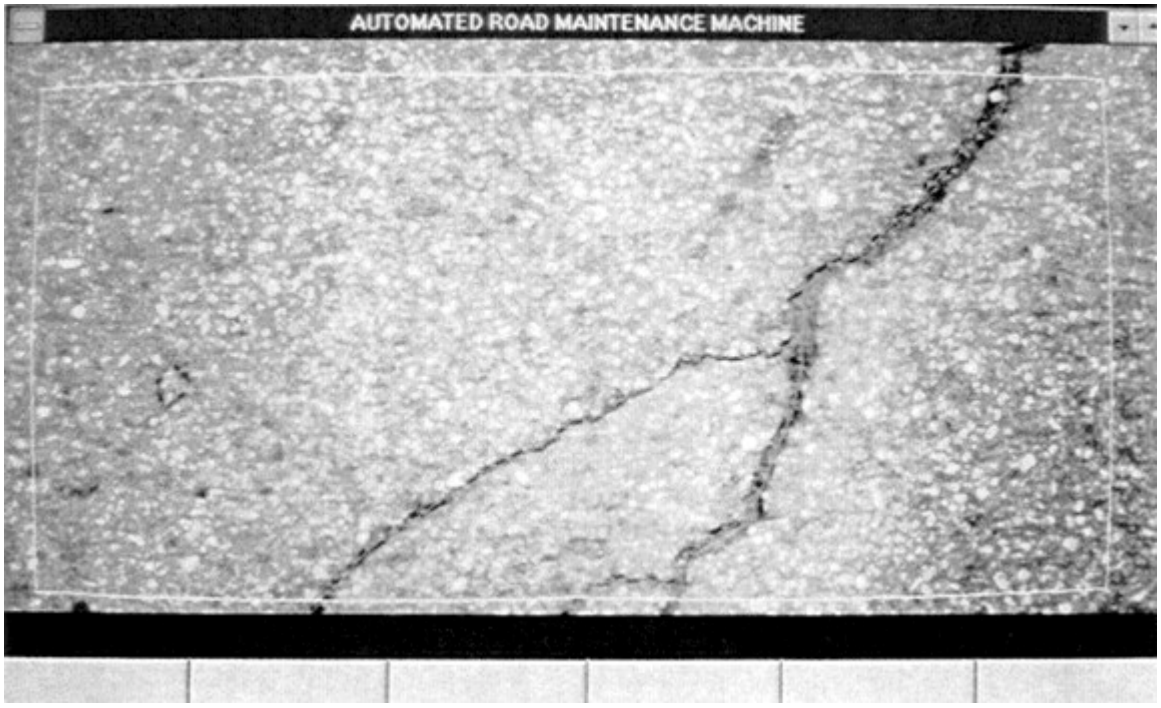

Tested Image No.28

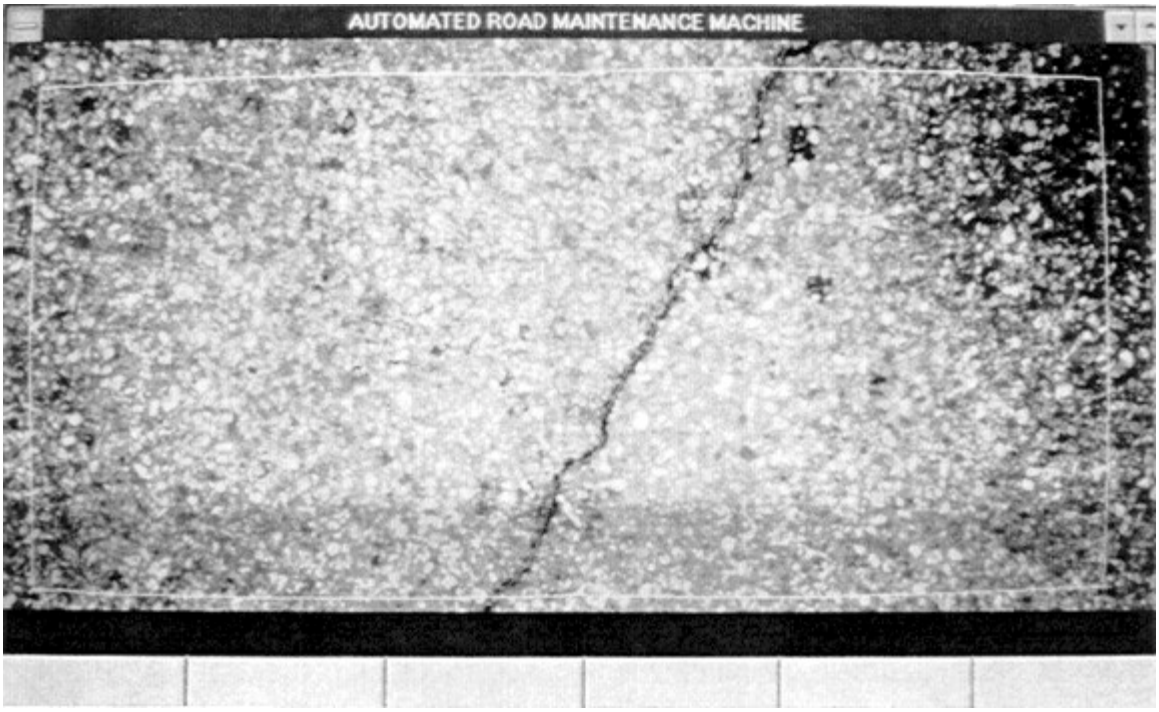

Tested Image No.29

Tested Image No.30

APPENDIX. B

Time and Accuracy Comparison Results Between Options I and II

Experimental Results of the Time and Accuracy Evaluation

Participant 1	Cracking type Longitudinal (L) Transverse (T) Blocking (B)	Total no. of node points by manual **mapping (point)**			**Total no. of errors by manual mapping (point)**			**Accuracy of the manual mapping (%)**			**Time taken for manual mapping (second)**		
		Trial			Trial			Trial			Trial		
		1st	2nd	3rd	1st	2nd	3rd	1st	2nd	3rd	1st	2nd	3rd
Image 1	B	68	68	67	14	13	9	79.41	80.88	86.57	29.98	28.43	31.36
Image 2	T	52	54	53	9	5	6	82.69	90.74	88.68	24.61	26.27	20.99
Image 3	T	35	34	35	6	3	5	82.86	91.18	85.71	10.89	11.02	9.36
Image 4	L	42	42	41	11	5	3	73.81	88.10	92.68	18.27	25.21	21.59
Image 5	T	51	50	50	8	7	9	84.31	86.00	82.00	16.77	23.46	19.46
Image 6	L	18	18	18	1	0	2	94.44	100	88.89	8.21	12.02	11.92
Image 7	L+T	36	35	36	5	7	2	86.11	80.00	94.44	22.52	19.09	21.67
Image 8	B	61	61	61	8	11	10	86.89	81.97	83.61	29.55	23.14	33.68
Image 9	T	49	49	50	6	7	7	87.76	85.71	86.00	22.90	23.43	16.46
Image 10	T	45	44	44	5	8	5	88.89	81.82	88.64	21.28	20.37	20.71

Time and Accuracy Evaluation of Manual Mapping in Option I *[Participant 1]*

Participant 1	Cracking type Longitudinal (L) Transverse (T) Blocking (B)	**Total no. of node points by manual mapping (point)**			**Total no. of errors by manual mapping (point)**			**Accuracy of the manual mapping (%)**			**Time taken for manual mapping (second)**		
		Trial			Trial			Trial			Trial		
		1st	2nd	3rd	1st	2nd	3rd	1st	2nd	3rd	1st	2nd	3rd
Image 11	L+T	53	54	54	7	7	7	86.79	87.04	87.04	28.77	35.14	24.18
Image 12	L+T	48	47	47	4	5	3	91.67	89.36	93.62	36.49	34.27	28.39
Image 13	L+T	59	60	58	7	6	7	88.14	90.00	88.93	35.42	37.02	24.84
Image 14	L+T	42	40	41	8	7	5	80.95	82.50	87.80	23.30	20.89	17.02
Image 15	L+T	58	59	58	5	5	6	91.38	91.53	89.66	38.24	39.90	27.27
Image 16	L+T	52	52	52	4	7	10	92.31	86.54	80.77	36.55	33.68	22.83
Image 17	L+T	56	55	57	5	9	9	91.07	83.64	84.21	30.55	26.77	22.08
Image 18	T	35	34	34	0	0	0	100	100	100	7.42	9.42	7.58
Image 19	L	20	21	20	1	1	3	95.00	95.24	85.00	8.36	8.18	10.23
Image 20	T	36	36	37	2	3	3	94.44	91.67	91.89	13.06	16.05	12.34

Time and Accuracy Evaluation of Manual Mapping in Option I *[Participant 1]*

Participant 1	Cracking type Longitudinal (L) Transverse (T) Blocking (B)	**Total no. of node points by manual mapping (point)** Trial			**Total no. of errors by manual mapping (point)** Trial			**Accuracy of the manual mapping (%)** Trial			**Time taken for manual mapping (second)** Trial		
		1st	2nd	3rd	1st	2nd	3rd	1st	2nd	3rd	1st	2nd	3rd
Image 21	L	20	21	20	2	1	4	90.00	95.24	80.00	8.43	7.49	8.52
Image 22	T	35	36	36	4	6	3	88.57	83.33	91.67	10.49	12.24	12.24
Image 23	T	36	36	36	1	0	5	97.22	100	86.49	6.86	8.52	7.71
Image 24	L	40	42	41	10	6	3	75.00	85.71	92.68	19.11	24.27	20.55
Image 25	T	40	40	41	6	7	8	85.00	82.50	80.49	15.99	15.40	17.08
Image 26	B	56	59	58	6	8	10	89.29	86.44	82.76	18.81	19.99	20.68
Image 27	L	35	34	34	2	1	0	94.29	97.06	100	10.65	12.90	11.05
Image 28	L	46	46	46	0	5	1	100	89.13	97.83	13.74	12.27	14.89
Image 29	L	20	20	21	1	3	2	95.00	85.00	90.48	7.93	7.33	8.02
Image 30	B	51	52	52	3	5	5	94.12	90.38	90.38	13.73	15.33	13.68
Total		1295	1299	1299	151	158	152				588.88	609.50	538.48
Average		1298 node pts. for 30 images (wrkspcs.)			154 node pts. for 30 images (wrkspcs.)			88.34	87.84	88.30	19.63	20.32	17.95
								88.16%/image (wrkspc.)			**19.30sec.**/image (wrkspc.)		

Time and Accuracy Evaluation of Manual Mapping in Option I *[Participant 1]*

Participant 1											
Crack image	**Manual editing time (Sec.)** Trial			Crack image	**Manual editing time (Sec.)** Trial			Crack image	**Manual editing time (Sec.)** Trial		
	1st	2nd	3rd		1st	2nd	3rd		1st	2nd	3rd
Image 1	61.11	51.47	50.88	Image 11	52.19	47.41	36.87	Image 21	13.75	8.63	15.56
Image 2	39.25	31.28	28.37	Image 12	37.69	34.75	26.10	Image 22	17.16	22.66	19.18
Image 3	22.19	14.28	24.60	Image 13	41.38	35.94	29.68	Image 23	8.66	1.48	17.09
Image 4	44.22	27.06	30.12	Image 14	43.75	36.91	25.10	Image 24	42.28	30.88	21.63
Image 5	39.09	34.35	51.37	Image 15	42.97	42.09	36.10	Image 25	30.34	43.25	35.88
Image 6	7.74	1.13	10.16	Image 16	41.84	43.16	38.22	Image 26	31.18	40.69	41.25
Image 7	27.69	27.96	15.85	Image 17	40.82	39.37	40.63	Image 27	19.59	9.75	5.22
Image 8	38.85	42.47	46.40	Image 18	2.01	0.58	1.54	Image 28	8.10	28.47	8.28
Image 9	31.12	37.50	37.75	Image 19	8.12	9.19	15.63	Image 29	9.97	11,00	10.72
Image 10	37.51	48.64	41.78	Image 20	13.46	13.63	18.96	Image 30	19.97	23.00	24.90
Total (Sec.)	348.77	316.14	337.30	Total (Sec.)	324.23	303.03	268.83	Total (Sec.)	201.00	219.81	199.71
Total (sec.)	Trial										
	1st			2nd			3rd				
	(348.77+324.23+201.00) = 874			(316.14+303.03+219.81) = 838			(337.30+268.83+199.71) = 805.84				
Average	29.13 sec per image			27.97 sec. per image			26.86 sec. per image				
	(29.13+27.97+26.86) = 83.96 -> 83.96/3 = **27.99 sec.** per image (wrkspc.)										

Time Evaluation of Manual Editing in Option I *[Participant 1]*

Participant 2	Cracking type Longitudinal (L) Transverse (T) Blocking (B)	**Total no. of node points by manual mapping (point)** Trial			**Total no. of errors by manual mapping (point)** Trial			**Accuracy of the manual mapping (%)** Trial			**Time taken for manual mapping (second)** Trial		
		1st	2nd	3rd	1st	2nd	3rd	1st	2nd	3rd	1st	2nd	3rd
Image 1	B	72	71	70	15	12	14	79.17	83.10	80.00	41.74	53.14	42.61
Image 2	T	50	53	52	7	13	11	86.00	75.47	78.85	31.96	34.30	32.61
Image 3	T	36	36	36	11	9	7	69.44	75.00	80.56	16.99	21.17	20.24
Image 4	L	43	45	42	10	12	9	76.74	73.33	78.57	33.83	31.21	36.92
Image 5	T	55	56	55	12	11	11	78.18	80.36	80.00	28.06	31.24	32.55
Image 6	L	18	17	18	2	1	3	88.89	94.12	83.33	8.83	7.55	8.43
Image 7	L+T	32	32	32	10	8	2	68.75	75.00	93.75	15.80	21.39	23.30
Image 8	B	64	64	64	25	11	15	60.93	82.81	76.56	37.73	49.18	42.30
Image 9	T	47	48	46	11	7	13	76.60	85.42	71.74	22.24	33.06	23.71
Image 10	T	49	49	49	5	4	7	89.80	91.84	85.71	31.37	34.40	33.02

Time and Accuracy Evaluation of Manual Mapping in Option I *[Participant 2]*

Participant 2	Cracking type Longitudinal (L) Transverse (T) Blocking (B)	**Total no. of node points by manual mapping (point)**			**Total no. of errors by manual mapping (point)**			**Accuracy of the manual mapping (%)**			**Time taken for manual mapping (second)**		
		Trial			Trial			Trial			Trial		
		1st	2nd	3rd	1st	2nd	3rd	1st	2nd	3rd	1st	2nd	3rd
Image 11	L+T	58	58	57	10	7	9	82.76	87.93	73.47	34.40	43.42	43.96
Image 12	L+T	49	49	49	8	6	13	83.67	87.76	73.47	29.33	43.80	42.18
Image 13	L+T	60	60	60	15	10	19	75.00	83.33	68.33	46.24	45.58	50.11
Image 14	L+T	40	40	40	6	2	7	85.00	95.00	82.50	24.80	24.89	25.55
Image 15	L+T	57	58	60	12	17	12	78.95	70.69	80.00	43.86	41.62	32.89
Image 16	L+T	55	55	54	11	5	9	80.00	90.91	83.33	42.95	47.83	46.96
Image 17	L+T	51	53	53	13	12	11	74.51	77.36	79.25	37.70	42.49	48.46
Image 18	T	35	34	35	0	3	0	100	91.18	100	10.64	10.12	10.93
Image 19	L	20	20	20	3	5	2	85.00	75.00	90.00	10.68	10.64	10.18
Image 20	T	35	36	36	5	2	5	85.71	94.44	86.11	15.74	19.74	16.02

Time and Accuracy Evaluation of Manual Mapping in Option I *[Participant 2]*

Participant 2	Cracking type Longitudinal (L) Transverse (T) Blocking (B)	**Total no. of node points by manual mapping (point)**			**Total no. of errors by manual mapping (point)**			**Accuracy of the manual mapping (%)**			**Time taken for manual mapping (second)**		
		Trial			Trial			Trial			Trial		
		1st	2nd	3rd	1st	2nd	3rd	1st	2nd	3rd	1st	2nd	3rd
Image 21	L	19	19	18	4	0	4	78.95	100	77.78	10.37	12.67	10.30
Image 22	T	35	35	35	4	2	1	88.57	94.29	97.14	14.05	19.24	16.39
Image 23	T	36	37	37	0	0	0	100	100	100	6.39	7.49	8.73
Image 24	L	38	39	39	7	9	7	81.58	76.92	82.05	24.52	29.93	34.40
Image 25	T	42	40	41	6	7	6	85.71	82.50	85.37	36.99	23.89	21.84
Image 26	B	59	59	58	12	4	14	79.66	93.22	75.86	27.74	36.58	29.15
Image 27	L	35	34	35	5	5	5	85.71	85.29	85.71	17.74	19.33	19.52
Image 28	L	42	42	43	5	3	5	88.10	92.86	88.37	22.49	22.02	19.92
Image 29	L	20	21	21	3	4	3	85.00	80.95	85.71	13.21	14.33	11.11
Image 30	B	53	52	51	4	6	9	92.45	88.46	82.35	18.37	19.86	23.24
Total		1305	1312	1306	241	196	243				756.76	895.53	818.13
Average		1308 node pts. for 30 images (wrkspcs.)			227 node pts. for 30 images (wrkspcs.)			81.53	85.06	81.39	25.23	29.85	27.27
								82.67%/image (wrkspc.)			**27.45 sec.**/image (wrkspc.)		

Time and Accuracy Evaluation of Manual Mapping in Option I *[Participant 2]*

Participant 2											
Crack image	**Manual editing time (Sec.)** Trial			Crack image	**Manual editing time (Sec.)** Trial			Crack image	**Manual editing time (Sec.)** Trial		
	1st	2nd	3rd		1st	2nd	3rd		1st	2nd	3rd
Image 1	62.97	70.16	61.66	Image 11	49.81	47.31	45.94	Image 21	14.75	7.75	20.57
Image 2	38.03	57.85	49.16	Image 12	58.87	35.07	52.78	Image 22	19.57	21.59	15.43
Image 3	34.69	39.35	28.50	Image 13	58.90	50.41	55.03	Image 23	1.61	1.65	1.35
Image 4	36.91	49.09	41.54	Image 14	24.63	19.56	33.25	Image 24	32.78	32.03	42.37
Image 5	43.65	43.47	49.50	Image 15	53.69	78.14	70.75	Image 25	31.65	35.41	39.59
Image 6	10.87	5.88	10.72	Image 16	47.54	41.69	40.28	Image 26	58.85	32.15	51.29
Image 7	34.16	29.59	19.41	Image 17	53.88	55.65	48.19	Image 27	21.81	41.37	24.34
Image 8	95.34	42.93	80.10	Image 18	5.53	16.81	9.47	Image 28	22.43	24.75	48.94
Image 9	44.84	33.53	53.22	Image 19	12.19	14.03	15.47	Image 29	16.06	24.41	15.94
Image 10	42.37	42.78	41.57	Image 20	21.35	14.90	31.35	Image 30	56.21	39.59	29.66
Total (Sec.)	443.83	414.63	435.38	Total (Sec.)	386.39	373.57	402.41	Total (Sec.)	255.72	260.70	289.48
Total (sec.)	Trial										
	1st			2nd			3rd				
	(443.83+386.39+255.72) = 1085.96			(414.63+373.57+260.70) = 1048.90			(435.38+402.41+289.48) = 1127.27				
Average	36.20 sec per image			34.96 sec. per image			37.58 sec. per image				
	(36.20+34.96+37.58) = 108.74 -> 108.74/3 = **36.25 sec.** per image (wrkspc.)										

Time Evaluation of Manual Editing in Option I *[Participant 2]*

Participant 3	Cracking type Longitudinal (L) Transverse (T) Blocking (B)	**Total no. of node points by manual mapping (point)**			**Total no. of errors by manual mapping (point)**			**Accuracy of the manual mapping (%)**			**Time taken for manual mapping (second)**		
		Trial			Trial			Trial			Trial		
		1st	2nd	3rd	1st	2nd	3rd	1st	2nd	3rd	1st	2nd	3rd
Image 1	B	70	71	70	10	19	17	85.71	73.24	75.71	31.75	34.91	39.00
Image 2	T	54	52	52	7	8	6	87.04	84.62	88.46	38.84	27.44	29.59
Image 3	T	36	36	35	5	7	8	86.11	80.56	77.14	15.97	17.66	18.56
Image 4	L	44	43	42	9	8	9	79.56	81.40	78.57	31.65	34.50	31.72
Image 5	T	55	53	55	12	11	7	78.18	79.25	87.27	30.35	30.72	29.63
Image 6	L	18	18	18	2	3	4	88.89	83.33	77.78	10.78	11.66	12.66
Image 7	L+T	35	33	35	6	7	4	82.86	78.78	88.57	25.09	19.50	21.41
Image 8	B	63	64	64	13	12	9	79.37	81.25	85.94	50.00	39.78	35.65
Image 9	T	46	45	47	7	8	6	84.78	82.22	87.23	23.91	22.13	23.31
Image 10	T	50	50	48	10	7	10	80.00	86.00	79.17	26.40	24.47	28.50

Time and Accuracy Evaluation of Manual Mapping in Option I *[Participant 3]*

Participant 3	Cracking type Longitudinal (L) Transverse (T) Blocking (B)	**Total no. of node points by manual mapping (point)**			**Total no. of errors by manual mapping (point)**			**Accuracy of the manual mapping (%)**			**Time taken for manual mapping (second)**		
		Trial			Trial			Trial			Trial		
		1st	2nd	3rd	1st	2nd	3rd	1st	2nd	3rd	1st	2nd	3rd
Image 11	L+T	70	71	72	9	5	12	87.14	92.96	83.33	35.72	38.12	36.87
Image 12	L+T	54	52	53	11	10	12	79.63	80.77	77.34	33.25	32.03	30.88
Image 13	L+T	59	60	60	12	8	13	79.66	86.67	78.33	42.59	43.50	42.93
Image 14	L+T	40	39	39	4	2	2	90.00	94.87	94.87	21.91	22.84	20.50
Image 15	L+T	58	58	58	13	14	12	77.59	75.86	79.31	40.63	34.13	33.88
Image 16	L+T	53	52	55	6	7	8	88.68	86.54	85.45	30.28	31.66	29.54
Image 17	L+T	53	52	53	9	12	12	83.02	76.92	77.36	28.03	25.47	29.87
Image 18	T	34	34	34	0	0	1	100	100	97.06	2.01	1.99	1.87
Image 19	L	20	19	20	2	1	1	90.00	94.74	95.00	11.69	10.65	9.91
Image 20	T	36	35	35	5	5	3	86.11	85.71	91.43	16.84	17.69	15.11

Time and Accuracy Evaluation of Manual Mapping in Option I *[Participant 3]*

Participant 3	Cracking type Longitudinal (L) Transverse (T) Blocking (B)	**Total no. of node points by manual mapping (point)**			**Total no. of errors by manual mapping (point)**			**Accuracy of the manual mapping (%)**			**Time taken for manual mapping (second)**		
		Trial			Trial			Trial			Trial		
		1st	2nd	3rd	1st	2nd	3rd	1st	2nd	3rd	1st	2nd	3rd
Image 21	L	19	19	19	3	2	2	84.21	89.47	89.47	11.00	12.66	9.06
Image 22	T	35	35	34	1	0	0	97.14	100	100	11.10	11.22	10.09
Image 23	T	36	36	36	0	0	1	100	100	97.22	6.56	8.15	7.34
Image 24	L	39	37	38	6	8	5	84.62	78.38	86.84	26.75	23.12	31.19
Image 25	T	42	40	40	5	4	7	88.10	90.00	82.50	23.78	21.59	26.13
Image 26	B	59	59	57	7	10	7	88.14	83.05	87.72	38.62	32.57	36.47
Image 27	L	33	35	34	4	1	0	87.88	97.14	100	17.32	18.56	17.13
Image 28	L	42	42	41	3	1	1	92.86	97.62	97.56	20.41	21.46	18.47
Image 29	L	20	20	19	0	2	4	100	90.00	78.95	14.75	12.75	11.53
Image 30	B	52	53	53	2	0	0	96.15	100	100	17.90	18.94	15.53
Total		1325	1313	1316	183	182	183				735.88	701.87	704.33
Average		1318 node pts. for 30 images (wrkspcs.)			183 node pts. for 30 images (wrkspcs.)			86.19	86.14	86.09	24.53	23.40	23.48
								86.14%/image (wrkspc.)			**23.80 sec.**/image (wrkspc.)		

Time and Accuracy Evaluation of Manual Mapping in Option I *[Participant 3]*

Participant 3											
Crack image	**Manual editing time (Sec.)** Trial			Crack image	**Manual editing time (Sec.)** Trial			Crack image	**Manual editing time (Sec.)** Trial		
	1st	2nd	3rd		1st	2nd	3rd		1st	2nd	3rd
Image 1	46.53	50.62	45.65	Image 11	26.25	20.10	30.65	Image 21	11.22	8.39	6.91
Image 2	28.28	25.24	22.15	Image 12	30.16	28.87	34.59	Image 22	4.28	2.24	2.19
Image 3	16.37	21.47	25.00	Image 13	34.19	32.40	29.37	Image 23	2.47	2.60	3.22
Image 4	34.44	28.43	24.12	Image 14	12.28	9.16	10.38	Image 24	16.85	21.47	16.12
Image 5	40.28	34.00	27.06	Image 15	37.47	34.63	25.28	Image 25	16.11	16.79	25.92
Image 6	12.06	11.18	12.22	Image 16	18.53	19.57	24.10	Image 26	23.50	24.82	16.91
Image 7	20.03	21.40	16.15	Image 17	29.09	28.53	33.44	Image 27	12.72	6.69	2.99
Image 8	39.57	30.65	27.50	Image 18	7.47	7.78	6.98	Image 28	8.66	6.68	6.63
Image 9	19.47	28.59	18.69	Image 19	7.22	8.12	7.34	Image 29	2.17	5.88	12.12
Image 10	24.31	20.78	25.69	Image 20	14.78	15.09	12.00	Image 30	6.13	4.50	3.13
Total (Sec.)	281.34	272.36	244.23	Total (Sec.)	217.44	204.25	214.13	Total (Sec.)	104.11	100.06	94.70
Total (sec.)	Trial										
	1st			2nd			3rd				
	(281.34+217.44+104.11) = 602.89			(272.36+204.25+100.06) = 576.67			(244.23+214.13+94.70) = 553.06				
Average	20.10 sec per image			19.22 sec. per image			18.44 sec. per image				
	(20.10+19.22+18.44) = 57.76 -> 57.76/3 = **19.25 sec.** per image (wrkspc.)										

Time Evaluation of Manual Editing in Option I *[Participant 3]*

Participant 1	Cracking type Longitudinal (L) Transverse (T) Blocking (B)	**Total no. of node points by manual mapping (point)**			**Total no. of errors by manual mapping (point)**			**Accuracy of the manual mapping (%)**			**Time taken for manual mapping (second)**		
		Trial			Trial			Trial			Trial		
		1st	2nd	3rd	1st	2nd	3rd	1st	2nd	3rd	1st	2nd	3rd
Image 1	B	67	67	67	16	14	12	76.12	76.67	82.09	15.46	16.89	21.58
Image 2	T	50	52	52	13	8	15	74.00	84.62	71.15	11.90	12.30	9.67
Image 3	T	35	35	34	11	9	13	68.57	74.29	61.76	4.90	4.50	5.14
Image 4	L	42	41	41	10	5	10	76.19	87.80	75.61	11.06	12.47	8.81
Image 5	T	51	52	52	23	10	10	54.90	80.77	80.77	6.87	9.59	8.82
Image 6	L	19	20	19	6	3	6	68.42	85.00	68.42	3.07	3.00	2.78
Image 7	L+T	34	32	34	9	10	8	73.53	68.75	76.47	8.09	9.50	6.19
Image 8	B	61	61	60	20	16	17	67.21	73.77	71.67	10.18	11.87	9.38
Image 9	T	49	48	48	14	6	8	71.43	87.50	83.73	6.43	8.81	8.81
Image 10	T	45	45	45	12	13	10	73.33	71.11	77.78	6.12	6.18	8.94

Time and Accuracy Evaluation of Manual Mapping in Option II *[Participant 1]*

Participant 1	Cracking type Longitudinal (L) Transverse (T) Blocking (B)	**Total no. of node points by manual mapping (point)**			**Total no. of errors by manual mapping (point)**			**Accuracy of the manual mapping (%)**			**Time taken for manual mapping (second)**		
		Trial			Trial			Trial			Trial		
		1st	2nd	3rd	1st	2nd	3rd	1st	2nd	3rd	1st	2nd	3rd
Image 11	L+T	56	55	55	17	13	17	69.64	76.36	69.09	9.69	12.34	10.87
Image 12	L+T	48	48	49	21	8	10	56.25	83.33	79.59	10.06	10.63	9.78
Image 13	L+T	58	58	57	18	21	15	68.97	63.79	73.68	11.75	9.13	11.21
Image 14	L+T	41	41	42	11	8	10	73.17	80.49	76.19	5.25	5.18	6.03
Image 15	L+T	59	58	59	9	11	11	84.75	81.03	81.36	12.47	11.84	12.19
Image 16	L+T	50	50	51	12	13	14	76.00	74.00	72.55	9.90	11.16	8.96
Image 17	L+T	54	56	55	12	11	6	77.78	80.36	89.09	8.46	9.34	9.19
Image 18	T	31	32	34	0	6	8	100	81.25	76.47	3.97	2.47	3.50
Image 19	L	20	19	19	5	5	8	75.00	73.68	58.89	2.12	2.15	2.59
Image 20	T	35	35	34	14	8	9	60.00	77.14	73.53	3.19	4.32	4.85

Time and Accuracy Evaluation of Manual Mapping in Option II *[Participant 1]*

Participant 1	Cracking type Longitudinal (L) Transverse (T) Blocking (B)	**Total no. of node points by manual mapping (point)**			**Total no. of errors by manual mapping (point)**			**Accuracy of the manual mapping (%)**			**Time taken for manual mapping (second)**		
		Trial			Trial			Trial			Trial		
		1st	2nd	3rd	1st	2nd	3rd	1st	2nd	3rd	1st	2nd	3rd
Image 21	L	21	21	21	12	8	7	42.86	61.90	80.56	2.07	3.53	4.75
Image 22	T	36	35	36	14	8	7	61.11	77.14	80.56	2.25	2.69	4.03
Image 23	T	37	36	37	2	1	4	94.59	97.22	86.67	4.28	3.09	3.9
Image 24	L	38	38	37	12	14	14	68.42	63.16	62.16	5.44	5.25	5.03
Image 25	T	40	40	40	18	19	11	55.00	52.50	72.50	3.69	4.00	3.87
Image 26	B	57	55	55	10	12	13	82.46	78.18	76.36	6.66	10.19	7.09
Image 27	L	34	34	36	8	4	7	76.47	88.24	80.00	5.28	5.66	4.94
Image 28	L	46	44	46	8	5	8	82.61	88.64	82.61	6.72	6.41	6.28
Image 29	L	20	19	19	7	4	9	65.00	78.95	52.63	2.07	2.97	2.56
Image 30	B	51	52	52	11	9	4	78.43	82.69	92.31	4.12	6.47	5.75
Total		1285	1279	1285	355	282	301				203.52	223.93	216.78
Average		1283 node pts. for 30 images (wrkspcs.)			313 node pts. for 30 images (wrkspcs.)			72.37	77.95	76.58	6.78	7.46	7.23
								75.63%/image (wrkspc.)			**7.16 sec.**/image (wrkspc.)		

Time and Accuracy Evaluation of Manual Mapping in Option II *[Participant 1]*

Participant 1	Cracking type Longitudinal (L) Transverse (T) Blocking (B)	**Total no. of node points by line snapping (point)**			**Total no. of errors by line snapping (point)**			**Accuracy of the line snapping (%)**			**Time taken for line snapping (second)**		
		Trial			Trial			Trial			Trial		
		1st	2nd	3rd	1st	2nd	3rd	1st	2nd	3rd	1st	2nd	3rd
Image 1	B	133	133	133	3	4	4	97.74	96.99	96.99	1.82	1.82	1.81
Image 2	T	99	103	103	0	1	2	100	99.03	98.06	1.26	1.37	1.37
Image 3	T	69	69	67	0	2	0	100	97.10	100	0.93	0.94	0.88
Image 4	L	83	81	81	4	4	4	95.18	95.06	95.06	1.10	1.05	1.04
Image 5	T	101	103	103	3	1	1	97.03	99.03	99.03	1.43	1.48	1.48
Image 6	L	37	39	37	0	0	0	100	100	100	0.44	0.49	0.44
Image 7	L+T	67	63	67	0	0	0	100	100	100	0.94	0.82	0.94
Image 8	B	121	121	119	1	2	2	99.17	98.35	98.32	1.70	1.70	1.65
Image 9	T	97	95	95	2	1	2	97.94	98.95	97.89	1.32	1.27	1.27
Image 10	T	89	89	89	0	1	1	100	98.88	98.88	1.21	1.21	1.21

Time and Accuracy Evaluation of the Line Snapping Function *[Participant 1]*

Participant 1	Cracking type Longitudinal (L) Transverse (T) Blocking (B)	**Total no. of node points by line snapping (point)**			**Total no. of errors by line snapping (point)**			**Accuracy of the line snapping (%)**			**Time taken for line snapping (second)**		
		Trial			Trial			Trial			Trial		
		1st	2nd	3rd	1st	2nd	3rd	1st	2nd	3rd	1st	2nd	3rd
Image 11	L+T	111	109	109	4	2	4	96.40	98.17	96.33	1.54	1.48	1.48
Image 12	L+T	95	95	97	2	2	5	97.89	97.89	94.85	1.27	1.26	1.32
Image 13	L+T	115	115	113	2	5	1	98.26	95.65	99.12	1.59	1.59	1.54
Image 14	L+T	81	81	83	0	1	1	100	98.77	98.80	1.05	1.04	1.10
Image 15	L+T	117	115	117	3	1	1	97.44	99.13	99.15	1.53	1.48	1.54
Image 16	L+T	99	99	101	0	0	0	100	100	100	1.32	1.32	1.37
Image 17	L+T	107	111	109	1	1	0	99.07	99.10	100	1.26	1.38	1.32
Image 18	T	61	63	67	0	1	0	100	98.41	100	0.82	0.88	0.98
Image 19	L	39	37	37	2	0	0	94.87	100	100	0.55	0.49	0.49
Image 20	T	69	69	67	1	1	0	98.55	98.55	100	0.99	0.99	0.94

Time and Accuracy Evaluation of the Line Snapping Function *[Participant 1]*

Participant 1	Cracking type Longitudinal (L) Transverse (T) Blocking (B)	**Total no. of node points by line snapping (point)**			**Total no. of errors by line snapping (point)**			**Accuracy of the line snapping (%)**			**Time taken for line snapping (second)**		
		Trial			Trial			Trial			Trial		
		1st	2nd	3rd	1st	2nd	3rd	1st	2nd	3rd	1st	2nd	3rd
Image 21	L	41	41	41	1	1	1	97.56	97.56	97.56	0.49	0.50	0.49
Image 22	T	71	69	71	0	2	0	100	97.10	100	0.93	0.87	0.94
Image 23	T	73	71	73	0	0	1	100	100	98.63	1.05	0.99	1.04
Image 24	L	75	75	73	1	1	2	98.67	98.67	97.26	0.99	0.99	0.93
Image 25	T	79	79	79	0	1	0	100	98.73	100	1.04	1.05	1.04
Image 26	B	113	109	109	1	0	1	99.12	100	99.08	1.59	1.49	1.48
Image 27	L	67	67	69	0	0	0	100	100	100	0.88	0.88	0.93
Image 28	L	91	87	91	0	1	0	100	98.85	100	1.15	1.05	1.16
Image 29	L	39	37	37	3	0	0	92.31	100	100	0.55	0.50	0.50
Image 30	B	101	103	103	2	3	2	98.02	97.09	98.06	1.21	1.26	1.26
Total		2540	2528	2540	36	39	35				33.95	33.64	33.94
Average		2356 node pts. for 30 images (wrkspcs.)			37 node pts. for 30 images (wrkspcs.)			98.58	98.46	98.62	1.13	1.12	1.13
								98.50%/image (wrkspc.)			**1.13 sec.**/image (wrkspc.)		

Time and Accuracy Evaluation of the Line Snapping Function *[Participant 1]*

Participant 1											
Crack image	**Manual editing time (Sec.)** Trial			Crack image	**Manual editing time (Sec.)** Trial			Crack image	**Manual editing time (Sec.)** Trial		
	1st	2nd	3rd		1st	2nd	3rd		1st	2nd	3rd
Image 1	13.27	15.12	13.33	Image 11	13.56	9.16	14.10	Image 21	3.50	4.06	5.28
Image 2	6.11	6.30	9.00	Image 12	9.72	7.31	13.60	Image 22	2.25	6.47	2.81
Image 3	2.00	6.00	3.14	Image 13	9.93	14.40	8.90	Image 23	3.84	2.28	3.28
Image 4	17.00	18.44	13.38	Image 14	3.53	3.47	4.50	Image 24	6.49	5.88	5.47
Image 5	12.85	8.68	6.43	Image 15	10.84	9.34	5.12	Image 25	3.53	3.72	3.12
Image 6	2.82	2.50	2.63	Image 16	3.75	4.41	5.21	Image 26	8.38	6.83	7.50
Image 7	4.43	4.07	4.12	Image 17	6.56	6.50	4.25	Image 27	5.53	4.63	4.31
Image 8	6.68	6.53	8.97	Image 18	2.25	3.97	3.53	Image 28	3.91	4.50	3.94
Image 9	7.88	6.15	9.29	Image 19	4.50	2.66	2.99	Image 29	4.75	2.35	2.84
Image 10	4.47	7.04	6.87	Image 20	7.28	5.31	3.28	Image 30	7.72	11.19	7.28
Total (Sec.)	77.51	80.83	77.16	Total (Sec.)	71.92	66.53	65.48	Total (Sec.)	49.90	51.91	45.83
Total (sec.)	Trial										
	1st			2nd			3rd				
	(77.51+71.92+49.90) = 199.33			(80.83+66.53+51.91) = 199.27			(77.16+65.48+45.83) = 188.47				
Average	6.64 sec per image			6.64 sec. per image			6.28 sec. per image				
	(6.64+6.64+6.28) = 19.56 -> 19.56/3 = **6.52 sec.** per image (wrkspc.)										

Time Evaluation of Manual Editing in Option II *[Participant 1]*

Participant 2	Cracking type Longitudinal (L) Transverse (T) Blocking (B)	**Total no. of node points by manual mapping (point)**			**Total no. of errors by manual mapping (point)**			**Accuracy of the manual mapping (%)**			**Time taken for manual mapping (second)**		
		Trial			Trial			Trial			Trial		
		1st	2nd	3rd	1st	2nd	3rd	1st	2nd	3rd	1st	2nd	3rd
Image 1	B	70	71	69	28	32	30	60.00	54.93	56.52	17.74	19.43	21.97
Image 2	T	51	50	51	20	18	14	60.78	64.00	72.55	12.69	16.28	12.13
Image 3	T	36	35	35	12	11	11	66.67	68.57	68.57	6.13	7.00	5.12
Image 4	L	39	39	39	22	22	15	43.59	43.59	61.54	10.09	10.29	9.72
Image 5	T	53	51	52	18	23	24	66.04	54.90	53.85	9.00	7.53	7.06
Image 6	L	17	17	17	13	9	6	23.53	47.06	64.71	2.09	2.38	2.22
Image 7	L+T	31	30	32	14	10	10	54.84	66.67	68.75	6.69	6.12	5.13
Image 8	B	62	61	62	38	21	29	38.71	65.57	53.23	9.56	10.75	10.09
Image 9	T	46	46	45	20	17	16	56.52	63.04	64.44	8.31	7.84	7.03
Image 10	T	48	49	48	22	19	20	54.17	61.22	58.33	7.65	10.28	9.16

Time and Accuracy Evaluation of Manual Mapping in Option II *[Participant 2]*

Participant 2	Cracking type Longitudinal (L) Transverse (T) Blocking (B)	**Total no. of node points by manual mapping (point)**			**Total no. of errors by manual mapping (point)**			**Accuracy of the manual mapping (%)**			**Time taken for manual mapping (second)**		
		Trial			Trial			Trial			Trial		
		1st	2nd	3rd	1st	2nd	3rd	1st	2nd	3rd	1st	2nd	3rd
Image 11	L+T	55	55	58	26	25	30	52.73	54.55	48.28	10.63	13.12	12.44
Image 12	L+T	49	50	49	26	29	26	46.94	42.00	46.94	10.65	10.59	10.87
Image 13	L+T	59	59	59	30	27	31	49.15	54.24	47.46	11.34	11.75	12.00
Image 14	L+T	40	39	39	16	15	17	60.00	61.54	56.41	5.19	6.00	4.22
Image 15	L+T	55	57	57	26	23	31	52.73	59.65	45.61	8.66	11.97	9.75
Image 16	L+T	55	53	54	28	22	24	49.09	58.49	55.56	12.19	13.03	10.25
Image 17	L+T	53	52	53	29	29	27	45.28	44.23	49.06	12.56	14.87	15.00
Image 18	T	33	35	34	3	0	0	90.90	100	100	1.93	3.84	4.43
Image 19	L	19	20	19	13	11	15	31.57	42.85	21.05	2.22	3.19	3.44
Image 20	T	34	35	35	20	19	19	41.18	45.71	45.71	2.98	4.93	4.10

Time and Accuracy Evaluation of Manual Mapping in Option II *[Participant 2]*

Participant 2	Cracking type Longitudinal (L) Transverse (T) Blocking (B)	**Total no. of node points by manual mapping (point)**			**Total no. of errors by manual mapping (point)**			**Accuracy of the manual mapping (%)**			**Time taken for manual mapping (second)**		
		Trial			Trial			Trial			Trial		
		1st	2nd	3rd	1st	2nd	3rd	1st	2nd	3rd	1st	2nd	3rd
Image 21	L	18	19	18	3	5	10	83.33	73.68	44.44	2.85	3.59	3.25
Image 22	T	33	34	33	9	12	14	72.73	64.71	27.27	3.19	3.65	3.06
Image 23	T	35	36	36	0	2	0	100	94.44	100	2.81	2.25	2.25
Image 24	L	37	38	37	15	17	8	59.46	55.26	51.35	8.31	8.06	6.78
Image 25	T	40	41	40	24	24	23	40.00	41.46	42.50	6.62	6.13	6.22
Image 26	B	59	58	58	22	24	28	62.71	58.62	51.72	11.22	11.97	9.78
Image 27	L	33	35	35	3	17	10	90.91	51.43	71.43	8.09	5.59	7.72
Image 28	L	43	43	43	14	13	5	67.44	69.77	88.37	9.41	8.63	9.31
Image 29	L	19	20	20	8	5	6	57.89	75.00	70.00	2.41	3.28	3.75
Image 30	B	47	47	48	17	11	13	64.83	76.60	72.92	6.79	6.13	5.38
Total		1269	1275	1275	539	512	532				230.00	250.55	233.63
Average		1273 node pts. for 30 images (wrkspcs.)			528 node pts. for 30 images (wrkspcs.)			57.53	59.84	58.27	6.78	7.46	7.23
								58.55%/image (wrkspc.)			**7.94 sec.**/image (wrkspc.)		

Time and Accuracy Evaluation of Manual Mapping in Option II *[Participant 2]*

Participant 2	Cracking type Longitudinal (L) Transverse (T) Blocking (B)	**Total no. of node points by line snapping (point)**			**Total no. of errors by line snapping (point)**			**Accuracy of the line snapping (%)**			**Time taken for line snapping (second)**		
		Trial			Trial			Trial			Trial		
		1st	2nd	3rd	1st	2nd	3rd	1st	2nd	3rd	1st	2nd	3rd
Image 1	B	139	141	137	3	5	1	97.84	96.45	99.27	1.82	1.81	1.81
Image 2	T	101	99	101	0	0	3	100	100	97.03	1.32	1.32	1.32
Image 3	T	71	69	69	2	0	2	97.18	100	97.10	0.94	0.93	0.99
Image 4	L	77	77	77	0	0	0	100	100	100	0.99	0.99	0.99
Image 5	T	105	101	103	3	2	2	97.14	98.02	98.06	1.48	1.43	1.42
Image 6	L	33	33	33	6	0	0	81.81	100	100	0.44	0.44	0.44
Image 7	L+T	61	59	63	0	0	1	100	100	98.41	0.76	0.77	0.82
Image 8	B	123	121	123	4	2	0	96.75	98.35	100	1.65	1.60	1.60
Image 9	T	91	91	89	1	0	0	98.90	100	100	1.26	1.26	1.21
Image 10	T	95	97	95	0	0	0	100	100	100	1.21	1.20	1.26

Time and Accuracy Evaluation of the Line Snapping Function *[Participant 2]*

Participant 2	Cracking type Longitudinal (L) Transverse (T) Blocking (B)	**Total no. of node points by line snapping (point)**			**Total no. of errors by line snapping (point)**			**Accuracy of the line snapping (%)**			**Time taken for line snapping (second)**		
		Trial			Trial			Trial			Trial		
		1st	2nd	3rd	1st	2nd	3rd	1st	2nd	3rd	1st	2nd	3rd
Image 11	L+T	109	109	115	2	0	2	98.17	100	98.26	1.42	1.43	1.54
Image 12	L+T	97	99	97	1	2	0	98.97	97.98	100	1.26	1.32	1.32
Image 13	L+T	117	117	117	2	2	2	98.29	98.29	98.29	1.59	1.59	1.54
Image 14	L+T	79	77	77	0	0	0	100	100	100	1.04	0.99	0.94
Image 15	L+T	109	113	113	5	1	2	95.41	99.12	98.23	1.48	1.42	1.49
Image 16	L+T	109	105	107	0	0	0	100	100	100	1.32	1.32	1.37
Image 17	L+T	105	103	105	6	2	1	94.29	98.06	99.05	1.32	1.37	1.37
Image 18	T	65	69	67	3	0	0	95.38	100	100	0.77	0.93	0.94
Image 19	L	37	39	37	1	0	1	97.30	100	97.30	0.49	0.50	0.49
Image 20	T	67	69	69	0	1	1	100	98.55	98.55	0.94	0.98	0.93

Time and Accuracy Evaluation of the Line Snapping Function *[Participant 2]*

Participant 2	Cracking type Longitudinal (L) Transverse (T) Blocking (B)	**Total no. of node points by line snapping (point)**			**Total no. of errors by line snapping (point)**			**Accuracy of the line snapping (%)**			**Time taken for line snapping (second)**		
		Trial			Trial			Trial			Trial		
		1st	2nd	3rd	1st	2nd	3rd	1st	2nd	3rd	1st	2nd	3rd
Image 21	L	35	37	35	0	1	0	100	97.30	100	0.44	0.55	0.43
Image 22	T	65	67	65	0	0	2	100	100	96.92	0.88	0.88	0.82
Image 23	T	69	71	71	0	0	0	100	100	100	0.93	0.99	0.99
Image 24	L	73	75	73	0	1	0	100	98.67	100	0.93	0.93	0.93
Image 25	T	79	81	79	0	0	1	100	100	98.73	1.04	1.10	1.09
Image 26	B	117	115	115	0	0	4	100	100	96.52	1.48	1.49	1.43
Image 27	L	65	69	69	0	0	3	100	100	95.65	0.82	0.82	0.88
Image 28	L	85	85	85	1	1	3	98.82	98.82	96.47	1.16	1.04	1.05
Image 29	L	37	39	39	0	0	0	100	100	100	0.55	0.55	0.50
Image 30	B	93	93	95	0	0	0	100	100	100	1.27	1.26	1.21
Total		2508	2520	2520	40	20	31				33.05	33.21	33.12
Average		2516 node pts. for 30 images (wrkspcs.)			31 node pts. for 30 images (wrkspcs.)			98.41	99.21	98.77	1.10	1.07	1.10
								98.79%/image (wrkspc.)			**1.09 sec.**/image (wrkspc.)		

Time and Accuracy Evaluation of the Line Snapping Function *[Participant 2]*

Participant 2											
Crack image	**Manual editing time (Sec.)** Trial			Crack image	**Manual editing time (Sec.)** Trial			Crack image	**Manual editing time (Sec.)** Trial		
	1st	2nd	3rd		1st	2nd	3rd		1st	2nd	3rd
Image 1	24.96	23.14	6.72	Image 11	10.22	4.78	8.37	Image 21	1.43	3.00	2.31
Image 2	3.03	3.43	13.75	Image 12	5.50	10.59	3.38	Image 22	1.72	1.50	6.50
Image 3	7.03	2.59	5.81	Image 13	9.72	8.66	9.79	Image 23	1.50	1.43	1.10
Image 4	3.88	4.19	3.51	Image 14	1.87	2.21	1.78	Image 24	3.13	4.97	2.65
Image 5	9.81	9.87	9.15	Image 15	17.78	6.41	9.25	Image 25	3.53	1.91	8.22
Image 6	10.82	1.62	1.78	Image 16	3.94	4.50	4.28	Image 26	3.87	3.47	12.65
Image 7	3.91	2.10	4.01	Image 17	36.41	11.56	5.94	Image 27	3.03	3.60	6.21
Image 8	11.01	6.41	2.96	Image 18	8.33	1.56	1.72	Image 28	5.03	4.37	7.37
Image 9	4.90	4.16	3.00	Image 19	2.43	1.85	2.53	Image 29	2.25	1.09	1.93
Image 10	3.53	3.96	5.87	Image 20	1.72	619	4.22	Image 30	3.72	3.94	3.12
Total (Sec.)	82.88	61.47	56.56	Total (Sec.)	97.92	58.40	51.26	Total (Sec.)	29.21	29.28	52.06
Total (sec.)	Trial										
	1st			2nd				3rd			
	(82.88+97.92+29.21) = 210.01			(61.47+58.40+29.28) = 149.15				(56.56+51.26+52.06) = 159.88			
Average	7.00 sec per image			4.97 sec. per image				5.33 sec. per image			
	(7.00+4.97+5.33) = 17.30 -> 17.30/3 = **5.77 sec.** per image (wrkspc.)										

Time Evaluation of Manual Editing in Option II *[Participant 2]*

Participant 3	Cracking type Longitudinal (L) Transverse (T) Blocking (B)	**Total no. of node points by manual mapping (point)**			**Total no. of errors by manual mapping (point)**			**Accuracy of the manual mapping (%)**			**Time taken for manual mapping (second)**		
		Trial			Trial			Trial			Trial		
		1st	2nd	3rd	1st	2nd	3rd	1st	2nd	3rd	1st	2nd	3rd
Image 1	B	67	68	68	24	21	29	64.18	69.12	57.35	14.13	17.19	15.75
Image 2	T	49	50	49	19	18	20	61.22	64.00	59.18	10.50	8.65	10.78
Image 3	T	35	35	35	17	15	15	51.43	57.14	57.14	4.68	6.16	6.31
Image 4	L	40	41	41	19	11	20	52.50	73.17	52.50	11.88	10.06	9.00
Image 5	T	51	50	52	21	11	15	58.82	78.00	71.15	8.21	8.28	8.00
Image 6	L	17	17	17	7	10	5	58.82	41.18	70.59	3.07	2.81	2.72
Image 7	L+T	31	30	30	15	13	9	51.62	56.67	70.00	6.62	6.09	6.12
Image 8	B	60	61	61	22	19	17	63.33	68.85	72.13	11.59	11.21	10.16
Image 9	T	47	47	46	21	20	14	55.32	57.45	69.57	10.00	6.62	6.75
Image 10	T	45	46	45	15	18	14	66.67	60.87	68.89	6.53	7.22	7.12

Time and Accuracy Evaluation of Manual Mapping in Option II *[Participant 3]*

Participant 3	Cracking type Longitudinal (L) Transverse (T) Blocking (B)	**Total no. of node points by manual mapping (point)**			**Total no. of errors by manual mapping (point)**			**Accuracy of the manual mapping (%)**			**Time taken for manual mapping (second)**		
		Trial			Trial			Trial			Trial		
		1st	2nd	3rd	1st	2nd	3rd	1st	2nd	3rd	1st	2nd	3rd
Image 11	L+T	55	55	55	23	13	16	58.18	76.36	70.91	11.22	10.25	10.28
Image 12	L+T	48	49	48	15	18 .	10	68.75	63.27	79.17	10.16	11.16	11.19
Image 13	L+T	58	58	59	19	13	22	67.24	77.59	62.71	12.38	11.09	10.25
Image 14	L+T	39	40	39	11	15	15	71.79	62.50	61.54	5.13	5.62	5.00
Image 15	L+T	57	57	56	25	28	20	56.14	50.88	64.29	11.31	10.40	10.71
Image 16	L+T	54	54	53	23	15	16	57.41	72.22	69.81	10.53	10.79	11.10
Image 17	L+T	52	52	52	27	17	18	48.08	67.31	65.38	12.22	12.03	13.47
Image 18	T	34	34	33	0	0	1	100	100	96.97	3.94	3.03	2.43
Image 19	L	19	19	19	8	8	108	57.89	57.89	47.37	3.59	3.75	3.15
Image 20	T	35	34	35	14	10	11	60.00	70.59	68.57	4.34	4.62	4.34

Time and Accuracy Evaluation of Manual Mapping in Option II *[Participant 3]*

Participant 3	Cracking type Longitudinal (L) Transverse (T) Blocking (B)	**Total no. of node points by manual mapping (point)**			**Total no. of errors by manual mapping (point)**			**Accuracy of the manual mapping (%)**			**Time taken for manual mapping (second)**		
		Trial			Trial			Trial			Trial		
		1st	2nd	3rd	1st	2nd	3rd	1st	2nd	3rd	1st	2nd	3rd
Image 21	L	18	19	19	4	7	9	77.78	63.16	52.63	2.97	3.34	2.79
Image 22	T	34	34	34	11	6	7	67.65	82.35	67.50	3.16	3.75	3.22
Image 23	T	36	35	36	0	1	1	100	97.14	97.22	3.31	3.25	2.78
Image 24	L	36	36	34	12	14	15	66.67	61.11	55.88	7.41	7.65	7.03
Image 25	T	38	39	39	10	15	19	73.68	61.54	51.28	5.84	5.88	5.44
Image 26	B	59	60	60	17	20	14	71.19	66.67	76.67	11.18	9.54	9.44
Image 27	L	33	32	33	5	7	5	84.84	78.13	84.85	6.28	7.01	6.69
Image 28	L	44	43	43	19	13	6	56.82	69.77	86.05	7.75	7.09	6.16
Image 29	L	20	21	19	3	9	8	85.00	57.14	57.89	3.28	3.31	3.34
Image 30	B	48	48	48	14	15	10	70.83	68.75	79.17	7.38	6.84	6.12
Total		1259	1264	1258	440	400	391				230.59	224.69	217.64
Average		1260 node pts. for 30 images (wrkspcs.)			411 node pts. for 30 images (wrkspcs.)			62.05	68.35	68.92	7.69	7.49	7.25
								67.44%/image (wrkspc.)			**7.48 sec.**/image (wrkspc.)		

Time and Accuracy Evaluation of Manual Mapping in Option II *[Participant 3]*

Participant 3	Cracking type Longitudinal (L) Transverse (T) Blocking (B)	**Total no. of node points by line snapping (point)**			**Total no. of errors by line snapping (point)**			**Accuracy of the line snapping (%)**			**Time taken for Line snapping (second)**		
		Trial			Trial			Trial			Trial		
		1st	2nd	3rd	1st	2nd	3rd	1st	2nd	3rd	1st	2nd	3rd
Image 1	B	133	135	135	3	2	3	97.74	98.52	97.78	1.76	1.82	1.70
Image 2	T	97	99	97	3	4	2	96.91	95.96	97.94	1.32	1.21	1.32
Image 3	T	69	69	69	2	2	1	97.10	97.10	98.55	0.93	0.93	0.88
Image 4	L	79	81	81	1	1	2	98.73	98.77	97.53	1.05	1.05	0.99
Image 5	T	101	99	103	2	2	3	98.02	97.98	97.09	1.37	1.37	1.31
Image 6	L	33	33	33	0	0	0	100	100	100	0.44	0.44	0.38
Image 7	L+T	61	59	59	1	1	0	98.36	98.31	100	0.77	0.77	0.77
Image 8	B	119	121	121	1	2	1	99.16	98.35	99.17	1.60	1.59	1.60
Image 9	T	93	93	91	1	0	0	98.92	100	100	1.10	1.15	1.21
Image 10	T	89	91	89	0	0	1	100	100	98.88	1.09	1.10	1.10

Time and Accuracy Evaluation of the Line Snapping Function *[Participant 3]*

Participant 3	Cracking type Longitudinal (L) Transverse (T) Blocking (B)	**Total no. of node points by line snapping (point)**			**Total no. of errors by line snapping (point)**			**Accuracy of the line snapping (%)**			**Time taken for line snapping (second)**		
		Trial			Trial			Trial			Trial		
		1st	2nd	3rd	1st	2nd	3rd	1st	2nd	3rd	1st	2nd	3rd
Image 11	L+T	109	109	109	2	1	0	98.17	99.08	100	1.43	1.43	1.49
Image 12	L+T	95	97	95	1	2	2	98.95	97.94	97.89	1.21	1.31	1.20
Image 13	L+T	115	115	117	2	1	1	98.26	99.13	99.15	1.54	1.42	1.42
Image 14	L+T	77	79	77	1	0	0	98.70	100	100	1.04	0.99	0.93
Image 15	L+T	113	113	111	3	1	2	97.35	99.12	98.20	1.43	1.49	1.54
Image 16	L+T	107	107	105	0	0	0	100	100	100	1.31	1.38	1.32
Image 17	L+T	103	103	103	3	1	1	97.09	99.03	99.03	1.32	1.32	1.32
Image 18	T	67	67	65	0	0	0	100	100	100	0.77	0.82	0.94
Image 19	L	37	37	37	0	0	0	100	100	100	0.49	0.44	0.50
Image 20	T	69	67	69	2	0	0	97.10	100	100	0.94	0.93	0.94

Time and Accuracy Evaluation of the Line Snapping Function *[Participant 3]*

Participant 3	Cracking type Longitudinal (L) Transverse (T) Blocking (B)	**Total no. of node points by line snapping (point)**			**Total no. of errors by line snapping (point)**			**Accuracy of the line snapping (%)**			**Time taken for line snapping (second)**		
		Trial			Trial			Trial			Trial		
		1st	2nd	3rd	1st	2nd	3rd	1st	2nd	3rd	1st	2nd	3rd
Image 21	L	35	37	37	0	1	0	100	97.30	100	0.44	0.44	0.44
Image 22	T	67	67	67	0	0	0	100	100	100	0.88	0.82	0.77
Image 23	T	71	69	71	0	0	0	100	100	100	0.99	0.99	0.98
Image 24	L	71	71	67	0	1	0	100	98.59	100	0.88	0.82	0.93
Image 25	T	75	77	77	4	2	3	94.67	97.40	96.10	0.99	1.04	1.10
Image 26	B	117	119	119	1	1	2	99.15	99.16	98.32	1.43	1.49	1.48
Image 27	L	65	63	65	0	0	1	100	100	98.46	0.77	0.82	0.88
Image 28	L	87	85	85	0	0	0	100	100	100	1.10	0.98	1.10
Image 29	L	39	41	37	1	1	0	97.44	97.56	100	0.50	0.50	0.50
Image 30	B	95	95	95	2	0	0	97.89	100	100	1.21	1.21	1.26
Total		2488	2498	2486	36	26	25				32.15	32.04	31.80
Average		2491 node pts. for 30 images (wrkspcs.)			29 node pts. for 30 images (wrkspcs.)			98.55	98.96	98.99	1.07	1.07	1.06
								98.84%/image (wrkspc.)			**1.07 sec.**/image (wrkspc.)		

Time and Accuracy Evaluation of the Line Snapping Function *[Participant 3]*

Participant 3												
Crack image	**Manual editing time (Sec.)**			Crack image	**Manual editing time (Sec.)**			Crack image	**Manual editing time (Sec.)**			
	Trial				Trial				Trial			
	1st	2nd	3rd		1st	2nd	3rd		1st	2nd	3rd	
Image 1	25.26	10.72	10.41	Image 11	4.79	4.66	3.66	Image 21	1.75	3.16	2.09	
Image 2	15.01	13.32	11.94	Image 12	4.47	7.78	7.37	Image 22	1.88	1.53	1.56	
Image 3	8.06	7.71	5.41	Image 13	5.90	4.66	5.75	Image 23	2.34	2.85	2.16	
Image 4	3.49	4.56	7.19	Image 14	3.37	2.50	2.41	Image 24	2.87	4.14	2.68	
Image 5	8.63	7.44	9.84	Image 15	10.12	4.66	8.78	Image 25	10.91	7.00	7.31	
Image 6	2.47	2.66	1.98	Image 16	3.25	2.93	2.57	Image 26	5.99	4.59	6.21	
Image 7	3.78	3.22	2.12	Image 17	10.18	4.81	4.06	Image 27	2.56	2.41	4.47	
Image 8	6.69	8.10	6.75	Image 18	1.18	1.91	1.04	Image 28	3.00	3.28	2.97	
Image 9	2.97	2.19	3.96	Image 19	1.69	1.53	1.59	Image 29	4.14	4.00	1.38	
Image 10	4.32	3.78	6.99	Image 20	5.12	2.72	2.25	Image 30	7.12	3.01	3.25	
Total (Sec.)	80.68	63.70	66.59	Total (Sec.)	54.86	38.16	39.48	Total (Sec.)	42.56	35.97	34.08	
Total (sec.)	Trial											
	1st			2nd			3rd					
	(80.68+54.86+42.56) = 178.10			(63.70+38.16+35.97) = 137.83			(66.59+39.48+34.08) = 140.15					
Average	5.94 sec per image			4.59 sec. per image			4.67 sec. per image					
	(5.94+4.59+4.67) = 15.20 -> 15.20/3 = **5.07 sec.** per image (wrkspc.)											

Time Evaluation of Manual Editing in Option II *[Participant 3]*

Option / Participant & Trial		OPTION I			Option II				
		Manual mapping		Manual editing	Manual mapping		**Line snapping**		**Manual editing**
		ACCURACY (%)	Time (Sec.)	Time (Sec.)	**Accuracy** (%)	**Time** (Sec.)	**Accuracy** (%)	**Time** (Sec.)	**Time** (Sec.)
	1st	88.34	19.63	29.13	72.37	6.78	98.58	1.13	6.64
Participant 1	2ndt	87.84	20.32	27.97	77.95	7.46	98.46	1.12	6.64
	3rd	88.30	17.95	26.86	76.58	7.23	98.62	1.13	6.28
	1st	81.53	25.23	36.20	57.53	7.67	98.41	1.10	7.00
Participant 2	2ndt	85.06	29.85	34.96	59.84	8.35	99.21	1.07	4.97
	3rd	81.39	27.27	37.58	58.27	7.79	98.72	1.10	5.33
	1st	86.19	24.53	20.10	65.05	7.67	98.55	1.07	5.94
Participant 3	2ndt	86.14	23.40	19.22	68.35	7.49	98.96	1.07	4.59
	3rd	86.09	23.48	18.44	68.92	7.25	98.99	1.06	4.67
AVERAGE		**85.66**	**23.52**	**27.83**	**67.21**	**7.53**	**98.71**	**1.10**	**5.79**

Overall Time and Accuracy Comparison Between Options I and II

APPENDIX. C

Graphical User Interface (GUI) of the ARMM's Vision Software

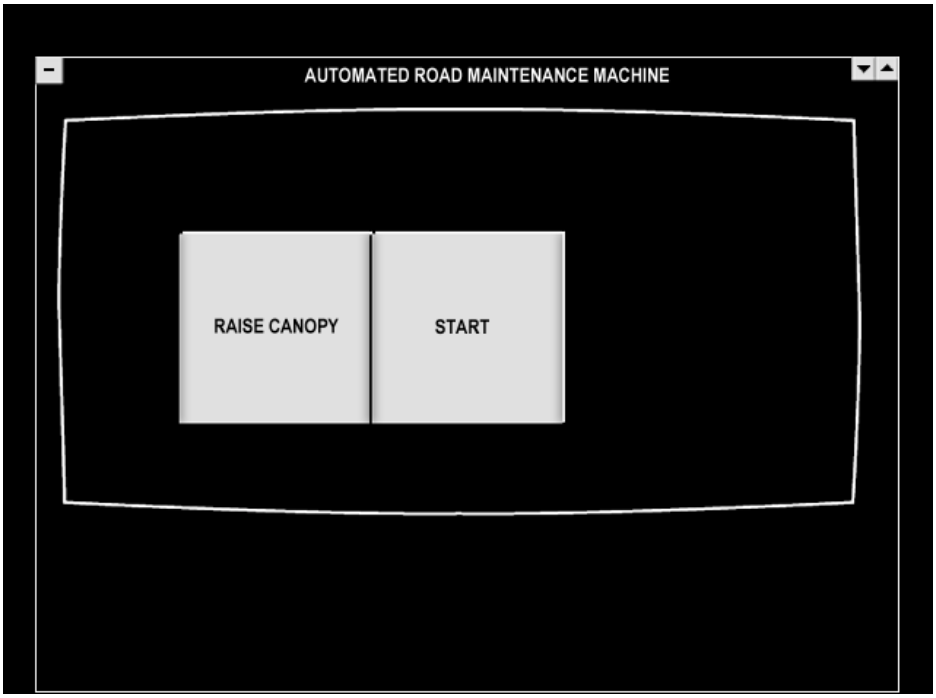

1. Raise Canopy and Image Start

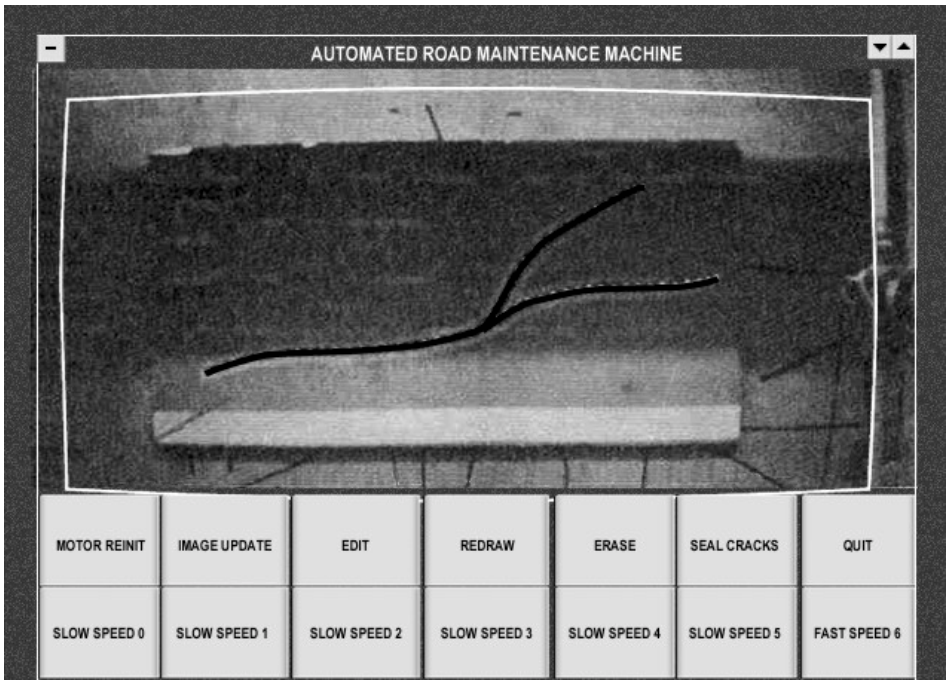

2. Image Acquisition and GUI of the ARMM's Vision Software

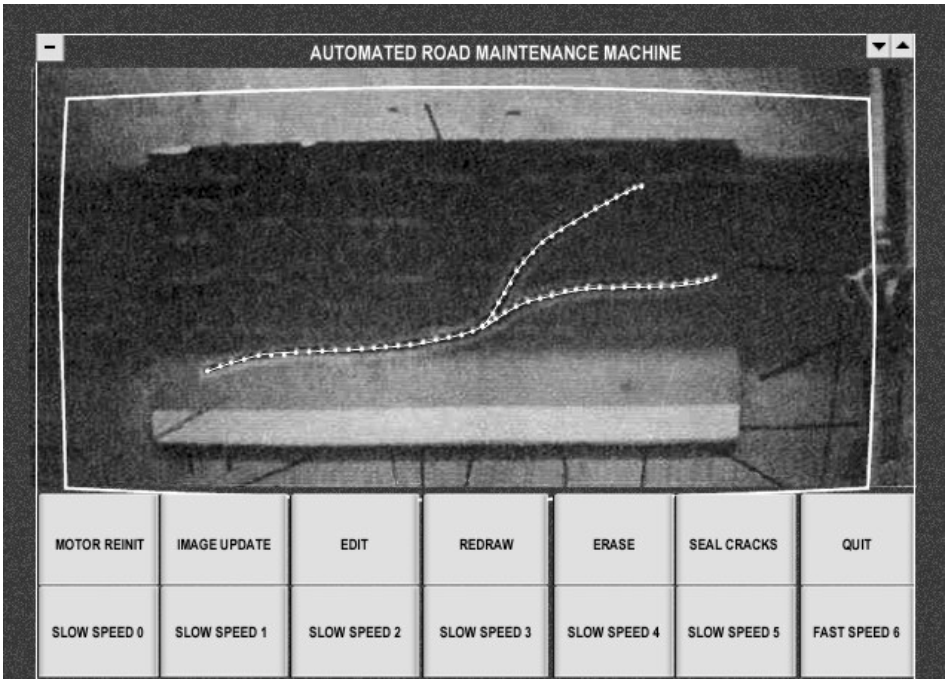

3.Manual Mapping and Line Snapping, and Preparation for Crack Sealing

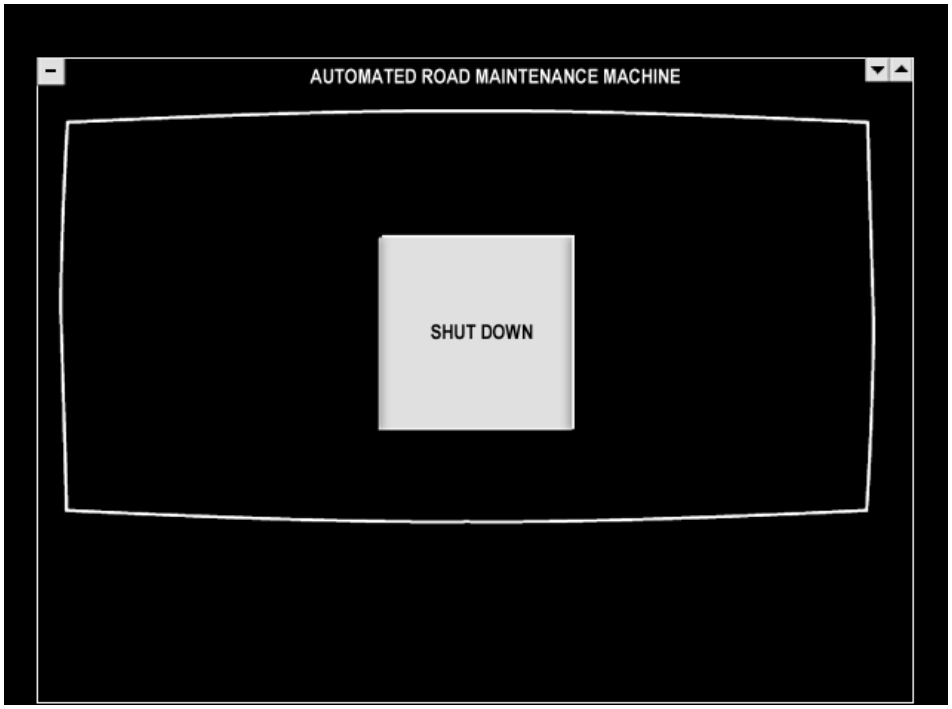

4.System Shutdown